STUDY OF THE ACTIN-RELATED PROTEIN 2/3 COMPLEX AND OSTEOCLAST BONE RESORPTION

By

IRENE RITA MARAGOS HURST

A DISSERTATION PRESENTED TO THE GRADUATE SCHOOL
OF THE UNIVERSITY OF FLOIRDA IN PARTIAL FULFILLMENT
OF THE REQUIREMENTS FOR THE DEGREE OF
DOCTOR OF PHILOSOPHY

UNIVERSITY OF FLORIDA

2006

COPYRIGHT

ACKNOWLEDGEMENTS

There are many individuals to whom I owe my success in this scholastic endeavor. First, I would like to thank my parents for their constant support. Through their parenting, I was able to understand the importance of advanced education, and it is what propelled me to further my education. Second, I would like to thank the faculty members that have helped me through this difficult period. My work in research began in embryology under the guidance of Gertrude Hinsch, Ph.D., at the University of South Florida, Tampa, FL. I furthered my research work at the University of Louisville studying microbiological contamination of dental unit air lines under Robert Staat, Ph.D. It was under his guidance that I was able to obtain my MS in oral biology and made the decision to continue my research work and obtain a Ph.D. For the last 5 years, I have had the explicit pleasure working under L. Shannon Holliday, Ph.D., as well as Timothy T. Wheeler, DMD, Ph.D., and Calogero Dolce, DDS, Ph.D. Their support and guidance have been invaluable. The strength of this program, in both clinical and basic science research, has allowed me to learn and utilize many research techniques as well as become an independent thinker. Last, I would like to thank my husband who has traveled from city to city to support my endeavors. Without him, I would never have made it to this point.

TABLE OF CONTENTS

page

ACKNOWLEDGMENTS iii

LIST OF TABLES vi

LIST OF FIGURES vii

ABSTRACT x

CHAPTER

1 INTRODUCTION 1

Osteoclast Differentiation: RANKL Signalling 2
Hormonal Control of Bone Resorption 5
Mechanism of Action of Oseoclast 5
Sealing Zone 7
Podosomes 7
Transportation of V-ATPase to the Ruffled Membrane 9
Ruffled Membrane 10
Osteoclast Adhesion 10
Osteoclasts and Disease 11
Treatment of Osteoporosis and Osteopetrosis 14
Osteoclast and Dentistry 19
General Purpose of Research 21

2 THE ACTIN RELATED PROTEIN (ARP) 2/3 COMPLEX: AN ELEMENT OF ACTIN RINGS 27

Introduction 27
Materials and Methods 29
Results 38
Discussion 41

3 THE ARP2/3 COMPLEX: A POSSIBLE LINK IN THE TRANSLOCATION OF V-ATPASE TO AND FROM THE RUFFLED MEMBRANE 59

Introduction 59
Materials and Methods 62
Results 64
Discussion 66

4 THE ROLE OF CORTACTIN IN OSTEOCLASTOGENESIS 77

Introduction 77
Materials and Methods 79
Results 84
Discussion 85

5 THE ROLE OF VASP IN OSTEOCLASTOGENESIS 97

Introduction 97
Materials and Methods 99
Results 103
Discussion 105

7 MODEL AND FUTURE DIRECTIONS 115

The Model and Hypothesis 115
Future Directions 121
Significance of Study 124

LIST OF REFERENCES 127

BIOGRAPHICAL SKETCH 148

LIST OF TABLES

Table page

2.1 PCR primers used for identification of Arp3 isoforms 58

3.1 PCR primers used for identification of Arp2/3 related proteins 76

LIST OF FIGURES

Figure page

1.1 Resorbing osteoclast 22

1.2 The OPG/RANK/RANKL triad plays an important role in the bone, immune, and vascular systems 23

1.3 Binding of the adaptor protein TRAF6 is the initial step in RANKL signaling 24

1.4 The dynamic nature of the podosomes of actin rings 25

1.5 In unactivated osteoclasts, V-ATPase is not present at the plasma membrane but is stored in cytoplasmic vesicles; but upon activation, it is transported via actin filaments to the ruffled membrane. 26

2.1 The Arp2/3 complex 45

2.2 Purification of the Arp2/3 complex from human platelets 46

2.3 Upregulation of Arp2 and Arp3 during osteoclastogenesis 47

2.4 Two isoforms of Arp3, Arp3 and Arp3-beta, are present in unactivated and activated osteoclasts 48

2.5 Arp2/3 complex is present in actin rings of osteoclasts 48

2.6 Arp2/3 complex is enriched relative to F-actin near the sealing zone 49

2.7 Arp2/3 does not co-localize with vinculin in actin rings 50

2.8 Treatment with chemical agents, cytochalasin B, echistatin, and wortmannin, causes a disruption of the actin rings of osteoclasts 51

2.9 The Arp2/3 remains co-localized in the actin based podosomal core regardless of actin ring disruption by wortmannin 52

2.10 Wortmannin and echistatin treatment of osteoclasts results in a decrease in the number of actin rings 52

2.11 siRNA 19942 but not 19944 reduces the Arp2 content of osteoclast-like cell extract 70% after 30 hours compared with actin 53

2.12 Actin rings are disrupted in Arp2 knockdown 54

2.13 Actin rings are disrupted in marrow osteoclasts on coverslips or on bone slices by siRNA directed against Arp2 55

2.14 Experimental siRNA reduces the number of actin rings on coverslips by over 95% 56

2.15 Dendritic nucleation model 57

3.1 The structure of V-ATPase 70

3.2 The B1 (1-106) fusion protein of V-ATPase and the Arp2/3 complex do not show a direct interaction by binding assay 71

3.3 The B1 (1-106) fusion protein of V-ATPase and the Arp2/3 complex do not show a direct interaction by immunoprecipitation of B1 subunit 72

3.4 Cortactin is preferentially upregulated during osteoclastogenesis as identified by PCR 73

3.5 Vasodilator stimulated phosphoprotein is identified to have a possible interaction with V-ATPase 74

3.6 Immunoprecipitation experiments with the B subunit of V-ATPase suggest a possible direct linkage between VASP and V-ATPase 75

4.1 Cortactin, N-WASP, and Arp2/3 form a synergistic, ternary complex to initiate actin polymerization 88

4.2 Cortactin is upregulated in response to RANKL stimulation 89

4.3 Cortactin co-localizes with the podosomal core proteins, actin and the Arp2/3 complex 90

4.4 siRNA 120649, but not a control siRNA (120653), effectively knocks down the cortactin content to an undetectable level of osteoclast-like cell extract after 30 hours compared with actin 91

4.5 Actin rings are disrupted in cortactin knockdown 92

4.6 An siRNA known to downregulate cortactin (Ambion) effectively knocks down the cortactin content of osteoclast-like cell extract to an undetectable level after 30 hours compared with actin 93

4.7 Actin rings are disrupted in cortactin knockdown 94

4.8 Transformation and purification of GST-cortactin fusion protein 95

4.9 Immunoprecipitation experiments with GST-cortactin show a linkage between cortactin and Arp3, VASP, N-WASP, and the E subunit of V-ATPase 96

5.1 The ENA/VASP family 108

5.2 VASP is present in the actin rings of osteoclasts 109

5.3 VASP is phosphorylated at Serine 157 in response to calcitonin treatment and results in the disruption of the actin ring..... 110

5.4 Calcitonin induces a three fold increase in phosphorylation levels of VASP at Serine 157 111

5.5 Identification of VASP null mice from breeding of homozygous females with a heterozygous male 112

5.6 Osteoclasts of mice lacking the VASP gene are able to form actin rings and respond to calcitonin in the same fashion as control cells..... 113

5.7 Evl, a member of the ENA/VASP family, is upregulated in response to osteoclastogenesis 114

Abstract of Dissertation Presented to the Graduate School
Of the University of Florida in Partial Fulfillment of the
Requirements for the Degree of Doctor of Philosophy

STUDY OF THE ACTIN-RELATED PROTEIN 2/3 COMPLEX
AND OSTEOCLAST BONE RESORPTION

By

Irene Rita Maragos Hurst

August 2006

Chair: Lexie Shannon Holliday
Major Department: Medical Sciences--Molecular Cell Biology

To resorb bone, osteoclasts form an extracellular acidic compartment segregated by a sealing zone. This is dependent on an actin ring that is composed of filamentous actin organized into dynamic structures called podosomes. The molecular basis of actin rings and their association with vacuolar H+-ATPase (V-ATPase) mediated-acidification during bone resorption were examined.

Immunoblotting and immunocytochemical studies showed for the first time that the actin-related protein (Arp) 2/3 complex is upregulated during osteoclastogenesis and expressed in actin rings. Knockdowns of Arp2, a component of the Arp2/3 complex, with short interfering RNAs (siRNAs) revealed that it is essential for actin ring formation. No direct associations between V-ATPase and Arp2/3 complex were detected. Two proteins involved in regulating Arp2/3 mediated actin polymerization were identified in in vitro binding studies as

interacting with V-ATPase: cortactin and vasodilator-stimulated phosphoprotein (VASP). Cortactin binds and activates Arp2/3 complex. It was upregulated during osteoclastogenesis and localized to the cores of podosomes. siRNA knockdowns showed that it was required for actin ring formation. Binding studies suggest that it may interact with V-ATPase indirectly through the glycolytic enzyme aldolase. VASP was shown to be present in actin rings and phosphorylated in response to calcitonin, which disrupts actin rings. VASP knockout mice did not demonstrate osteoclast or bone defects. ENA-VASP-like protein (Evl), a protein closely related to VASP, was also expressed in osteoclasts and may substitute for the lack of VASP. These data demonstrate that the Arp2/3 complex and cortactin play significant roles in osteoclastic bone resorption and may provide targets for therapeutic agents designed to limit the activity of osteoclasts.

CHAPTER 1
INTRODUCTION

Bone remodeling is a result of the processes of bone resorption and formation and primarily involves two types of cells (1). Osteoblasts, cells of the mesenchymal lineage, form bone and regulate osteoclast differentiation and activation (1). Osteoclasts, the bone resorbing cells, are derived from hematopoietic precursors and are close relatives of macrophages (2-4). Upon activation, the osteoclast undergoes profound reorganizations (5, 6) and becomes polarized, forming morphologically and functionally distinct basolateral and resorptive domains (3, 7, 8) (Figure 1.1). The bone-apposing resorptive domain contains three primary functional structures: the sealing or clear zone, the ruffled membrane, and integrin-mediated adhesions. The ability of the osteoclast to resorb bone is dependent on its ability to generate an extracellular acidic compartment between itself and the bone (7-9). This local acidification is maintained by the presence of the sealing zone, which forms tight contact with the bone surface (6, 9, 10). The acidic pH of this compartment is created by vacuolar H^+ATPases (V-ATPases) (8, 11), in the ruffled membranes which are bounded by sealing zones. V-ATPases pump protons into the extracellular space, solubilizing hydroxyapatite crystals (2), and providing the acidic environment required for the acid cysteine

protease, Cathepsin K, which is involved in the digestion of the organic bone matrix (2, 5, 9, 12).

Osteoclast Differentiation: RANKL Signalling

Osteoclasts differentiate from circulating hematopoietic stem cells that are recruited to the bone to fuse and form multinucleated osteoclasts (13-16). The osteoclast has phenotypic features that distinguish it from other members of the macrophage/monocyte family such as the expression of tartrate-resistant acid phosphatase (TRAP) and the calcitonin receptor and the formation of the ruffled membrane (4, 13).

Osteoclastogenesis is dependent on two important factors, receptor activator of nuclear factor kappa B ligand (RANKL), a tumor necrosis factor (TNF) related cytokine, and colony stimulating factor-1 (CSF-1) (Figure 1.2) (4, 13, 17). These factors induce the osteoclast to express genes specific for osteoclastogenesis such as those encoding cathepsin K, TRAP, and β3-integrin (3). Once osteoclastogenesis has occurred, RANKL and interleukin 1 function to increase the osteoclast survival time by inducing nuclear factor kappa B (NFκB) activity (13).

RANKL is a TNF-related type II transmembrane protein found on osteoblasts either as a surface protein or in a proteolytically released soluble form (1, 4, 13). The expression of RANKL coordinates bone remodeling by stimulating bone resorption in the osteoclast by binding and activating the tumor necrosis factor receptor (TNFR)-related protein, RANK, a transmembrane receptor expressed on the surface of hematopoietic precursors (1, 4, 13). The

requirement of these two proteins in osteoclastogenesis is indicated as mice deficient in either RANK or RANKL are severely osteopetrotic with the inability to resorb bone (1). In addition, antibodies neutralizing RANKL inhibit bone resorption induced by stimulants such as parathyroid hormone (PTH) and prostaglandin E2 (PGE2) (16).

Activation of RANK leads directly to the expression of osteoclast specific genes by the association of various TNF-receptor associated factor proteins (TRAFs) relaying the signal to at least five major signaling cascades: inhibitor of NF-κB kinase (IKK), c-Jun N-terminal kinase (JNK), p38, extracellular signal-related kinase (ERK), and Src pathways (1, 13, 17) (Figure 1.3). The initial step is the binding of TRAFs, cytoplasmic adaptor proteins, to specific domains of the cytoplasmic portion of RANK, in which three putative TRAF binding domains have been identified (1, 13, 17). The binding sites of TRAF-2, -5, and -6 to RANK have been identified; however, only mutations in TRAF-6 result in a loss of osteoclast activity, resulting in osteopetrosis (1, 13, 18). TRAF6 is the key adaptor linking the expression of NF-κB and activator protein-1 (AP-1) to RANK (1, 13). Osteoclastogenesis is inhibited by mutations in the p50/p52 component of NF-κB or the c-Fos component of AP-1, resulting in osteopetrosis (1, 13). TRAF2 and 5 are also able to activate NF-κB pathways, but their contributions to osteoclastogenesis are minor. TRAF3, however, has been shown to serve as a negative regulator of NF-κB activation (1, 13).

Activation of the protein kinase p38 by RANK results in the activation of the transcriptional regulator mi/Mitf (13). This regulator controls the gene

expression of both TRAP and Cathepsin K, which are both required for the osteoclast phenotype (13). ERK-1 kinase is also regulated by RANKL through upstream activation by MEK-1 (13). ERK appears to negatively regulate osteoclastogenesis as inhibitors of ERK potentiate RANKL induced osteoclastogenesis (13).

Src protein binds TRAF6, permitting RANK-mediated signaling to continue through the tyrosine phosphorylation of phosphatidylinositol 3-OH kinase (PI3K) and the serine/threonine protein kinase (AKT) (13). Both PI3K and AKT are involved in various cellular processes, such as motility, cytoskeletal rearragements, and cell survival (13). Mutations in the Src protein have been shown to cause osteopetrosis in mice (13, 19).

Multiple factors are responsible for both positively and negatively regulating osteoclastogenesis by affecting expression of RANKL. Interluekin-1, c-Fms, tumor necrosis factor (TNF)-α, prostaglandin (PG) E2, and transforming growth factor (TGF)-β activate surface receptors on the osteoclast to potentiate osteoclastogenesis and bone resorption (13, 17). It is known that IL1-R and TNFR1 signal through the TRAF6 pathway and have a synergistic effect on RANK mediated TRAF6 activation, while c-Fms and TGF-β affect osteoclastogenesis by upregulation of its components, such as the surface receptor RANK (13, 17).

Negative regulation of osteoclastogenesis through RANKL occurs by osteoprotegerin (OPG), a soluble protein secreted by osteoblasts (1, 13, 17). OPG is a TNFR-related protein and acts as a decoy receptor by binding to

RANKL and blocking its ability to bind RANK (1, 13, 17). It is controlled hormonally by bone anabolic agents such as bone morphogenic proteins (BMPs) (13). These factors cause an overproduction of OPG which blocks osteoclast differentiation, leading to osteopetrosis (13).

Hormonal Control of Bone Resorption

Stimulation of osteoclastogenesis by calciotropic factors and proresorptive cytokines such as parathyroid hormone related peptide (PTHrP), parathyroid hormone (PTH), interleukin (IL)-1b, tumor necrosis factor (TNF)-α, 1,25 dihydroxyvitamin D3, or prostaglandin (PG) E2 (13, 20, 21), acts indirectly via osteoblastic stromal cells (16, 22) by inducing mRNA expression of RANKL. In converse, factors such as estrogens cause a decrease in RANKL expression and an increase in OPG expression, causing reduced numbers of osteoclasts (13). The cytokine, thrombopoietin, has also been identified to induce OPG expression. Calcitonin also is known to inhibit bone resorption (13).

Mechanism of Action of Osteoclast

Once the osteoclast attaches to bone, there is segregation of an extracellular compartment between it and the bony surface (1). The area of tight adhesion segregating this extracellular compartment is termed the sealing zone (1). Bounded by the sealing zone is the ruffled membrane (1). The ruffled membrane is a convoluted membrane packed with vacuolar proton ATPase (VATPase), the osteoclast proton pump (23). The protons, which are pumped by the V-ATPase and are responsible for bone demineralization, are obtained by various mechanisms. One mechanism is the hydration of carbon dioxide to

carbonic acid by carbonic anhydrase II (CA II) (3). The carbonic acid then dissociates into protons and bicarbonate ions. Although traditionally described as the primary mechanism of proton production in the osteoclast, osteopetrosis caused by mutations in carbonic anhydrase II is mild and improves with age (24, 25). This would suggest an alternative source of protons is available. Osteoclastic glycolysis provides the mechanism for an alternative source of protons. In the glycolytic process, one or two hydrogen ions are generated for every ATP molecule produced or glucose molecule consumed respectively (26). Recent data indicate that several glycolytic enzymes bind directly to the V-ATPase and that V-ATPase assembly requires the glycolytic enzyme aldolase (26, 27). These data suggest that V-ATPase, by directly interacting with glycolytic enzymes, forms an acidifying metabolon. Regardless of their source, at the resorptive membrane, the protons are utilized by the V-ATPase to acidify the extracellular compartment (23, 28). At the basolateral membrane, bicarbonate is exchanged for chloride ions in an energy dependent manner (3). The chloride ions, which have entered the osteoclast, pass into the extracellular compartment through a voltage gated anion channel coupled to the V-ATPase (3, 23). The V-ATPase generates a membrane potential and the chloride channel dissipates this potential formed by the protons from the V-ATPase allowing the pH to decrease in the extracellular compartment to approximately 4.5 (3, 23). The highly acidic nature of the extracellular compartment dissolves the bone mineral, which in turn, exposes the organic matrix of the bone (3). Cathepsin K, an acid cysteine proteinase generated by the osteoclast, is then able to degrade

the bone matrix, which is primarily composed of type I collagen and non collagenous proteins (3). The degraded bone, both protein and mineral, are then transcytosed through the osteoclast and secreted into the microenvironment through the basolateral membrane (3).

Sealing Zone

The sealing zone segregates the acidic resorption compartment from the surrounding environment, analogous to creation of an extracellular lysosome (7, 8). By electron microscopy, this area of the plasma membrane demonstrates extremely tight adhesion, less than 10 nm, between the plasma membrane and the adjacent bone surface (29). The molecular mechanisms accounting for the sealing zone are still unknown. Several actin binding proteins, including vinculin and gelsolin, have been localized to the sealing zone (30). In addition, there is much evidence that the formation of an actin ring is required for formation of the sealing zone (5-7, 31, 32). When actin rings are disrupted by calcitonin, herbimycin A, or bisphosphonates, ruffled membrane formation and bone resorption are inhibited (31). Thus, this region is critical in osteoclastic bone resorption.

Podosomes

Podosomes are small, discrete but highly dynamic F-actin based structures. Structural studies indicate that there are two main domains of podosomes, a cylindrical dense actin core with a surrounding ring enriched with $\alpha_v\beta_3$ and focal adhesion proteins, such as integrins, vinculin, paxillin, and talin (33, 34). Along with actin, additional core components include Wiskott-Aldrich

Syndrome protein (WASP) family members, the Actin Related Protein (Arp) 2/3 complex, and cortactin (35, 36). The core and ring may be linked by a bridging protein such as α-actinin. Peripheral to the ring domain, it is hypothesized that a "cloud" of monomeric actin resides (33, 37). Although podosomes are typically found in monocytic cells and are not specific to the osteoclast (38), it is only in the osteoclast that they arrange themselves into a defined actin ring and are associated with a sealing zone (33, 39). Podosomes can also be found or induced in several other cell types, such as endothelial cells, and cells transformed with v-src (33, 35, 40, 41).

Podosomes are relatively small with a diameter of 0.5-1 μm and a depth of approximately 0.2-0.4 μm (33). Although small, they are found in great numbers in osteoclasts (33, 42). Current research suggests that the actin ring of osteoclasts is formed by a rearrangement and fusion of individual podosomes with a slightly different 3-dimensional structure (43). This structure still maintains an actin based core but the "cloud of proteins" is now proposed to surround the entire actin ring structure rather than each individual podosome (43). These actin ring structures can become as large as 4 μm in height and diameter (43). Regardless, podosomes are highly dynamic turning over every 2-12 minutes, with the the length of the actin core turning over multiple times within the lifespan of the podosome, likely facilitated by gelsolin (44) and dynamin (36, 42). Figure 1.4 depicts the dynamic nature of podosomal structures in the actin ring. Rhodamine actin was introduced into saponin-permeabilized activated osteoclasts to allow for the fluorescent visualization of incorporation of actin into

the actin ring. If the actin ring is static, no incorporation would occur; however, within 10 minutes, the rhodamine actin was incorporated into the actin ring, verifying the dynamic nature of the actin ring. To confirm this dynamic nature, the activated osteoclasts were treated with latrunculin A, which binds monomeric actin (45, 46). Due to the inability to add new actin monomers, a loss of podosomal structures and actin ring is observed. Podosome assembly and disassembly occurs from front to end with F-actin continuously adding at the leading edge and treadmilling through to the basolateral region (33, 35).

It is of note that podosomes are only present on adherent cells, indicating that attachment may be the initiating factor with regulation occurring by a variety of mechanisms. Signaling pathways which regulate podosomal formation include Rho family GTPases, such as RhoA, Rac1, or CDC42, and tyrosine phosphorylation by Src or Csk. (35, 47). It has been noted that both dominant active and inactive mutations in Rho family GTPases affect the formation and localization of podosomes; however, the mechanism of disruption has been shown to be dependent on cell type (47). In addition, the use of Src kinase inhibitors causes failure of podosomes while the use of phosphotyrosine phosphatase inhibitors induces podosomal formation (48, 49).

Transportation of V-ATPase to the Ruffled Membrane

The vacuolar H^+-ATPase plays a vital role in bone resorption, as it is the proton pump responsible for acidification of the extracellular compartment and demineralization of the bone (8, 9, 11, 12, 23). In unactivated osteoclasts, V-ATPase is not present at the plasma membrane but rather stored in cytoplasmic

vesicles (23, 50). In the inactivated state, the V-ATPase is bound to F-actin (9, 51); but upon activation, the mechanism by which translocation of actin and V-ATPase to the plasma membrane occurs is still unknown (Figure 1.5) (9).

Ruffled Membrane

The ruffled membrane is the resorption organelle of the osteoclast (8). Its name is derived from the brush border-like appearance of the plasma membrane (8). The ruffled border is formed by the fusion of intracellular acidic vesicles with the plasma membrane, adjacent to the bone surface (6, 8, 11). The fusion of these vesicles causes an enrichment of vacuolar proton ATPase in the plasma membrane (7, 11), which pumps protons to acidify the resorption compartment (23, 50).

Osteoclast Adhesion

Adhesion of the osteoclast to bone is integral in the resorption process. The integrin, $\alpha_v\beta_3$, is a key player in adhesion of the osteoclast to bone (30, 52) by recognizing Arginine-Glycine-Aspartic Acid (RGD) moieties in extracellular matrix (ECM) proteins (53). This integrin has been localized to the basolateral membrane, intracellular vesicles and ruffled border (30, 54). Bone resorption, osteoclast formation and attachment have been shown to be inhibited by disintegrins, blocking antibodies, and RGD mimetic peptides, indicating the importance of $\alpha_v\beta_3$ in osteoclast adhesion (55-57). Echistatin, an RGD containing disintegrin which binds $\alpha_v\beta_3$ tightly, induces osteoclastic detachment from its substrate (55, 58). The use of echistatin *in vivo* causes an inhibition of bone resorption without significantly altering the number of osteoclasts (59),

resulting in a decreased osteoclastic efficiency without effects on osteoclast differentiation and recruitment (60). In addition, a deletion of the β_3 integrin subunit did not affect osteoclast recruitment, which is thought to be mediated by $\alpha_3\beta_5$, or the formation of resorption lacunae (52). The β_3 -/- mice did show decreased bone resorption, abnormal ruffled membranes, and increased osteoclast number, most likely caused from stimulation by hyperparathyroidism secondary to the hypocalcemia produced by decreased bone resorption (52). Skeletal remodeling in the β_3 -/- mice proceeds even in the absence of $\alpha_v\beta_3$; it is hypothesized that an adequate resorption rate is achieved by the increased number of osteoclasts, even in the presence of decreased resorption per osteoclast (52). However, with age, the compensation decreases, and osteosclerosis occurs (52). Although once thought to mediate the extremely tight seal of the sealing zone, Lakkakorpi et al. (57) and Masarachia et al. (59) have shown the specific exclusion of $\alpha_v\beta_3$ from the sealing zone. However, its absence from the sealing zone does not preclude its ability to cause a visible disruption of the sealing zone as was shown by Nakamura et al. (60). It seems likely that proper stimulation of integrin-based signal transduction pathways normally plays a role in the acquisition and maintenance of osteoclast polarity during bone resorption (61).

Osteoclasts and Disease

As previously stated, bone homeostasis is dependent on a delicate balance between bone resorption and bone formation (62). When one is in excess of the other, bone diseases occur. Most commonly, skeletal diseases are

a result of an excessive amount of bone resorption, resulting in osteoporosis (1, 62). Osteoclastic bone diseases are caused by reduced number of osteoclasts, reduced or loss of function or overactivity of osteoclasts (62).

There are several diseases which result in reduced osteoclast activity and thus, osteopetrosis, which often leads to brittle bones and fractures (62-64). Autosomal recessive malignant osteopetrosis is a result of a mutation in the TCIRG1 gene (65, 66). This gene encodes for the 116 kD a3 subunit of V-ATPase (65, 66). The resultant phenotype is osteoclast-rich but with poor resorptive abilities (65, 66). Autosomal dominant osteopetrosis type II (Albers-Schonberg disease) results from a mutation in the CLCN7 gene, which encodes for the CLC7 chloride channel (67-69). As a result of this mutation, normal numbers of osteoclasts are present; however, resorption is inhibited as acidification of the resorption lacunae is hindered (67-69). Autosomal dominant osteopetrosis type I has been linked to a gain of function mutation in the LRP5 gene (70-72). In this disease, osteoclast function is not impaired; however, abnormally low numbers are present (70). It is hypothesized that the mutations in the LRP5 gene alter the osteoblast, decreasing the potential to support osteoclastogenesis (70). Pycnodyostosis has been showed to be a result from mutations in the Cathepsin K gene, an acid cysteine protease responsible for the degradation of organic bone matrix (73-75). A deficiency in this protease results in elevated numbers of osteoclasts and disorganized bone structure (73-75). Another osteopetrotic disease is the autosomal recessive syndrome of osteopetrosis with renal tubular acidosis and cerebral calcification; which is, most

frequently referred to as carbonic anhydrase isoenzyme II deficiency (24, 25, 76). CAII is responsible for one of the mechanisms by which the protons, which are responsible for acidification of the resorption compartment, are produced (3). Thus, prevention of normal acidification occurs (24, 25, 76).

A decrease in osteoclast number may result from defects in the CSF1 (colony stimulating factor) gene (62). Defect in this gene in the murine model results in a broad spectrum of pathology from a delay in osteoclast formation to a complete inhibition of osteoclast formation. In addition, polarization can be affected and there may be a loss of the ruffled border (62). However, to date, there have been no human cases of osteopetrosis attributed to a lack of CSF-1 (62).

The diseases of increased osteoclastic activity include Paget's disease (PD), expansile skeletal hyper-phosphatasia and familial expansile osteolysis (FEO) (77). The second most common bone disease, after osteoporosis, is Paget's disease of bone (77). This disease primarily occurs as a result from a mutation in SQSTM1, which encodes sequestosome 1, an ubiquitin binding protein involved in multiple signaling pathways, including RANKL, IL-1 and TNF (78, 79). However, recent cases have reported a mutation in the TNFRSF11A gene as well which encodes RANK (80-83). Unlike Pagets, familial expansile osteolysis and expansile skeletal hyper-phosphatasia result primarily from defects in the TNFRSF11A, which is the gene encoding RANK (80, 83). Regardless of mutation location, these defects result primarily in an enlargement of the osteoclasts with an increased number of nuclei (80-83). In addition, there

can be an increase in osteoclast number as well as in activity (80-83). A striking finding in both FEO and PD are nuclear inclusions similar to those seen by viral infections (83).

The osteoclast is also implicated in diseases in which skeletal pathology results from inflammation (84-86). In rheumatoid diseases, such as rheumatoid arthritis, seronegative spondyloarthropathies, and systemic lupus erythematosis, as well as periodontal disease, the osteoclast has been identified as the dominant cell type which mediates the inflammatory bone loss (84-86). Activation of the osteoclasts occurs due to increases in proinflammatory cytokines, such as TNF-α, Interferon (INF)-γ, and interleukins, which then modulate expression of RANKL and OPG (84, 85).

Treatment of Osteoporosis and Osteopetrosis

Osteoporosis occurs as a result of an imbalance in the bone remodeling cycle resulting in excessive bone loss (87-89). For the past decade, the treatment of osteoporosis was based on the retardation of bone mineral density loss (88). However, bone formative medications have recently come on the market. The anti-resorptive medications slow bone resorption and formation, but the effect on formation is less dramatic, allowing bone formation to exceed bone resorption and bone density to increase modestly (88). Anti-resorptive medications include the bisphosphonates, estrogens, selective estrogen receptor modulators, and calcitonin.

Calcium is important in the prevention and treatment of osteoporosis (90, 91). Adequate calcium is important for individuals at all ages. Individuals, with

high calcium intake as children, have increased bone mass, which is an important variable in future fracture risk, as the risk for osteoporotic fractures is inversely related to bone mineral density (91). Post-menopausal use of calcium has been shown to decrease bone loss and prevent tooth loss but there is little or no reduction in the risk of spinal fractures (90, 91). Calcium intake should be between 1000-2000 mg/daily (91). Although calcium may slow the loss of bone mineral density, most physicians support the use of additional pharmacologic intervention to prevent/treat osteoporosis (91).

Estrogens and SERMS function as estrogen receptor agonists (88, 89, 92, 93). Estrogen therapy, also known as hormone replacement therapy, has been approved primarily for the prevention of osteoporosis. It has also been shown to increase bone density modestly, reduce bone loss and reduce the risk of fractures in postmenopausal women (92, 93). Selective Estrogen Receptor Modulators (SERMS) bind to the estrogen receptor. Although their mechanism of action is not fully understood, these agents may function by inducing conformational changes in the estrogen receptor, causing differential expression of specific estrogen-regulated genes in different tissues (92, 93). SERMS (raloxifene) are used for both the prevention and treatment of post-menopausal osteoporosis. They function like the estrogens but without the disadvantages of estrogens, such as the increase in uterine cancer (92, 93). Raloxifene has been shown to increase bone mass and reduce spinal fractures; however, as of yet, there is no evidence indicating a decrease in non-spinal fractures (92, 93). Recent data have shown significant risks for breast cancer, venous

thromboembolism and stroke with the use of estrogens and SERMS (94, 95). Data on the incidence of breast cancer have identified an increased risk in ductal and lobular cancer with the use of medium potency estrogens and an increase in lobular cancer with low potency estrogens (94). In addition, if additional risk factors are added, such as alcohol consumption and the use of oral contraceptives, an increase in all three breast cancer subtypes (ductal, lobular or tubular) was observed (94). An examination of the literature identified increased risks of thromboembolism in patients in their first year of therapy and those taking an estrogen-progesterone or high dose estrogen preparation (95). Route of administration also increases the risk as oral administration had significantly higher incidence of thromboembolism than transdermal (95).

The bisphosphonates, alendronate, ibandronate and risedronate, are used for the prevention and treatment of postmenopausal bone loss (88, 89, 92, 93, 96, 97). They function to slow bone loss, increase bone density and reduce the risk of skeletal fractures (97). There are two main categories of bisphosphonates (96). Amino bisphosphonates inhibit osteoclastogenesis by blocking isoprenylation of Rho and Rap and inducing apoptosis while the non-amino bisphosphonates are metabolized to cytotoxic ATP analogues thus inducing cell death (69, 98). Although very effective in the treatment of osteoporosis, the use of bisphosphonates carries significant side effects (99). Several studies have demonstrated a high risk of gastric, duodenal, and esophageal ulcers with administration (100). In addition, two percent of bisphosphonate users demonstrate acute systemic inflammatory reactions, ocular complications, acute

and chronic renal failure, and electrolyte imbalances (99). Osteonecrosis of the mandible or maxilla has recently been identified as sequelae of treatment with bisphosphonates (99, 101-103). These lesions presented as non-healing, usually as the result of dental surgical intervention (99, 101, 102). Although the large majority of these patients were receiving parenteral administration of the drug, several patients were on oral doses (99, 101, 102). Many researchers strongly support further studies to identify the risks and benefits of continuing bisphosphonate therapy (99, 101-103).

Calcitonin is also used for the prevention and treatment of osteoporosis (104, 105). This naturally occurring hormone is involved in calcium regulation and bone metabolism (104, 106, 107). It is administered nasally rather than orally, as it is a protein and would be degraded prior to its function (104). Calcitonin has been shown to increase bone mass and reduce spinal fractures. In addition, studies have shown a decrease in pain post-fracture with the use of calcitonin (105). Non-spinal fractures, however, have not been shown to be reduced with calcitonin treatment (105). A resistance to continuous treatment with calcitonin, with a loss of inhibitory effects on bone resorption, has been shown to occur within 12-18 months after initiation of treatment due to a downregulation of the calcitonin receptor, by both internalization of the receptor and a reduced concentration of de novo receptor synthesis (106, 107). Recent data have shown that this resistance can be avoided by the use of intermittent administration of calcitonin, as calcitonin receptor mRNA expression returns to normal by 96 hours after discontinuation (106, 107).

Teraparatide (Forteo), parathyroid hormone [1-34], is a newly approved medication to treat osteoporosis via bone formation (108-110). Its mechanism of action is to increase bone formation by the osteoblasts (108-110). It has been shown to stimulate bone formation and increase bone mass to a greater extent than the anti-resorptive agents (108-110). Reductions in spinal and non-spinal fractures have been shown (108-110). Like calcitonin, it is a peptide but it is given by injection daily which is a disadvantage of this treatment (108, 110). The most common adverse effects of treatment with teraparatide include headache, nausea, dizziness, and cramping; however, only dizziness and cramping differed from placebo in a randomized clinical trial (111). Other less common complications include hypercalcemia and hyperuricemia (111). These complications can often be inhibited by a reduction of the dosage but may require complete cessation of the drug (111). Animal studies have shown an increased risk for osteosarcoma with the use of teraparatide; however, osteosarcoma has not been identified in over 2800 patients in human clinical trials (111).

Several new treatment modalities are on the horizon for osteoporosis. Zolendronic acid, an injectable bisphosphonate, is currently being studied. It has been shown to increase bone mineral density modestly as do the other bisphosphonates (93). In addition, strontium ranelate, the only current drug known to decrease bone resorption and increase bone formation concomitantly, has just recently finished Phase III trials (93, 112). It has been shown to reduce both vertebral and non-vertebral fractures (93). Its efficacy and safety have been shown; and therefore, it should be marketed soon (112). In addition, as the proof

of concept for bone anabolic therapy has been established with the use of parathyroid hormone, other parathyroid hormone analogues are being investigated as well as the development of non-peptide small molecules targeted against the parathyroid hormone receptor.

The treatment of osteopetrosis has focused on the stimulation of host osteoclasts with calcium restriction, calcitrol, steroids, parathyroid hormone, and interferon (113, 114). Infantile malignant osteopetrosis has also been treated with bone marrow transplantation (113, 114). Coccia et al. (115) documented a case of successful bone-marrow transplantation in a five month old girl in 1980. Prior to transplantation, the patient exhibited anemia, thrombocytopenia, low serum calcium and elevated serum alkaline phosphatase and acid phosphatase all of which normalized within 12 weeks post-transplantation (115). In addition, histologic sections prior to transplantation showed an increase in osteoclast number but no bone resorption occurring (115). Post-transplantation, active osteoclastic bone resorption occurred (115). Unfortunately, although there have been some reports of successful treatment of osteopetrosis, most research indicates ineffectiveness of treatment and patients are usually given poor prognosis (113). Difficulty in treatment also stems from the multiple etiologies of osteopetrosis, and therefore, treatment must be individualized to each patient (113).

Osteoclasts and Dentistry

Osteoclasts play a significant role in the oral cavity, both through physiologic and pathologic processes. The osteoclast is central to the bone loss

observed in periodontal disease. In the inflammatory process in the periodontium, recent data have shown increased levels of RANKL and decreased levels of OPG in patients with periodontal disease (116-118). Recent data have also identified RANKL expression on both T and B lymphocytes (117). It is suggested that the bacterial biofilm initiates an immune response with expression of RANKL which in turn stimulates osteoclastogenesis and bone resorption (117). This hypothesis is confirmed by data showing an abrogation of bone resorption when RANKL is inhibited or knocked out (117).

Dental root resorption is another pathologic process mediated by the osteoclast. Dental root resorption is fairly unpredictable and the etiology is still unknown (119). Recent studies however identify increased levels associated with the IL-1β gene (120). Studies on RANKL and OPG expression when heavy forces are applied during orthodontic tooth movement show increased levels of RANKL to OPG associated with root resorption (121). In contrast, root resorption has been shown to be inhibited with echistatin treatment, a known inhibitor of osteoclasts (119).

Osteoclasts do not always play a pathologic role in the oral cavity. In fact, resorption can be accelerated or inhibited based on the needs of the orthodontic patient. Several studies have shown that osteoclastic bone resorption can be decreased with the addition of chemical mediators or cytokines (122-126). Mice lacking the TNF type 2 receptor show less bone resorption than wild type mice (126). Addition of OPG to the periodontal tissues of mice has also been shown to decrease osteoclastogenesis (125). In addition, inhibition of orthodontic tooth

movement has been observed when treated with matrix metalloproteinase inhibitors, echistatin or an RGD peptide (123). In contrast, orthodontic tooth movement can be accelerated by the removal of OPG. Compared to wild type OPG littermates, OPG knock out mice show increased osteoclast number and increased alveolar bone resorption (127). In the future, the power of the osteoclast may be able to be harnessed to enhance the treatment of the dental patient.

General Purpose of Research

The general purpose of the work presented in this dissertation has been to learn more about the actin ring of osteoclasts, its characteristics and composition and requirements for formation. In addition, we sought to identify a relationship between components of the actin ring and V-ATPase, another specialized structure of the osteoclast.

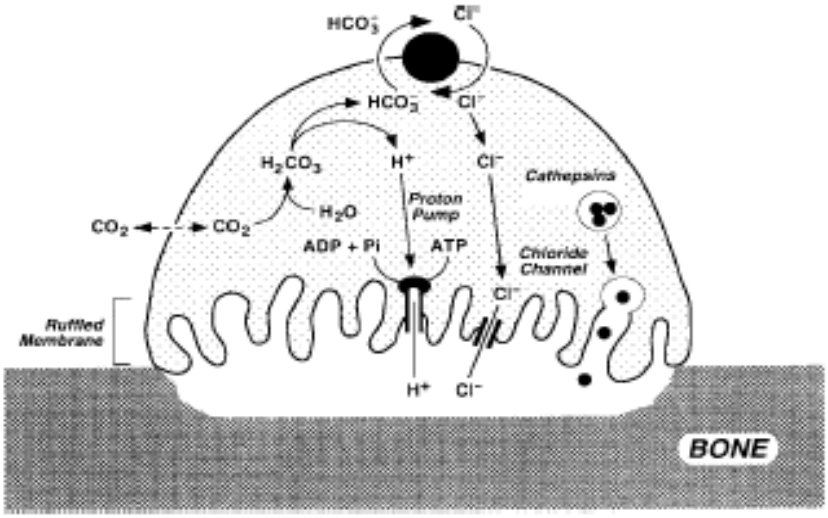

Figure 1.1. Resorbing osteoclast. Once the osteoclast attaches to bone, there is segregation of an extracellular compartment between it and the bony surface. The area of tight adhesion segregating this extracellular compartment is termed the sealing zone. Bounded by the sealing zone is the ruffled membrane. The ruffled membrane is a convoluted membrane packed with vacuolar proton ATPase (VATPase), the osteoclast proton pump (3). Bone degradation is initiated by hydration of carbon dioxide to carbonic acid by carbonic anhydrase II (CA II). The carbonic acid then dissociates into protons and bicarbonate ions. At the apical membrane, the protons are pumped into the extracellular compartment via the V-ATPase. At the basolateral membrane, bicarbonate is exchanged for chloride ions in an energy dependent manner. The chloride ions, which have entered the osteoclast, pass into the extracellular compartment through an anion channel coupled to the V-ATPase. The protons and chloride ions form hydrochloric acid and reduce the pH in the extracellular compartment to approximately 4.5, which allows the demineralization of the bone mineral and exposes the organic matrix of the bone. Cathepsin K, an acid cysteine proteinase, is then able to degrade the bone matrix. The degraded products, collagen and calcium, are then transcytosed through the osteoclast and secreted into the microenvironment through the basolateral membrane. (Teitelbaum et al. J Bone Miner Res 2000; 18:344-349) (3)

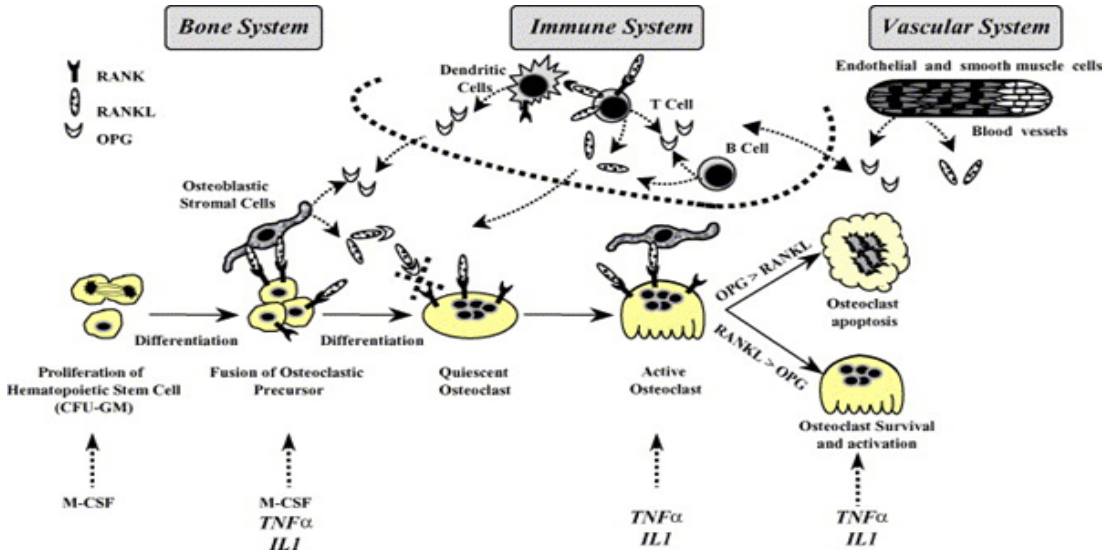

Figure 1.2. The OPG/RANK/RANKL triad plays an important role in the bone, immune, and vascular systems. In the bone system, the interaction between OPG and RANKL promotes either osteoclast differentiation and survival or osteoclast apoptosis. (Theoleyre et al. Cytokine and Growth Factor Reviews. 2004; 15:457-475) (17)

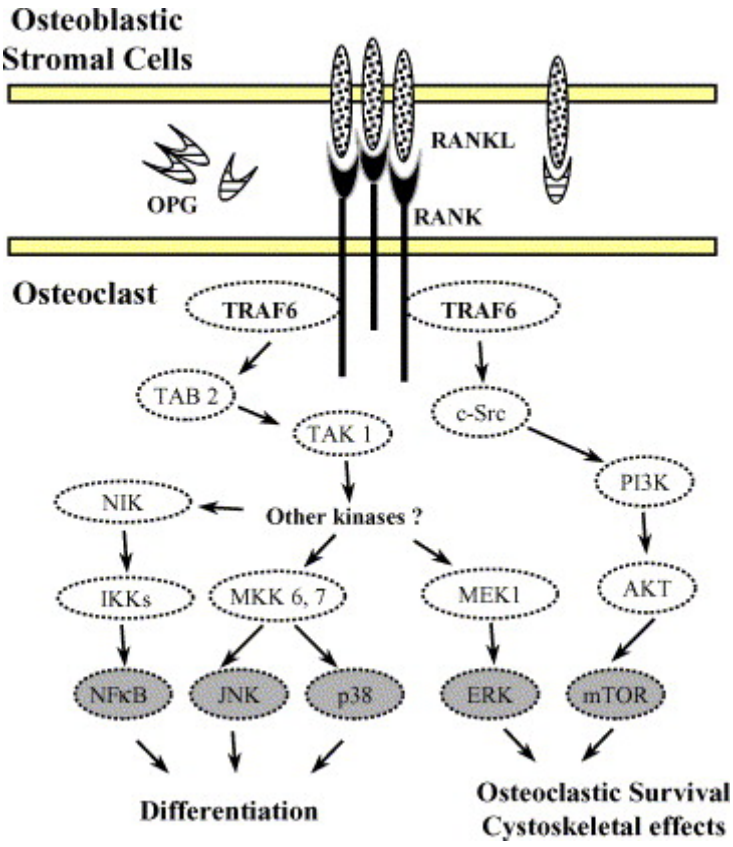

Figure 1.3. Binding of the adaptor protein TRAF6 is the initial step in RANKL signaling. Down stream targets of TRAF6 include nuclear transcription factors, such as NFκB, and signal transduction molecules, such as c-Src. (Theoleyre et al. Cytokine and Growth Factor Reviews. 2004; 15:457-475) (17)

CONTROL **LATRUNCULIN A**

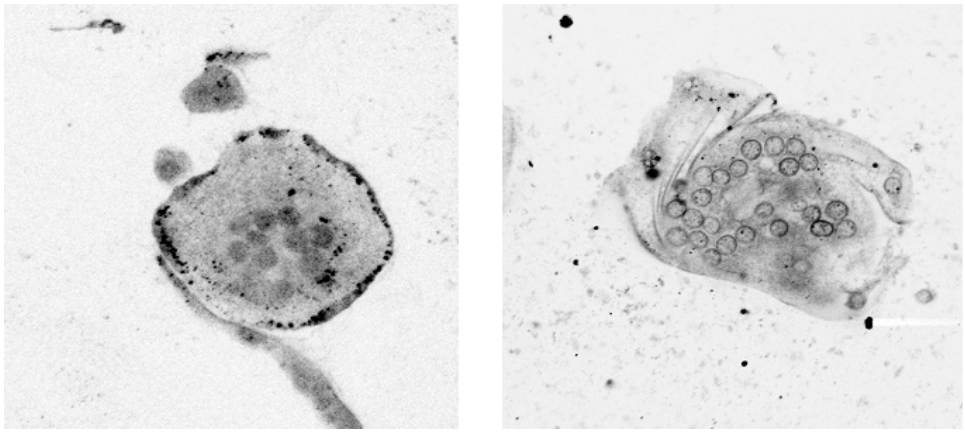

Figure 1.4. The dynamic nature of the podosomes of actin rings**.** Rhodamine actin was incorporated into saponin permeabilized osteoclast like cells. In the control cells, the rhodamine actin was quickly incorportated (within 10 minutes) into the actin rings of osteoclasts. In the latrunculin A treated cells, which inhibits G-actin from polymerization, a complete loss of the actin ring was observed. (Hurst and Holliday, unpublished)

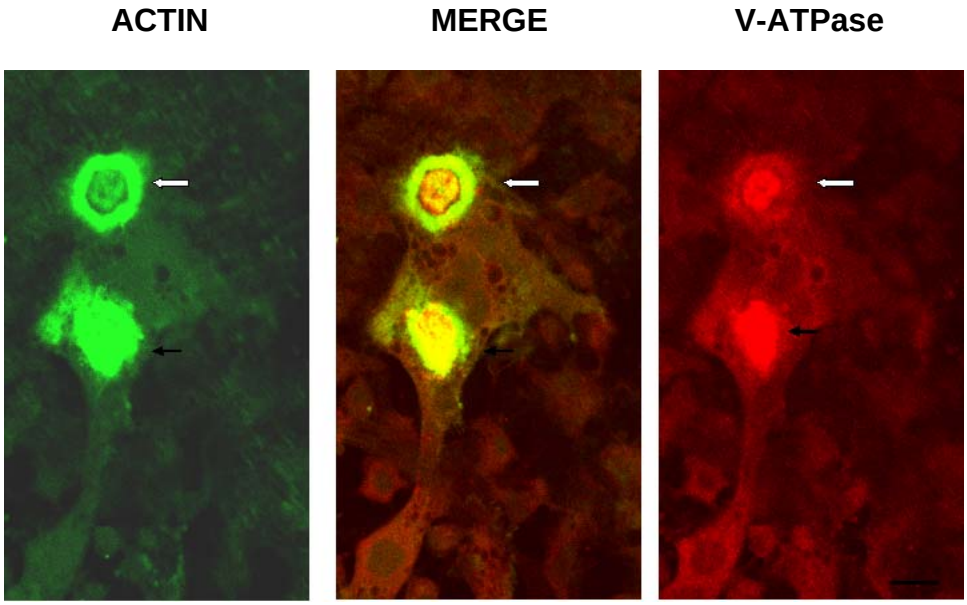

Figure 1.5. In unactivated osteoclasts, V-ATPase is not present at the plasma membrane but is stored in cytoplasmic vesicles, but upon activation, it is transported via actin filaments to the ruffled membrane. Mouse marrow osteoclasts were loaded onto bovine cortical bone slices cultured for 2 days, and fixed and stained with anti-V-ATPase antibody and phalloidin. This micrograph is representative of an early resorptive osteoclast. The white arrow identifies a region where the V-ATPase has been transported to the ruffled membrane which is bounded by actin. The black arrow, below, identifies a unactivated region, where the V-ATPase and actin are still found to be co-localized in cytoplasmic vesicles**.** (Lee et al. J Biol Chem. 1999; 274(41):29164-29171) (9)

CHAPTER 2
ACTIN RELATED PROTEIN (ARP) 2/3 COMPLEX: AN ELEMENT OF ACTIN RINGS

Introduction

The Arp2/3 complex was originally identified by Machesky et al, 1994 (128) as a contaminant during affinity chromatography of profilin from *Acanthamoeba castellani*. Further studies have shown the Arp2/3 complex to be ubiquitous (129). It has been isolated and studied in detail from sources including human platelets, bovine brain extract, Xenopus laevis and *Sacchromyces cerevisiae* (130-133). The Arp2/3 complex is a globular particle of 220 kD (134, 135) and is composed of seven subunits (131, 136-139), which have been highly conserved during evolution (136). Arp2 and Arp3 are actin related proteins, sharing sequence homology with actin in the nucleotide and divalent cation binding domains (131). The other five subunits are novel (131, 137, 139). The subunits are present in stoichiometric amounts (131, 140). Two isoforms of both the Arp3 and p40 subunits have been identified (130, 133, 139, 141). The two isoforms of the Arp3 subunit, Arp3 and Arp3B, share 92% identity (139). Expression of the two isoforms differs with tissue (139). Arp3 is present ubiquitously, while Arp3B is found predominantly in the brain, liver, muscle and pancreas (142). The two isoforms of the p40 subunit share only 68% sequence similarity (130, 133, 139, 141).

The Arp2/3 complex is a key regulator and nucleator of actin polymerization (32, 129). The Arp2/3 complex functions to stimulate actin polymerization at the barbed end of actin filaments, form a nucleation core to trigger actin polymerization de novo, and bind to the side of actin filaments where actin polymerization is triggered, resulting in the formation of an orthogonal actin network (134, 136, 137). Neither Arp2 nor Arp3 is able to independently induce polymerization of actin (133, 136). The formation of a dimer between the two subunits in the complex is required to form the nucleation core to trigger polymerization of actin (Figure 2.1) (138); this process is considered a possible rate limiting step (137, 138, 143, 144). The formation of the dimer is a result of activators such as the WASP family proteins, VASP via ActA, and cortactin (138, 143-146).

Arp2/3 complex driven polymerization is thought to be required for centrally-important cell processes including amoeboid movement and phagocytosis (147-150). The fact that the Arp2/3 complex is a central player in the actin-based motility of certain pathogens has proven to be invaluable to understanding how Arp2/3 works (130, 148-150). Activation of the Arp2/3 complex by WASP family members and small G-proteins results in actin polymerization resulting in the movement of bacterial pathogens such as *Listeria, Shigella*, and *Rickettsia* as well as the enveloped virus vaccinia (129, 151-153). This motility actin polymerization that serves as the basis for this movement results in an “actin comet tail”. This movement is involved in the spread of the pathogens from cell to cell (145, 149, 150). Reconstitution of actin-based

motilities *in vitro* has been successful using F-actin, the Arp2/3 complex, actin depolymerizing complex (ADF), and capping protein (154). The motility of this system proceeds at slow speeds; however, with the addition of Arp2/3 regulators, such as profilin, α–actinin, and VASP, there is an increase in motility (154).

In this study, we examined the presence of the Arp2/3 complex in osteoclasts and its localization during osteoclastogenesis. In addition, we tested its requirement for actin ring formation.

Materials and Methods

Materials

Anti-Arp2 and anti-Arp3 antibodies were purchased from Santa Cruz Biotechnology (Santa Cruz, CA, USA). Rhodamine labeled phalloidin was obtained from Sigma-Aldrich (St. Louis, MO). All CY2 and Texas Red-labeled secondary antibodies were obtained from Jackson-ImmunoResearch (West Grove, PA, USA). The expression vector containing a RANKL [158-316] glutathione-S-transferase fusion protein construct was a kind gift of Dr. Beth S Lee (Ohio State University, Columbus, OH, USA)

Arp 2/3 purification

The Arp2/3 complex was purified from outdated human platelets (Civitan Blood Bank, Gainesville, FL, USA) by a method previously described by Welch and Mitchison (155) based on conventional chromatography. The platelets were centrifuged at 160g for 15 minutes. The platelet pellet was resuspended in 20 volumes of wash buffer (20 mM PIPES, pH 6.8, 40mM KCL, 5 mM ethylene-bis(oxyethylenenitrilo)tetraacetic acid (EGTA), 1 mM Ethylenediaminetetraacetic

acid (EDTA) per volume of packed platelets and centrifuged at 2000g for 15 minutes. The wash was repeated two times. After the final spin, the pellet was resuspended in five volumes of wash buffer on ice for 10 minutes. An equal volume of lysis buffer (Wash buffer plus 10 ug/ml leupeptin, pepstatin, and chymostatin (LPC protease inhibitors), 1 mM benzamidine, 1 mM phenylmethylsuflonyl fluoride (PMSF), 1% Triton X-100, and 0.05 mM adenosine triphosphate) was added on ice for 5 minutes. The lysate was centrifuged at 2000g for 2 minutes at 4^{o}C to pellet the triton-insoluble cytoskeleton. The pellet was resuspended in 5 volumes of resuspension buffer (Wash buffer plus LPC protease inhibitors, 100mM sucrose, 0.05 mM ATP and 1 mM dithiothreitol (DTT)). The resuspended lysate was centrifuged at 2000g for 2 minutes at 4^{o}C. The pellet was gently resuspended in 10 volumes of low salt buffer (20 mM PIPES, pH 6.8, 10mM KCl, 5 mM EGTA, 1 mM EDTA, 1 mM DTT, LPC protease inhibitors) and repelleted by centrifugation at 2000g for 2 minutes. The pellet was resuspended in 5 volumes of extraction buffer (20 mM PIPES, pH 6.8, 0.6 M KCl, 5 mM EGTA, 1 mM EDTA, 1 mM DTT, 0.2 mM ATP, LPC protease inhibitors). This suspension was homogenized for 2 minutes using a Teflon tissue homogenizer. The homogenate was incubated on ice for 30 minutes and then centrifuged at 25,000g for 15 minutes. The supernatant was collected – the first fraction of the cytoskeletal extract. The pellet was resuspended in 5 volumes of extraction buffer, and homogenized for 1 minute, followed by incubation on ice for 2 hours. This step was repeated two times; after which, the homogenate was centrifuged at 25,000g for 15 minutes at 4^{o}C. The supernatant was collected and

added to the first fraction of the cytoskeletal extract. Figure 2.2 lane 1 shows the total protein extract from the human platelets. ATP was added to a 5 mM final concentration and EGTA was added to a 10 mM final concentration. The extract was incubated at 4^{o}C for 16 hours. The extract was centrifuged at 25,000g for 15 minutes. The extract was desalted by use of a 10 ml gel filtration column preequilibrated with Q-Buffer A supplemented with 100 mM KCl (20 mM Tris, pH 8.0, 2 mM $MgCl_2$, 5 mM EGTA, 1 mM EDTA, 0.5 mM DTT, 0.2 mM ATP, 2.5% v/v glycerol). The desalted extract was passed over a 5 ml-Hi-trap Q-Sepharose HP Column pre-equilibrated with Q Buffer A plus 100 mM KCl. The column was presaturated with ATP prior to loading the desalted extract. The Arp2/3 complex is isolated in the flow through fractions. Figure 2.2 lane 2 shows the protein composition of the Q-Sepharose flow through fraction. The flow-through fractions were pooled and the pH was adjusted to pH 6.1 by the addition of MES, pH 6.1 to a final concentration of 40 mM. Glycerol to 10% v/v and LPC protease inhibitors were added and the KCl concentration was adjusted to 50 mM by the 1:2 dilution of sample to S-buffer A (20 mM 2-[N-Morpholino]ethanesulfonic acid (MES), pH 6.1, 2 mM $MgCl_2$, 5 mM EGTA, 1 mM EDTA, 0.5 mM DTT, 0.2 mM ATP, 5-10% v/v glycerol). The diluted flow-through fractions were passed over a 1 ml Hi-trap SP-Sepharose HP column pre-equilibrated with S-buffer plus 50 mM KCl at a rate of 0.5 ml/min. The column was washed with 10 volumes of S buffer with 50 mM KCl. The Arp2/3 complex was eluted with a linearly increasing gradient of KCl from 50 mM to 500 mM. The Arp2/3 complex eluted at 175-200 mM KCl. The peak fractions were pooled and concentrated to 0.5 ml.

The concentrated fractions were loaded onto a Superose 6-HR 10/30 gel filtration column pre-equilibrated with gel filtration buffer (20 mM MOPS, pH 7.0, 100 mM KCl, 2 mM $MgCl_2$, 5 mM EGTA, 1 mM EDTA, 0.5 mM DTT, 0.2 mM ATP, 5-10% v/v glycerol). Fractions of 0.5 ml were collected and the Arp2/3 complex was the only detectable peak eluted from the column at A_{280}. The fractions containing the purified Arp2/3 complex were pooled and concentrated using Centricon 30 concentrators. The protein was frozen in liquid nitrogen and stored at –80^{o}C. Approximately 500 ug of protein was recovered from 10 ml of cytoskeletal extract (250 ml of plasma).

Cell culture

Osteoclasts were obtained from two sources. Mouse marrow osteoclasts were grown from marrow derived from the long bones of the hind legs of Swiss-Webster mice. The marrow cells were grown in α-MEM medium with 10% fetal bovine serum (FBS) plus 10^{-8} M 1,25-dihydroxyvitamin D_3 for a period of approximately seven days. Osteoclasts were also grown from the RAW 264.7 cell line, which is a mouse hematopoietic cell line. This protocol was approved by the University of Florida Institutional Animal Care and Usage Committee. RAW 264.7 cells were grown in Dulbecco's Modified Eagle's Medium (DMEM) containing gentamicin and 10% FBS for 4 days with fresh media being added on day 2. On day four, the cells were detached by scraping, gently triturated and counted with a hemacytometer. The cell density is crucial for osteoclast differentiation. A cell count of 15,000-20,000 cells/cm^2 was cultured with 50 ng/ml recombinant receptor activator of nuclear factor kappa b ligand

(RANKL)(amino acids 158-316)-GST for 4-5 days. With the addition of RANKL, the RAW 264.7 cells become large, multinucleated cells expressing characteristics of osteoclasts including actin ring formation, expression of tartrate-resistant acid phosphatase activity and the ability to resorb bone. The osteoclasts and RAW 264.7 cells were cultured in tissue-culture grade dishes. Once mature, the cells were scraped and replated on either glass coverslips or dentine bone slices.

Western blot analysis with quantitation of Arp2/3

Anti-Arp2/3 antibodies were obtained from Santa Cruz Biotechnology Inc (Santa Cruz, CA). The Anti-Arp2 antibody was generated against the carboxyl terminus of the Arp2 protein while the Anti-Arp3 antibody was generated against the amino terminus. The specificity of the antibodies was determined by Western Blot analysis, by probing the purified Arp2/3 complex (Figure 2.3A). RAW 264.7 cells were grown as previously described, plated on 6 well plates, and either left unstimulated or stimulated with RANKL. Cell lysates were collected from both the control and treated cells. Cells were washed twice with ice cold PBS and scraped from the plates. The cells were then detergent solubilized in 0.2% Triton X-100 in PBS. Equal amounts of the lysates were separated by SDS-PAGE, followed by Western Transfer. The nitrocellulose blots were then incubated with either anti-Arp3 or anti-Arp2 antibodies for one hour, washed three times, incubated with HRP conjugated secondary antibody, washed three times, and incubated with Super Signal Dura West Chemiluminescent Substrate (Pierce, Rockford, IL). The blots were then viewed on a Fluorochem 8000 (Alpha-

Innotech, San Leandro, CA), and quantitation was performed by Spot Densitometry (Fluor-Phor Software, Alpha-Innotech, San Leandro, CA). The integrated density values (IDV) were obtained (white = 65535, black = 0). Background values were subtracted, and the intensities were normalized against the value of actin in the sample. The values were then compared between stimulated and unstimulated cells. The stimulated and unstimulated values were statistically analyzed using the student's t-test, with statistical significance (p) being less than 0.05.

Immunofluorescence

Immunofluorescence was performed to visualize the distribution of the Arp2/3 complex in the resorptive osteoclast as well as its co-localization with actin. The marrow or RAW264.7-derived osteoclasts were fixed in 2% formaldehyde in PBS on ice for 20 minutes. The cells were then detergent-permeabilized by the addition of 0.2% Triton X-100 in PBS for 10 minutes, washed in PBS and blocked in PBS with 2% bovine serum albumin (BSA) for one hour. Cells were stained with rhodamine-phalloidin, or antibodies recognizing Arp3 or Arp2 at a dilution of 1:100 in PBS. Secondary antibodies were diluted according to manufacturer's instructions. Osteoclasts were visualized using the MRC-1024 confocal laser scanning microscope and LaserSharp software (Bio-Rad, Hercules, CA). Images were taken in sequential series to eliminate any overlap of emission and analyzed by confocal assistant software.

Additional immunofluorescence experimentation was performed to identify changes in the distribution of the Arp2/3 complex when introduced to agents

known to disrupt actin ring formation. Cell culture was performed as previously described. On day 6 of differentiation (many large multinucleated cells present), wortmannin (100 nM), cytochalasin D (20 μM) or echistatin (10 nM) were added to the cells and incubated for 10-30 minutes. The cells were then fixed in 2% formaldehyde, solubilized in 0.2% Triton X-100 in PBS and blocked in PBS with 2% BSA. Cells were stained with rhodamine-phalloidin, or antibodies recognizing Arp3 or Arp2 at a dilution of 1:100 in PBS. Secondary antibodies were diluted according to manufacturer's instructions. Osteoclasts were visualized using the MRC-1024 confocal laser scanning microscope and LaserSharp software (Bio-Rad, Hercules, CA). Images were taken in sequential series to eliminate any overlap of emission and analyzed by confocal assistant software.

Polymerase chain reaction of the two isoforms of Arp3

To determine the redundancy of the Arp3 protein, RNA was extracted from RANKL differentiated RAW 264.7 cells as well as from unstimulated RAW 264.7 cells using RNAeasy Mini Kit (Qiagen, Valencia, CA) and quantified by spectrophotometer. The sequences for Arp3 and Arp3-beta were obtained from Gen Bank. Primers were designed as described in Table 2.1. For standard RT-PCR, 3 μg of total RNA was annealed to an oligo-dt primer and first strand cDNA synthesis was performed using Thermoscript RT-PCR System (Invitrogen, Carlsbad, CA) following manufacturer's directions. One-twentieth of the cDNA was subjected to amplification by PCR. PCR was performed under the following conditions: 95^{o}C for 2 minutes, then 35 cycles of 90^{o}C, 30 seconds; 58^{o}C, 30

seconds; 72°C, 30 seconds. One-half of the PCR product was separated on 0.5% agarose gel with ethidium bromide staining for 1 hour. Images were detected using UV transillumination on a Fluorochem 8000 (Alpha-Innotech, San Leandro, CA).

Knock down of Arp2 with siRNA

Five siRNA complexes were designed against the Arp2 protein (accession no. XM_195339) and produced by Sequitur (Natick, MA, USA): 19941 (targeting bp 21-39) sense 5"-GGUGGUGGUGUGCGACAAUTT-3", antisense 5'-AUUGUCGCACACCACCACCTT-3'; 19942 (targeting bp 138-156) sense 5'-AGGGGGAAACAUUGAAAUCTT-3', antisense 5'-GAUUUCAAUGUUUCCCCC UTT-3'; 19943 (targeting bp 255-273) sense 5'-CAGAGAGAAGAUUGU AAAGTT-3', antisense 5'-CUUUACAAUCUUCUCUC UGTT-3'; 19944 (targeting bp 372-390) sense 5'-CUCUGGAGAUGGUGUCACUTT-3', antisense 5'-AGUGACACCAUCUCCAGAGTT-3'; 19945 (targeting bp 513-531) sense 5'-CCAUUCUGCUGAUUUUGAGTT-3', antisense 5'-CUCAAAAUCAGCAGAAUG GTT-3'. Initial experimentation showed that only siRNA 19942 was capable of producing downregulation of the Arp2 protein. The other siRNAs were used as ineffective controls. For morphological examination, RANKL stimulated RAW 264.7 cells on glass coverslips in 24-well plates were either not transfected or transfected using 1.5 U control or ineffective siRNA and 1.5 U fluorescent double stranded RNA combined with 2 ul Lipofectamine 2000 (Invitrogen) in Opti-Mem media supplemented with RANKL on day 5 of differentiation (at the appearance of multinucleated cells). Six hours after transfection, the media was replaced

with DMEM supplemented with FBS and RANKL. No antibiotics were used. The cells were incubated for 24–48 hours at 37^{o} C in a CO_2 incubator; after which, the cells were fixed in 2% paraformaldehyde. Rhodamine phalloidin was used to visualize actin ring morpholology. Only cells with uptake of the fluorescent oligomer were identified as having been transfected with the control or Arp2 siRNA. Morphological examination was performed using confocal microscopy. Mouse marrow osteoclasts were grown on tissue culture plates for 5 days and supplemented with calcitriol as described previously. The cells were then scraped and transfected as described for the RAW 264.7 cells, except αMEM was used in place of DMEM. Cells were analyzed as described above for RAW 264.7 cells. For assessment of protein expression, RANKL stimulated RAW 264.7 cells on 6 well plates were either not transfected or transfected using 7.5 U control or experimental siRNA combined with 10 ul Lipofectamine 2000 on day 5 of differentiation. Six hours after transfection, the media was replaced by DMEM with FBS and RANKL. The cells were incubated for 30 hours at 37^{o} C in a CO_2 incubator. Cells were scraped and washed twice with PBS. The pellets were lysed using 250 ul of cell extraction buffer (BioSource International, Camarillo, CA, USA) supplemented with protease inhibitor cocktail (Sigma P2714) and phenylmethylsulfonyl fluoride (PMSF) for 30 minutes on ice with vortexing every 10 minutes. The extract was centrifuged for 10 minutes at 13,000 rpm at 4^{o} C. Bradford assay was performed on the lysates. Equal concentrations of protein were separated by SDS-PAGE, followed by western transfer. The nitrocellulose blots were blocked in blocking buffer overnight and incubated with both anti-Arp2

and anti-actin antibodies for 2 hours. The blots were washed and incubated with a horseradish peroxidase (HRP)-labeled secondary antibody for 1 hour, followed by incubation with a chemiluminescent substrate. The blots were visualized using an Alpha Innotech Fluorochem 8000. Quantitation was performed using densitometry measuring integrated density values.

Results

Arp2 and Arp3 are upregulated during osteoclastogenesis

After the purified Arp2/3 complex was isolated from platelets, the specificities of the anti-Arp2 and anti-Arp3 antibodies were determined by western blot analysis (Figure 2.3A). Both antibodies recognized their target proteins. When observing total protein levels, by western blot analysis, from non-stimulated RAW 264.7 cells and RAW 264.7 cells induced to differentiate into osteoclasts by treatment with RANKL, both Arp2 and Arp3 were upregulated approximately three-fold in response to RANKL stimulation (Figure 2.3B and 2.3C).

Both isoforms of the Arp3 protein are present in osteoclasts

The Arp3 protein has been identified in two different isoforms. By PCR analysis, both isoforms are expressed in the activated osteoclast (Figure 2.4). This may allow for redundancy of the Arp3 protein, which would allow the maintenance of essential function of the Arp 2/3 protein even if one isoform was mutated or lost.

Expression of Arp2/3 complex in the actin ring

The actin rings on osteoclasts of either glass coverslips or bone slices were stained with anti-Arp3 and anti-Arp2 antibodies (Figure 2.5). In addition to actin ring staining, osteoclasts on coverslips often showed intense patches of Arp3-staining with little F-actin co-staining in the center of the cell.

Confocal z-sections of actin rings of osteoclasts on coverslips and on resorbing bone slices revealed that Arp3 was present throughout the actin ring and was enriched, relative to F-actin, at the apical membrane, in proximity to the sealing zone. Figure 2.6 A and B show a projection of 44 slices of the edge of a mouse marrow osteoclast on glass stained with anti-Arp3 (A) or phalloidin (B). These slices were stacked and digitally rotated 90^{o} so that the apical surface was at the bottom and the basolateral at the top. Figure 2.6C is the rotated version of 2.6A and Figure 2.6E is the rotated version of 2.6B. Figure 2.6E is the merged image of Figures 2.6C and 2.6D, with the Arp3 staining pseudocolored green and phalloidin staining pseudocolored red. Notice that Arp3 was enriched compared with F-actin at the apical boundary, and F-actin was relatively enriched near the basolateral boundary.

Figures 2.6F and G show a projection through the actin ring of a resorbing osteoclast stained with anti-Arp3 (F) or phalloidin (G). Figures 2.6H and 2.6I show a smaller portion of the rings found in Figures 2.6F and 2.6G. The smaller section was rotated 90^{o} so that the apical surface, which contacts bone, was down, and the basolateral surface was at the top (Figure 2.6J). Using a small section of the actin ring, the image was simplified and more easily interpreted.

Anti-Arp3 staining was pseudocolored green and phalloidin staining was pseudocolored red. Similar results were observed as with the unactivated osteoclasts. Arp3 was enriched relative to F-actin at the apical boundary.

Arp3 does not co-localize with the actin associated protein, vinculin

Osteoclasts were co-stained with another actin associated protein, vinculin. The vinculin staining (Figure 2.7) surrounded that of Arp3 with little co-localization occurring.

Disruption of Arp3 distribution by chemical agents

The distribution of the Arp2/3 complex was identified after disruption of the actin ring by the chemical agents, wortmannin, cytochalasin D and echistatin (Figure 2.8). Disruption of the actin ring occurred regardless of the chemical agent used; however, the Arp2/3 complex continued to co-localize with actin in podosomes (Figure 2.9). Figure 2.10 quantitatively describes the effects of wortmannin and echistatin treatment on osteoclast-like cells on glass coverslips.

Arp2 is required for actin ring formation

Five siRNAs were generated against targets in Arp2. Preliminary studies showed that one (19942) effectively knocked down Arp2 expression, whereas the others were ineffective. RAW 264.7 cells were stimulated with recombinant RANKL and transfected just as they began to fuse. Transfection efficiency was from 65 to 80% of the total giant cells, as judged by uptake of a fluorescent double-stranded oligomer. Western blot analysis (Figure 2.11) of osteoclasts 30 hours after transfection showed a 70% decrease in the amount of Arp2 found in the total cell extract.

Other RAW 264.7 osteoclast-like cells were fixed 30 hours after transfection with effective or ineffective siRNAs. Both nontransfected cells or cells transfected with ineffective siRNAs showed normal actin rings (Figure 2.11). In contrast, fewer structures that look like podosomes were apparent in the knock down cells, and actin rings were rarely observed (less than 1% of controls). Typically F-actin was concentrated in central regions of giant cells in which Arp2 was knocked down.

Mouse marrow osteoclasts were also transfected with effective or ineffective siRNAs (Figure 2.13). Transfection efficiency was very low, but a few transfected osteoclasts were identified based on the entry of the fluorescent double-stranded oligomer. Osteoclast transfection with 19942 did not have actin rings after 30 hours, whereas the majority of the osteoclasts transfected with the ineffective control did show actin rings. This was true for both activated and inactivated osteoclasts.

Discussion

These studies demonstrate for the first time that the Arp2/3 complex is a component of the actin ring of osteoclasts and is required for its formation. The Arp2/3 complex was upregulated three-fold during differentiation. This is consistent with the Arp2/3 playing a role in actin ring formation, specialized structures specific to osteoclasts. The Arp2/3 complex is abundant in actin rings, co-localizes with the actin core of podosomes and is enriched at the apical boundary near where the osteoclasts contact the substrate. Vinculin, a focal adhesion protein, was enriched at the apical border of actin rings but did not co-

localize with actin or the Arp2/3 complex but rather surrounded them in a cloud, which is consistent with current studies (33).

The organization of podosomes in the actin rings of osteoclasts has been shown to be disrupted by the addition of chemical agents such as wortmannin, echistatin and cytochalasin D. Cytochalasin D is a fungal toxin that reduces actin polymerization by inhibiting G-actin and is known to disrupt actin ring formation in the osteoclast (156, 157). The actin fibers of podosomes depolymerize as the effective concentration of G-actin becomes limiting (156, 157). Wortmannin is a fungal toxin and functions as a selective inhibitor of PI3 Kinase activity (158). Echistatin is a snake venom toxin and inhibits the integrin, $\alpha_v\beta_3$ (159, 123). In osteoclasts, echistatin causes a disruption of the sealing zone and an internalization of integrins from the basolateral membranes to intracellular vesicles. The treated osteoclasts tend to round up and collapse. Although the osteoclasts are still adherent to bone, osteoclastic resorptive ability is severely reduced as is seen by a reduction in resorptive pit number and size. Regardless of the type of inhibition, disruption of the actin ring occurs but with a continuous co-localization of the Arp2/3 complex with the podosomal core. These data support high integrity of the podosomal core.

It has become clear that much of the actin filament dynamics in cells depends on the Arp2/3 complex (160). Activated Arp2/3 complex interacts with actin monomers to promote filament assembly. Activation occurs in response to interactions with accessory proteins that are in turn activated in response to signal transduction. Recent data indicate that actin treadmills rapidly through

podosomes, entering apically and removed basolaterally (Figure 2.15) (161). The plasma membrane is pushed forward by this actin polymerization until capping of the barbed end occurs. As the filaments age, the ATP bound to each subunit is hydrolyzed, with slow dissociation of the γ-phosphate. ADF/cofilin cause severing of actin filaments and the dissociating of ADP–actin (161, 162). The exchange of ADP for ATP is catalyzed by profilin, and a regeneration of the pool of profilactin is available for the next generation of filaments (162). This mechanism suggests a role for the Arp2/3 complex. In addition, the enrichment of the Arp2/3 complex at the apical boundary of the podosomes of actin rings that we observed is consistent with the Arp2/3 complex playing a role in the entry of actin monomers into the actin ring filaments. The true function of the treadmilling is not currently known; however, it is plausible that the podosomes may be exerting force on the plasma membrane, causing it to conform to bone (160). It is known that actin polymerization can produce protrusive forces required for cell crawling as well as the intracellular propulsion of microbial pathogens and organelles. An important example of this force generation via actin polymerization occurs is in the propulsion of Listeria monocytogenes. Loisel et al. (154) have shown the reconstitution of sustained movement in *Shigella* and *Listeria* with the addition of purified Arp2/3 complex, actin, actin depolymerizing protein (cofilin), and capping protein. As the Arp2/3 complex is a known central player in the actin-based motility of certain pathogens, this same force generation may be within the realm of the Arp2/3 complex in the actin ring of osteoclasts (144-146).

In osteoclasts, gelsolin has been implicated in triggering actin ring formation (44, 163). This could potentially be accomplished by cleaving existing filaments and uncapping barbed ends in a regulated manner (164). Moreover, the gelsolin “knockout” mouse is mildly osteopetrotic, suggesting a role for gelsolin in bone resorption (165). However, the mildness of the osteopetrosis suggests other mechanisms contribute to the cytoskeletal dynamics required for bone resorption (166, 167). A strong possibility may be coordination between gelsolin and the Arp2/3 complex. A recent model describing podosomes suggests a balance of actin polymerization, which, based on our results, is likely regulated by the Arp2/3 complex, and filament cleavage, by proteins like gelsolin (33). This balance could account for the structure and dynamics of podosomes.

In summary, the Arp2/3 complex is present in the podosomal structures of the actin rings of osteoclasts. Knockdown of Arp2 using siRNA shows that the Arp2/3 complex is required for actin ring formation. These data suggest that the Arp2/3 complex plays a role in osteoclastic bone resorption and may provide a target for therapeutic agents designed to limit the activity of osteoclasts.

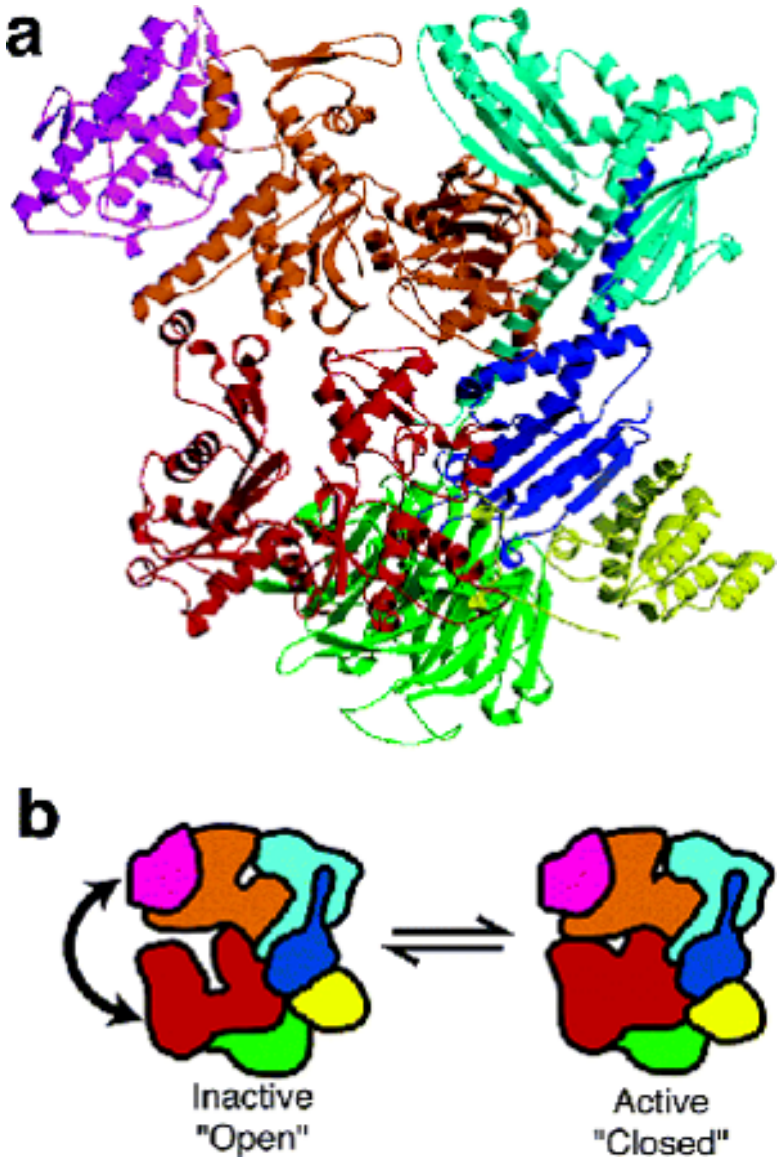

Figure 2.1. The Arp 2/3 complex. A) Crystal structure of the 7 subunits of the Arp2/3 complex. B) The Arp2/3 complex remains in an inactive conformation. Upon activation by WASP family members, the Arp2 and Arp3 subunits undergo a conformational change and allow the complex to become active and participate in actin polymerization. (Robinson et al. Science. 2001; 294:1679-1684) (138)

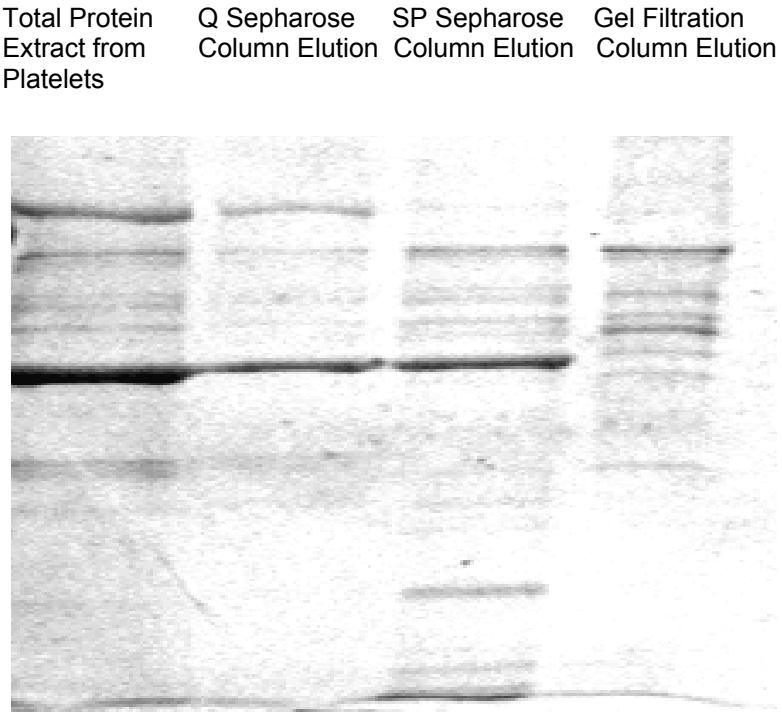

Figure 2.2. The purification of the Arp2/3 complex from human platelets**.** The Arp2/3 complex was purified from human platelets by a previously published method by Welch and Mitchison using conventional chromatography. Each lane depicts the elution from the columns run with purified Arp2/3 complex obtained after gel filtration.

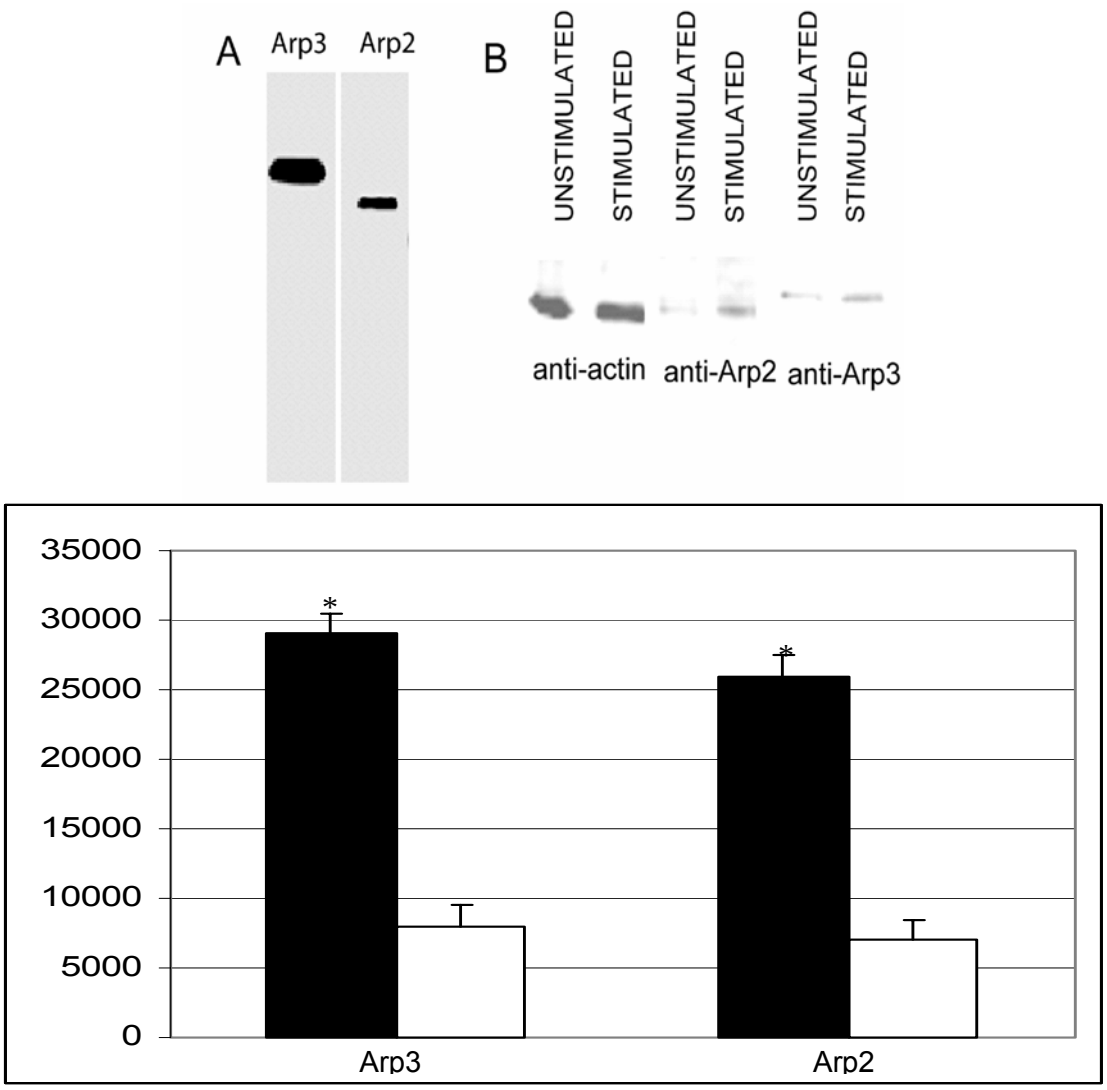

Figure 2.3. Arp2 and Arp3 are upregulated during osteoclastogenesis**.** (A) Human platelet Arp2/3 complex was subjected to SDS-PAGE, blotted to nitrocellulose, and probed with antibodies against Arp3 and Arp2, and the bound antibody was detected by chemiluminescence. B) RAW 264.7 cells were cultures with (black bars) or without (white bars) RANKL. Total protein was extracted and equal amounts of protein were loaded and separated by SDS-PAGE and transferred to nitrocellulose and probed with anti-actin, anti-Arp2 and anti-Arp3 antibodies. Arp2 and Arp3 expression was upregulated during osteoclastogenesis compared with actin. C) Quantitation of four independent blots confirmed upregulation of Arp2 and Arp3 as osteoclasts differentiated. Error bars represent standard error. * $p < 0.05$ by student's t-test.

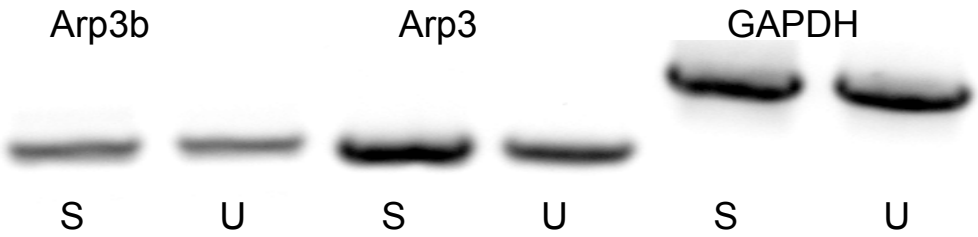

Figure 2.4. The two isoforms of Arp3, Arp3 and Arp3-beta, are present in unactivated and activated osteoclasts. RAW 264.7 cells were cultured with (stimulated) or without (unstimulated) RANKL. Cells were harvested and RNA was obtained using RNAeasy Mini Kit (Qiagen, Valencia, CA). RT-PCR was performed using primers specific to Arp3 and Arp3-beta. Both Arp3 and Arp3-beta were present and are upregulated in response to RANKL stimulation.

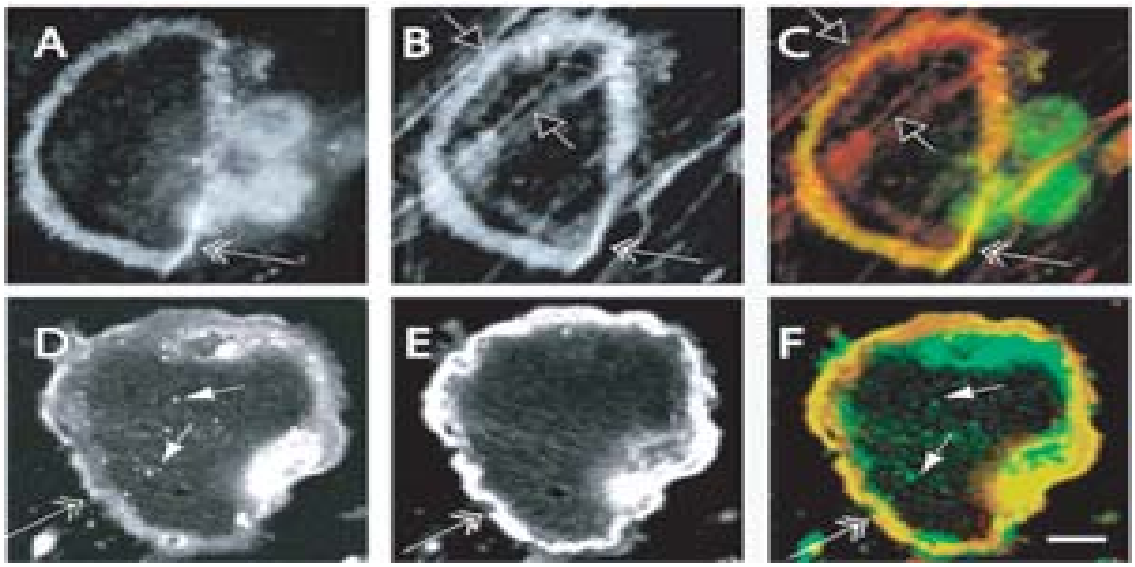

Figure 2.5. Arp2/3 complex is present in the actin rings of osteoclasts. Mouse marrow osteoclasts were loaded onto bovine cortical bone slices (A-C) or glass coverslips (D-E), cultured for 2 days, and fixed and stained with anti-Arp3 antibody (A and D) and phalloidin (B and E). Images were merged (C and F), with Arp3 staining pseudocolored green and phalloidin pseudocolored red. Co-localization of the two is yellow. A-C) A projection of 15 confocal slices (0.5 μm) is shown. The arrow indicated the actin ring. The green staining of the nuclei was the result of cross reactivity by the secondary antibody. Note the yellow staining of the actin ring in the merged image indicating co-localization. D-F) This is an image of a single optical section (0.5 μm) of a mouse marrow osteoclast on a glass coverslip. The small arrow points to Arp2/3-rich spots; the large arrow identifies the actin rings. The size bar is equivalent to 5 μm in A-C and 25 μm in D-F.

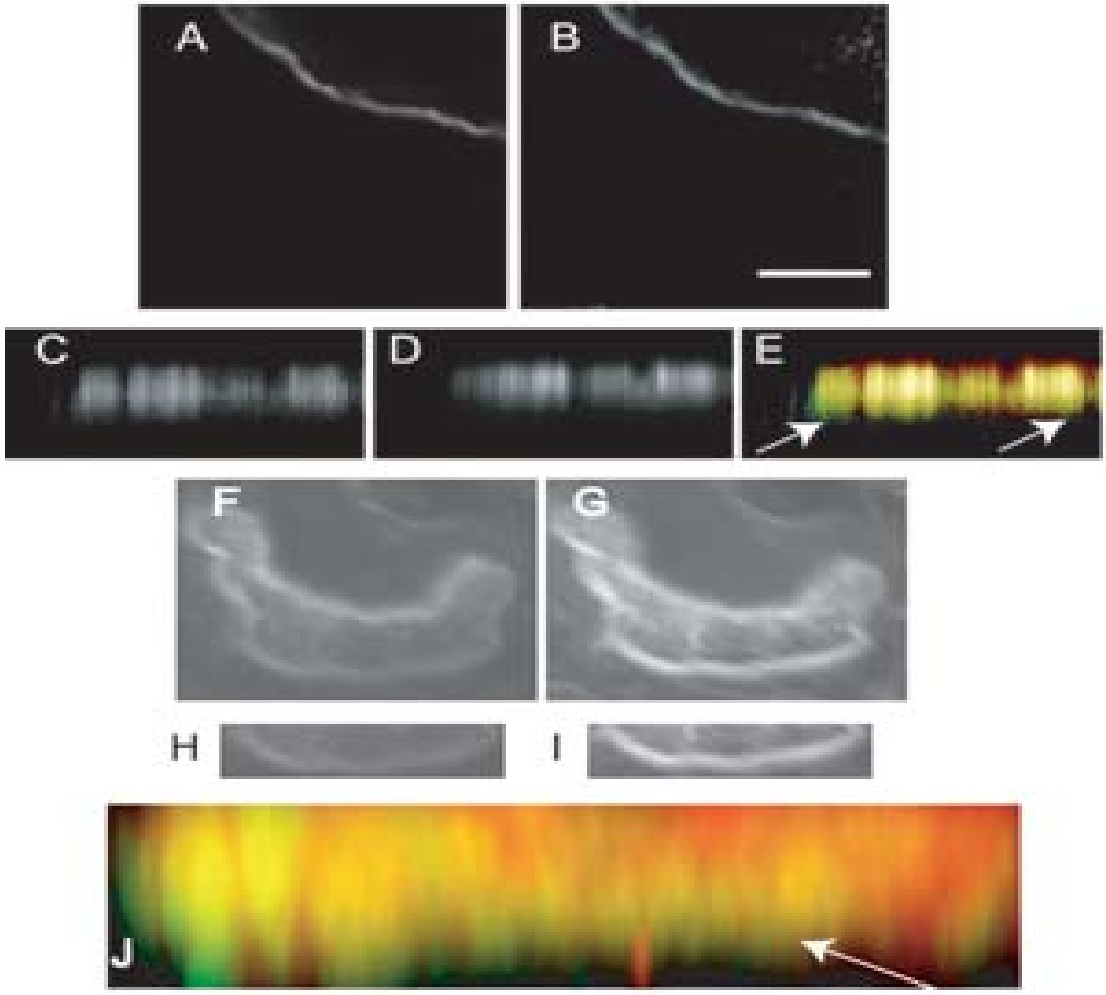

Figure 2.6. Arp2/3 complex is enriched relative to F-actin near the sealing zone. A and B) A projection of the edge of an osteoclast on a coverslip is shown, stained with (A) anti-Arp3 or (B) phalloidin. C-E) The images in A and B were computer rotated 90^{o} to examine the cell in side view. The apical side is down. The podosomal nature of the ring is readily apparent. As shown by the arrows, Arp3 (pseudocolored green) was enriched near the apical surface (the contact area with the coverslip), whereas microfilaments (pseudocolored red) were enriched at the basolateral boundary of the actin ring. Areas of co-localization are yellow. F and G) The image of a resorbing osteoclast on a bone slice is shown. H and I) A section of the actin ring is identified from F and G. J) The images in H and I were then merged and rotated 90^{o} so that the apical surface was down. Arp3 is pseudocolored green and phalloidin is red. As observed in the osteoclast on a glass coverslip, Arp3 is enriched near the apical boundary near the sealing zone (arrow). The size bar is 10 μm in A and B; 5 μm in C-I, and 2 μm in J.

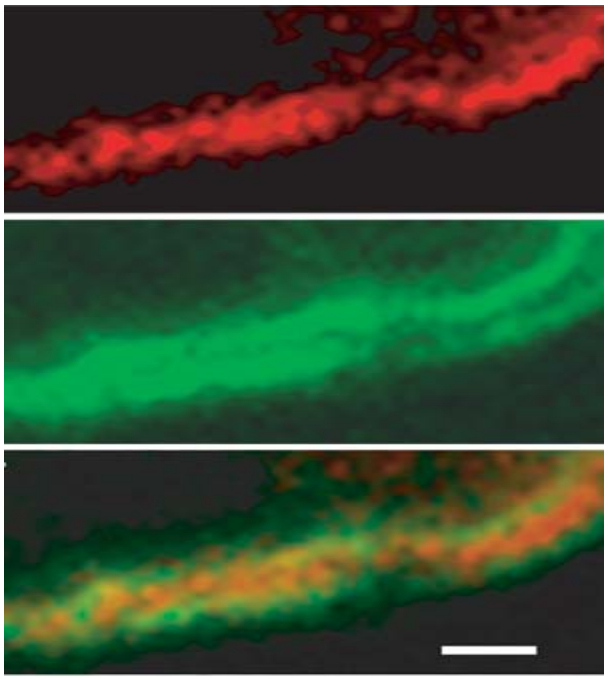

Figure 2.7. Arp2/3 does not co-localize with vinculin in actin rings. RAW 264.7 cells were stimulated with RANKL to differentiate into osteoclast-like cells and fixed and stained with either anti-Arp3 or anti-vinculin. The images were merged. A) Image of actin ring stained with anti-Arp3 and pseudocolored red. B) Image of actin ring stained with anti-vinculin and pseudocolored green. C) Merged image of A and B. Note there is little co-localization between Arp3 and vinculin. The size bar is 3 μm.

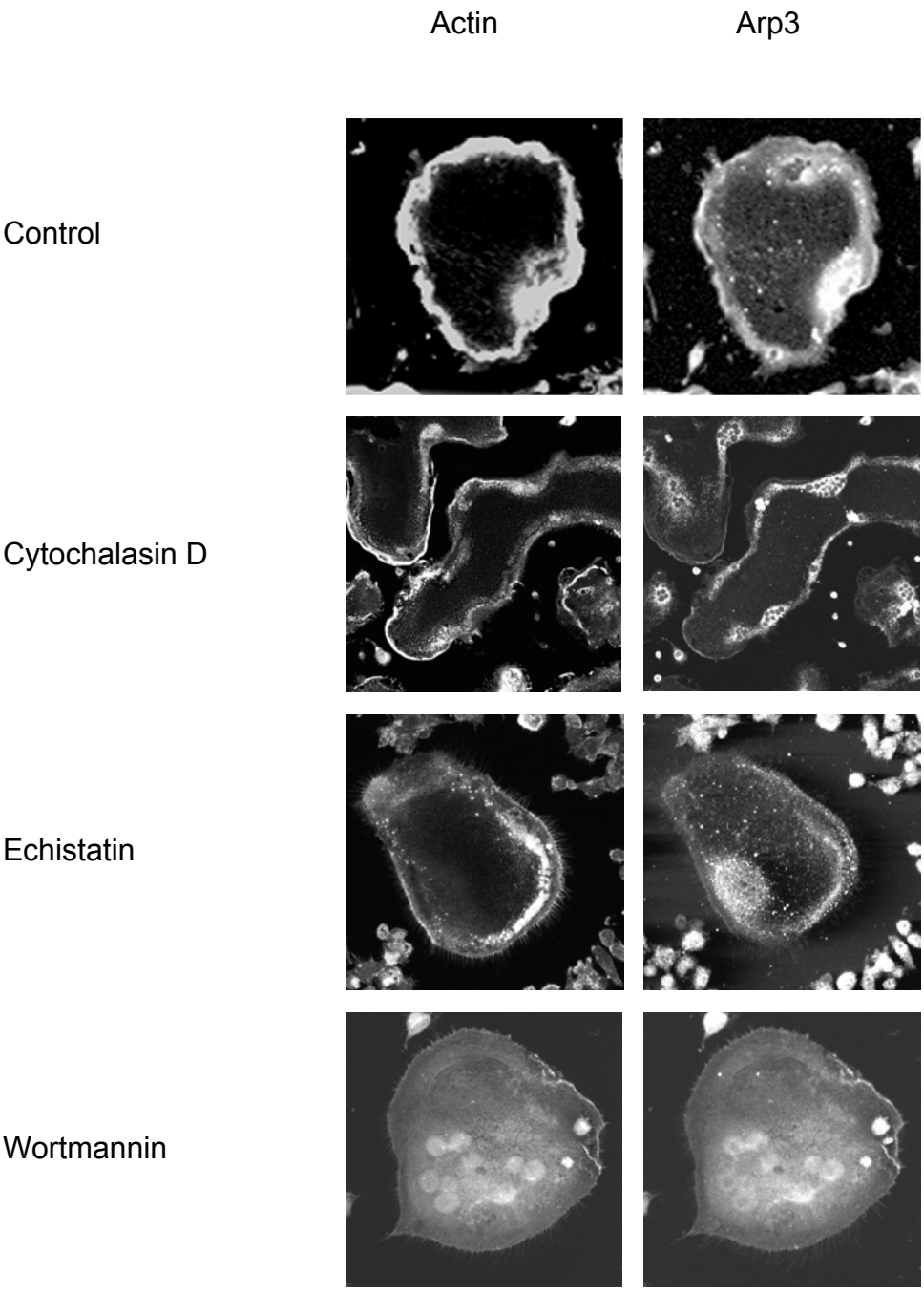

Figure 2.8. Treatment with the chemical agents, cytochalasin D, echistatin and wortmannin, cause a disruption of the actin rings of osteoclasts. Mouse marrow osteoclasts were loaded onto bovine cortical bone slices or glass coverslips, cultured for 2 days, and either untreated or treated with with cytochalasin D, echistatin or wortmannin for 30 minutes and fixed and stained with anti-Arp3 antibody and phalloidin. Note the disruption of the actin ring in all cells but co-localization of the Arp2/3 complex with actin remains stable.

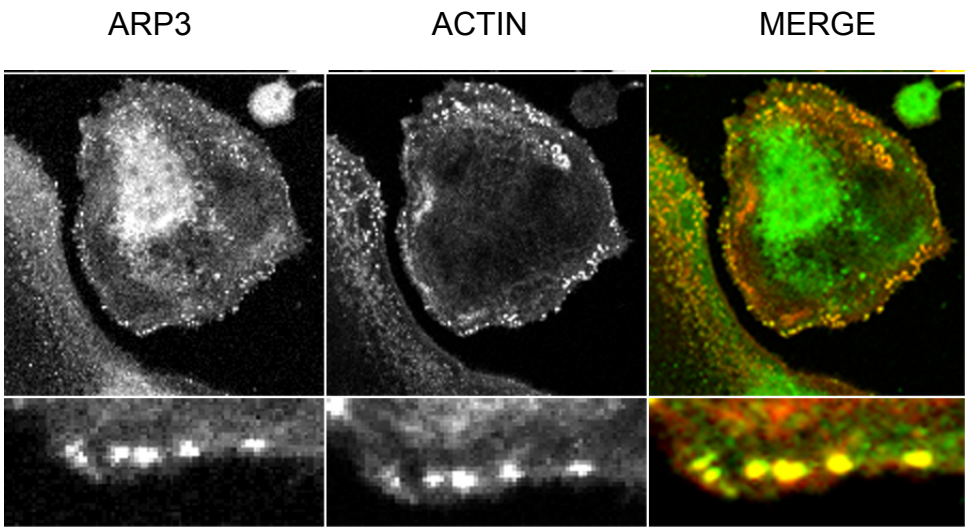

Figure 2.9. Arp2/3 remains co-localized in the actin based podosomal core regardless of actin ring disruption by wortmannin. RAW 264.7 cells were cultured with RANKL until osteoclast-like cells were observed. The cells were then treated with 100 nM wortmannin for 15 mintues, after which they were fixed and stained with either rhodamine phalloidin or anti-Arp3 antibody. Although actin ring structure has been disrupted, Arp3 continues to co-localize with actin in the podosomal core.

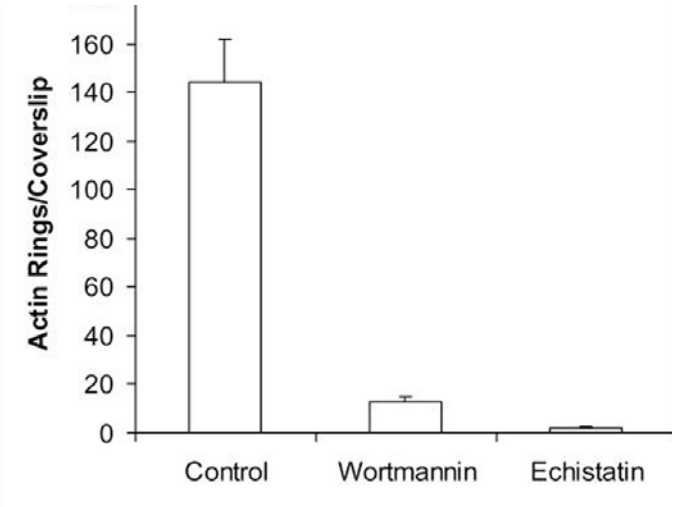

Figure 2.10. Wortmannin and echistatin treatment of osteoclasts results in a decrease in the number of actin rings. Actin rings were counted after either no treatment or treatment with wortmannin or echistatin. A significant decrease in actin rings, more than 90%, was observed after treatment with either inhibitor.

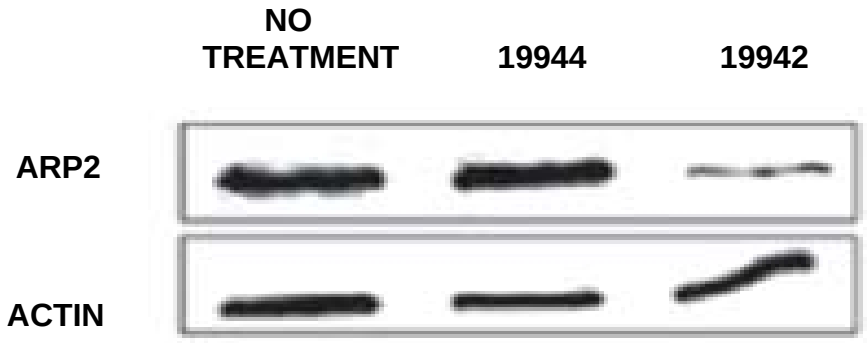

Figure 2.11. siRNA 19942 but not 19944 reduces the Arp2 content of osteoclast-like cell extract 70% after 30 hours compared with actin. RAW 264.7 cells were stimulated with RANKL. Just as large, multinucleated osteoclasts began to appear, cells were transfected as noted. Cells transfected with siRNA 19942, which had proved effective at knocking down Arp2 in preliminary experiments, reduced Arp2 levels dramatically compared with either control cells or cells transfected with an ineffective siRNA 19944.

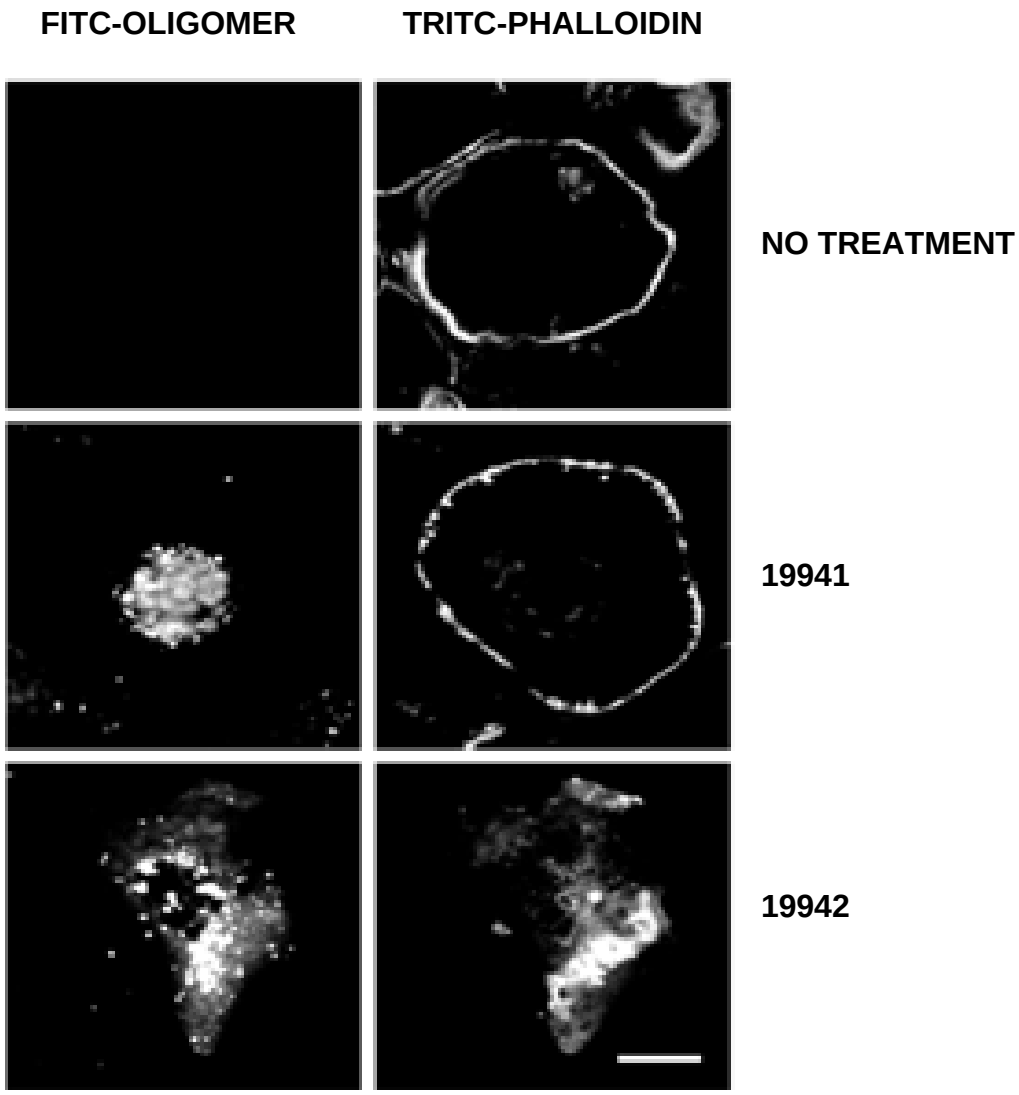

Figure 2.12. Actin rings are disrupted in Arp2 knockdown**.** Untransfected RAW 264.7 osteoclast-like cells or osteoclast-like cells transfected with ineffective siRNA (19941) or effective siRNA (19942) were fixed after 30 hours and examined for the presence of fluorescent oligo marker of transfection (left panels) or F-actin by staining with phalloidin (right panels). The photographs are representative cells. The effective siRNA disrupted the ability of the osteoclasts to form actin rings. The size bar equals 25 μm.

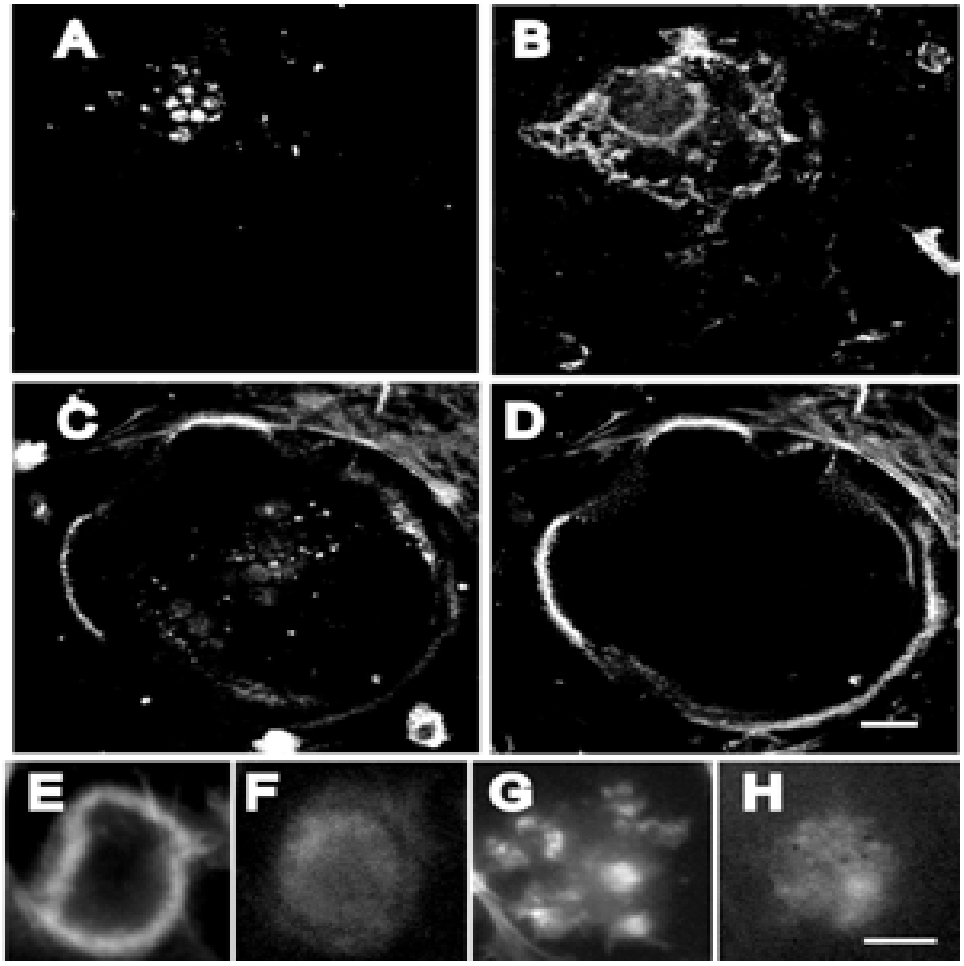

Figure 2.13. Actin rings are disrupted in marrow osteoclasts on coverslips or on bone slices by siRNA directed against Arp2**.** Mouse marrow in tissue culture plates was stimulated with calcitriol for 5 days to produce osteoclasts. These were scraped and loaded onto coverslips (A-D) or bone slices (E-H) and transfected with (A, B, G, and H) 19942 or (C-F) 19941. The cells were stained with phalloidin (B, D, E, and G) or the fluorescent oligomer (A, C, F, and H) was detected. Note that in osteoclasts transfected with the effective siRNA (19942), no actin rings were present. In cells transfected with the ineffective control siRNA (19941), actin rings appeared normal. Standard bar in D is for A-D and represents 10 μm. Standard bar in H is for E-H and represents 10 μm.

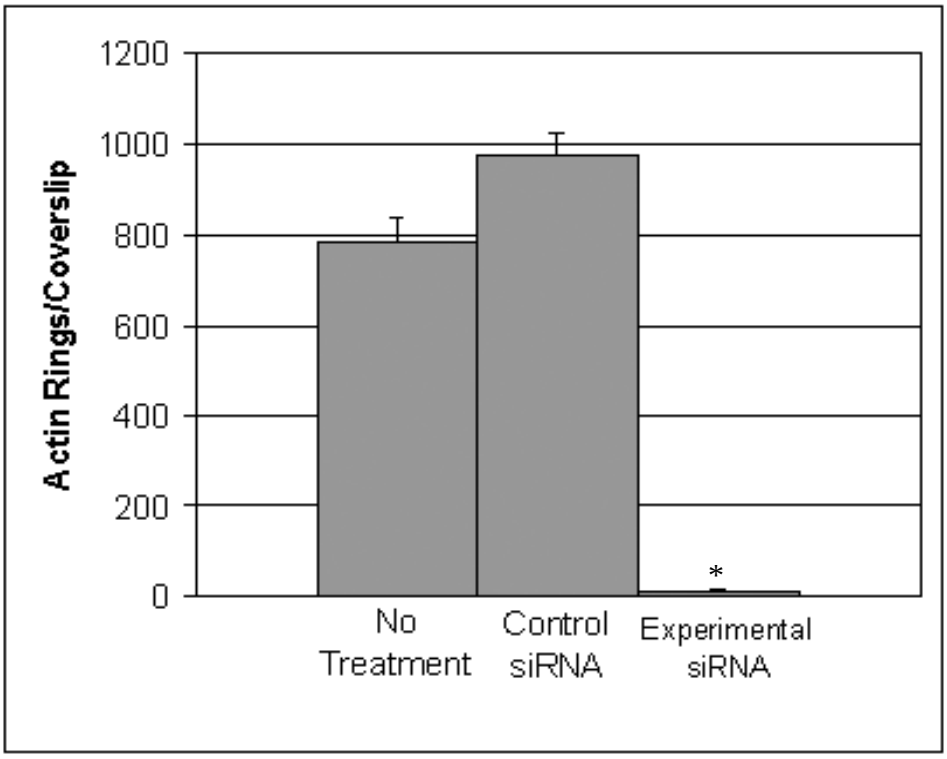

Figure 2.14. Experimental siRNA reduces the number of actin rings on coverslips by over 95%. RAW 264.7 osteoclast-like cells or osteoclast-like cells transfected with no siRNA, ineffective siRNA (19941) or effective siRNA (19942) were fixed after 30 hours and examined for the presence of fluorescent oligo marker of transfection. The actin rings of the cells with the marker of transfection present were counted to quantify changes in the number of actin rings formed. There was a significant decrease in the number of actin rings after treatment with effective siRNA. Error bars represent standard error. * $p < 0.05$ by student's t-test.

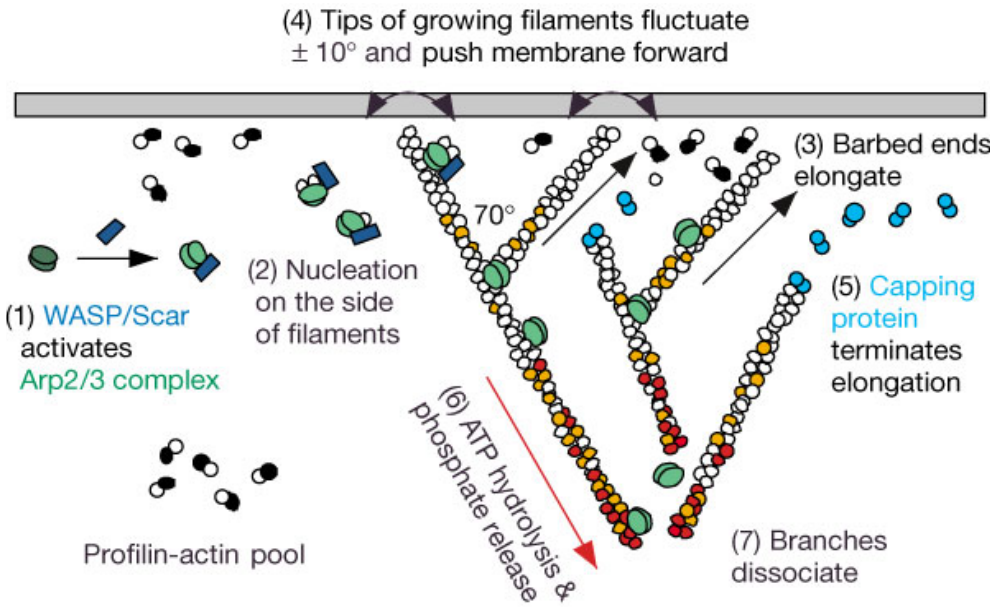

Figure 2.15. Dendritic Nucleation Model. Upon activation of WASP/Scar family proteins, the Arp2/3 complex is activated, resulting in actin polymerization and side-branching of new filaments on existing filaments. As the filaments elongate, they push the membrane forward. Profilactin is required for filament elongation at the barbed ends and may be localized to this region by VASP. (ATP-actin – white; ADP-P-actin – orange; ADP-actin –red; profilin - black) (Blanchoin L. et al. Nature. 2000;404:1007-1011) (37)

Table 2.1. PCR Primers Used for Identification of Arp3 Isoforms. The sequences of primers used for PCR as well as their positions numbered relative to the AUG start site and the expected product size. All primers were designed against murine sequences.

RT-PCR Target	Position of Primers	Size of Product	Sequence of Primers (5'-3")
Arp3	750-769	191 bp	AGAGCACCAGAGAGAGCAGA
	921-940		CACACCACACGGCTACTACA
GAPDH (Control)	380-403	711 bp	CCATGTTTGTGATGGGTGTGAACC
	1068-1091		TGTGAGGGAGATGCTCAGTGTTGG

\

CHAPTER 3
THE ARP2/3 COMPLEX:
A POSSIBLE LINK IN THE TRANSLOCATION OF V-ATPASE TO AND FROM THE RUFFLED MEMBRANE

Introduction

V-ATPase plays a vital role in the osteoclast as it is responsible for acidification of the extracellular compartment segregated by the osteoclast and subsequent demineralization of the bone mineral (11, 12). Mutations in the V1 subunit B1 result in distal renal tubular acidosis accompanied by osteopetrosis (64). In addition, recessive osteopetrosis, with deficient acid secretion, is caused by mutations in the V0 domain or in the chloride channel (64).

The vacuolar proton ATPase is composed of 13 or more different proteins and over 20 subunits and consists of two major functional domains, V_1 and V_o (Figure 3.1) (11-170). The V_1 domain, a peripherally located cytoplasmic section, contains at least eight different subunits (A-H) and contains three catalytic sites for ATP hydrolysis (168). These sites are formed from the A and B subunits (11, 168). The V_o domain, a proton channel, is composed of at least 5 subunits and allows for proton translocation across the ruffled membrane (168).

V-ATPase is present in osteoclast precursors at high levels (171); but upon osteoclastogenesis, the levels of V-ATPase increase significantly and

isoforms selective to the osteoclast are expressed (171, 172). Prior to activation of the osteoclast, the V-ATPase is stored in intracellular cytoplasmic vesicles (23, 50). As the cell is activated, V-ATPase binds to actin and is transported to the ruffled membrane, a specialized region of the plasma membrane. Once a resorption cycle has been completed, the V-ATPase is internalized into the cytosol (173).

V-ATPase binding to F-actin has been identified with the F-actin binding site localized to a profilin-like domain in subunit B (11). This domain is localized to amino acids 23-67 in the B1 subunit and binding is in a direct 1:1 relationship (174). Since there are three B subunits, there are at least three actin binding sites present on the V-ATPase, and two more may be associated with the C subunit as it has also been shown to bind actin (175). It is of note that the levels of actin bound to V-ATPase fluctuate with the resorptive state of the osteoclast. Binding of F-actin to V-ATPase appears to be physiologically controlled with evidence supporting signaling through $\alpha_v\beta_3$ and PI3K activity (12, 52, 163, 175-177).

During translocation of the V-ATPase to and from the ruffled membrane, F-actin and V-ATPase are components of discrete structures termed podosomes (178). There are several lines of evidence supporting the dependency of the cytoskeleton for transportation of V-ATPase to and from the ruffled membrane. The grey lethal mutation (gl), which causes osteopetrosis, results in defective cytoskeletal organization (179). In the majority of cases, a mutation is found in the gene, TCIRG1, which encodes the a3 subunit of the osteoclast V-ATPase

(179). Mutations of this protein may prohibit the V-ATPase from assembling which would be consistent with the lack of ruffled border formation and improper and disorganized localization of V-ATPase (180-182). In addition, the oc/oc "osteosclerotic" mouse shows a lack of association between the cytoskeleton and V-ATPase, hindering the localization of V-ATPase to the ruffled membrane (180-182). This mouse is characterized by extensive bone deformities (180-182). These data support the hypothesis that the detergent insoluble cytoskeleton plays a key role in transportation of the V-ATPase to the ruffled membrane.

As previously stated, the Arp2/3 complex is a central player in the actin-based motility of certain pathogens (144-147). The Arp2/3 complex has been shown to co-localize with actin in the actin ring and as a vital component of the actin ring of osteoclasts. In addition, the Arp2/3 complex responds by various proteins, such as cortactin and VASP, which are members of various signal transduction pathways. From this interaction with actin dynamics, its ability to be regulated by signal transduction mechanisms, and its sequence homology with actin, it might be hypothesized that the Arp2/3 complex may bind V-ATPase, as actin does, and function as a possible player in the transportation of V-ATPase to and from the ruffled membrane.

In this study, we tested for an association between V-ATPase and the Arp2/3 complex. Since no association could be determined, other potential V-ATPase binding partners were identified.

Materials and Methods

V-ATPase/Arp2/3 binding assay

To determine if the Arp2/3 complex binds to V-ATPase, a protein binding assay was performed. Twenty five μl of a maltose binding protein (MBP) -B1 fusion protein (B1-109) was incubated with 25 μl of purified Arp2/3 complex for 1 hour. Amylose beads, which are an affinity matrix used to isolate proteins fused to MBP, were prepared by sequential washes in column buffer followed by F-buffer. The amylose beads (25 μl) were then added to the Arp2/3-fusion protein mixture and incubated for 30 minutes. The solution was centrifuged at 13,000 rpm for 2 minutes. The supernatant was collected, and the beads were washed with F-buffer. This was repeated three times. The beads were then incubated with 25 μl of 100 mM maltose for 10 minutes and eluted by centrifugation. The supernatant was separated by SDS-PAGE and stained with Coomasie Blue.

Immunoprecipitation was performed to identify binding of Arp2/3 with V-ATPase. The MBP-tagged B1 fusion protein was incubated with purified Arp2/3 complex and protein G beads (to allow for clearance of any non-specific binding). The mixture was centrifuged and the supernatant collected. Anti-maltose binding protein antibody was incubated with the supernatant for 30 minutes. Protein G beads were added and incubated for 10 minutes. The mixture was centrifuged and the supernatant collected (to determine in which fraction the original sample was). The pellet was washed three times. The pellet was incubated with SDS and centrifuged at 13,000 rpm for 2 minutes. The supernatant was then separated by SDS-PAGE followed by western transfer. The nitrocellulose blots

were then incubated with anti-Arp2 antibodies for one hour, washed three times, incubated with anti-goat HRP conjugated secondary antibody, washed three times, and incubated with Super Signal Dura West Chemiluminescent Substrate (Pierce, Rockford, IL). The blots were then viewed on a Fluorochem 8000 (Alpha-Innotech, San Leandro, CA).

PCR to identify other actin associated proteins involved in V-ATPase translocation and actin ring dynamics

To identify other key proteins involved in osteoclastogenesis, RNA was extracted from RANKL differentiated RAW 264.7 cells as well as from unstimulated RAW 264.7 cells using RNAeasy Mini Kit and quantified by spectrophotometer. The sequences for WASP, n-WASP, VASP, Cortactin, and Arp3 were obtained from Gen Bank. Primers were designed as described in Table 3.1. For standard RT-PCR, 3μg of total RNA was annealed to an oligo-dt primer and first strand cDNA synthesis was performed using Thermoscript RT-PCR System (Invitrogen, Carlsbad, CA) following manufacturer's directions. One-twentieth of the cDNA was subjected to amplification by PCR using the primers listed in Table 3.1. PCR was performed under the following conditions: 95^{o}C for 2 minutes, then 35 cycles of 90^{o}C, 30 seconds; 58^{o}C, 30 seconds; 72^{o}C, 30 seconds. One-half of the PCR product was separated on 0.5% agarose gel with ethidium bromide staining for 1 hour. Images were detected using UV transillumination on a Fluorochem 8000 (Alpha-Innotech, San Leandro, CA).

Immunoprecipitation with the B subunit of V-ATPase suggests a possible direct linkage between VASP and V-ATPase.

To identify possible binding partners with the B2 subunit of V-ATPase, cell lysates were extracted from RANKL stimulated RAW 264.7 cells. The cell lysates were subjected to high speed centrifugation to pellet actin and to avoid the presence of actin filament complexes in the immunoprecipitate. The B2 antibody was biotinylated using EZ-link Sulfo-NHS-LC-biotinylation kit (Pierce, Rockford, IL). The lysates were incubated with either B2-biotinylated or B2 antibody. The B2 (non-biotinylated) antibody was used as a control. Complexes were pulled down with streptavidin agarose, which affinity purifies biotin labeled proteins. The agarose was washed and eluted with loading buffer. The elution was separated by SDS-PAGE and western transfer. The nitrocellulose blots were then probed with antibodies directed against various actin associated proteins such as N-WASP, cortactin, VASP, WASP, and Arp3. The blots were washed and incubated with secondary antibodies and incubated with Super Signal Dura West Chemiluminescent Substrate (Pierce, Rockford, IL). The blots were then viewed on a Fluorochem 8000 (Alpha-Innotech, San Leandro, CA).

Results

The B1 (1-106) subunit of V-ATPase does not bind purified Arp2/3 complex.

Purified Arp2/3 complex and the B1(1-106) maltose binding protein fusion protein, which contains the actin binding site, were incubated together. After being separated on amylose resin and eluted with maltose, the elution was separated by SDS-PAGE and Western transfer. The blots were then probed with

either anti-B1 or anti-Arp3 antibody. Only the B1 subunit was pulled down, suggesting that the Arp2/3 complex does not bind to V-ATPase in the actin binding region (Figure 3.2 and 3.3).

Cortactin is preferentially upregulated at the transcriptional level during osteoclastogenesis

To identify other actin associated proteins involved in V-ATPase translocation and actin ring dynamics, PCR was performed using primers to detect changes in gene expression in several actin-associated proteins during osteoclastogenesis. Unlike the other proteins tested, cortactin mRNA was the only gene preferentially upregulated during osteoclastogenesis, with a complete lack of detection prior to treatment of RAW 264.7 cells with RANK-L (Figure 3.4). This was expected based on a previous publication which identified an upregulation of cortactin protein in chicken osteoclasts. These data identify upregulation occurs at the transcriptional level.

Vasodilator stimulated phosphoprotein (VASP) is identified to have a possible interaction with V-ATPase.

A signal transduction assay was peformed using a standard array by Hypromatrix (work done by Sandra Vergara). The membrane was incubated with RANKL-induced RAW 264.7 whole cell extract. The membrane was then incubated with a biotinylated-B2 antibody, washed and labeled with a secondary antibody. Chemiluminescent substrate was applied and the membrane was viewed by a Fluorochem 8000. Among 29 responsive proteins, vasodilator

stimulated phosphoprotein was identified as having an interaction with the B2 subunit (Figure 3.5).

Immunoprecipitation with the B subunit of V-ATPase suggests a possible direct linkage between VASP and V-ATPase.

To identify possible binding partners with V-ATPase, cell lysates were extracted from RANKL stimulated RAW 264.7 cells. The cell lysates were subjected to high speed centrifugation to remove any contamination by actin complexes in the immunoprecipitate. The lysates were incubated with either biotinylated-B2 or non-biotinylated B2 antibody. Complexes were pulled down with streptavidin agarose, to isolate any protein complexes bound to the biotinylated antibody. The non-biotinylated B2 antibody was used as a control. Efforts to pull down cortactin in immunoprecipitations of V-ATPase were not successful; and of all the proteins tested, VASP was identified to form a complex with the B2 subunit of V-ATPase (Figure 3.6), suggesting a potential complex that includes VASP, cortactin and V-ATPase.

Discussion

The actin binding site on V-ATPase has been identified to amino acid sequence 23-67 of the B1 subunit of the V-ATPase (183). Based on the sequence homology between actin and the Arp2/3 complex, we hypothesized that V-ATPase might bind the Arp2/3 complex. Experiments with both binding assays and immunoprecipitation experiments with the B1 fusion protein failed to show a direct linkage between V-ATPase and the Arp2/3 complex. However, this result does not confirm an absence of a direct interaction between the two

proteins. Binding of the Arp2/3 complex may occur through a different amino acid sequence than that of the fusion protein or the Arp2/3 complex may not be in the correct structural conformation to bind to the V-ATPase in the performed experiments. Isolation of purified V-ATPase was attempted to determine binding with the Arp2/3 complex but has not been successful thus far.

As identification of a direct interaction between V-ATPase with Arp2/3 could not be established, research focused on the identification of other proteins which could play pivotal roles in osteoclast function. Semi-quantitative PCR analysis of several actin related proteins was performed to determine if there were any changes during osteoclastogenesis. Cortactin was identified as being preferentially upregulated during osteoclastogenesis at the transcriptional level (184), indicating a possible key role in actin ring formation or translocation of V-ATPase to the ruffled membrane. This finding is not surprising as previous research in chicken osteoclasts has shown the cortactin upregulation at the protein level (184); however, our findings identify for the first time that the upregulation occurs at a transcriptional level. Cortactin is involved in the activation and stabilization of actin based networks, inhibiting their disassembly (135, 185-187). Cortactin can bind and activate the Arp2/3 complex through binding the Arp3 subunit (186, 187). Cortactin, n-WASp, and Arp2/3 form a synergistic, ternary complex to initiate actin polymerization (186, 188). Although no additional proteins were found to have significant differences in levels of mRNA before and after osteoclastogenesis, real-time PCR would be of value in

determining minor variations in mRNA concentration not detectable by traditional PCR.

In addition to cortactin, we sought to identify other actin binding proteins that could have a possible interaction with V-ATPase. A signal transduction antibody array was performed by Sandra Vergara (University of Florida, Gainesville, FL) to determine possible interactions between signal transduction proteins and V-ATPase from RANK-L induced RAW264.7 whole cell extracts. The results from this array indicated that Vasodilator Stimulated Phosphoprotein might be linked with V-ATPase. Further immunoprecipitation experiments show that VASP is pulled down in a complex with the B2 subunit of V-ATPase. VASP plays a key role in actin based motility and is localized predominantly at focal adhesions, cell/cell contacts and regions of highly dynamic actin reorganizations such as podosomes (151, 185). VASP can bind directly to G-actin and F-actin as well as recruit profilactin complexes to the site of actin polymerization. In addition, VASP is known to enhance Arp 2/3 activity and prevent capping proteins. VASP is phosphorylated in response to protein kinase A (PKA) and protein kinase G (PKG) (189, 190). The ability of VASP to be phosphorylated allows it to be both a positive and negative regulator of actin polymerization. Calcitonin induces alterations in the cytoskeleton of the osteoclast through the protein kinase A pathway (191, 192). It is plausible that the disruption of the actin cytoskeleton by calcitonin could be mediated by VASP. Phosphorylation of VASP has also been shown to diminish F-actin binding, suppressing actin nucleation as well as inhibiting Arp2/3 triggered actin polymerization; thus, it can

be a negative regulator of actin polymerization (185). Thus, VASP may play an important role in the regulation of the translocation of V-ATPase to and from the plasma membrane.

In summary, the Arp2/3 complex did not bind the same amino acid sequence of the B1 subunit of V-ATPase as did actin. Further studies are required to determine if binding exists at another sequence. Two additional proteins, cortactin and VASP, were identified as having possible key roles in osteoclast function. Cortactin was found to be preferentially upregulated in response to RANKL stimulation while VASP was found to associate with the B2 subunit, either directly or indirectly through other V-ATPase subunits or other V-ATPase bound proteins.

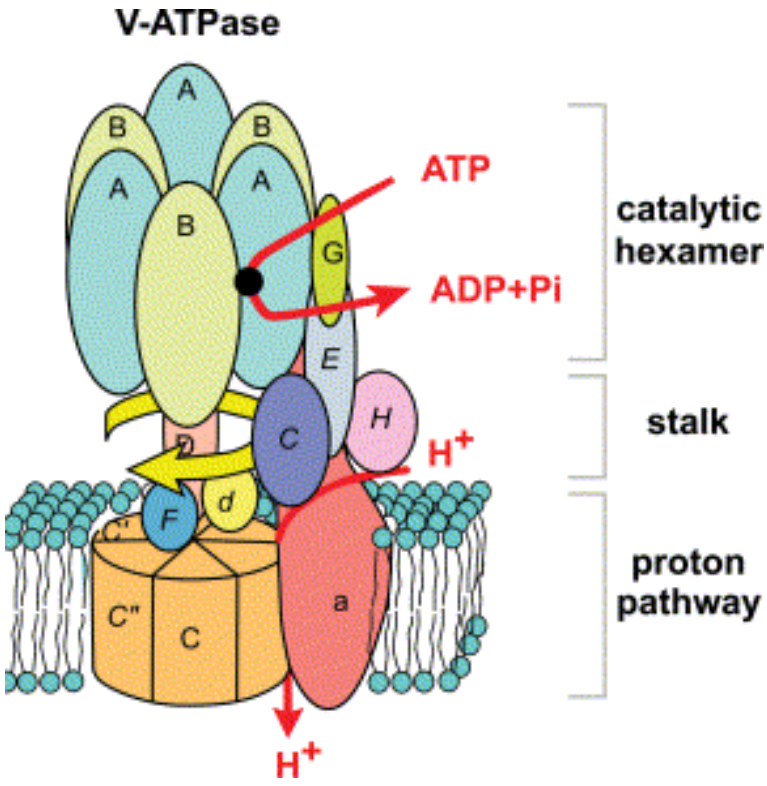

Figure 3.1. The structure of V-ATPase**.** The vacuolar proton ATPase is composed of 13 or more different proteins and over 20 subunits and consists of two major functional domains, V_1 and V_o. The V_1 domain, a peripherally located cytoplasmic section, contains at least eight different subunits (A-H) and contains three catalytic sites for ATP hydrolysis. These sites are formed from the A and B subunits. The V_o domain, a proton channel, is composed of at least 5 subunits and allows for proton translocation across the ruffled membrane. (Sun-Wada et al. Biochimica et Biophysica Acta. 2004; 1658: 106-114) (168)

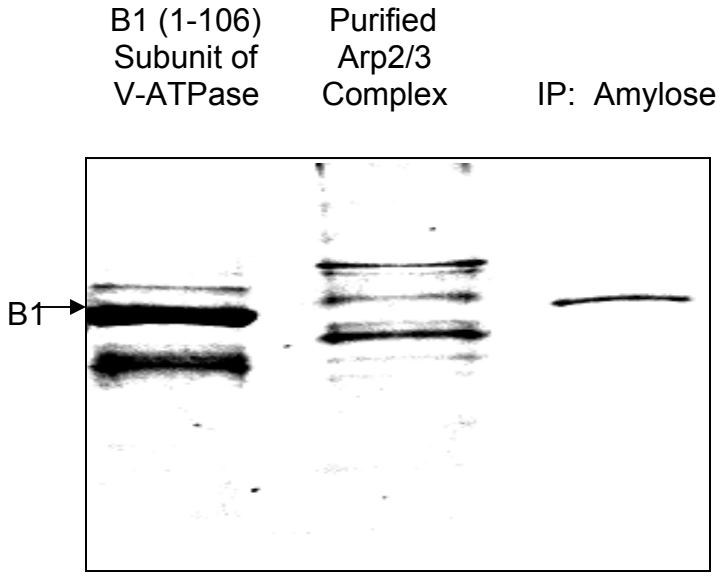

Figure 3.2. The B1 (1-106) fusion protein of V-ATPase and the Arp 2/3 complex do not show a direct interaction by binding assay. The B1-MBP fusion protein and the Arp2/3 complex were incubated together. The sample was then run on amylose resin to bind the maltose binding protein. The column was then eluted with maltose. The samples were separated by SDS-PAGE and stained with Coomasie. The B1 subunit was pulled down in the amylose column but Arp3 was not, indicating a lack of binding between the two proteins.

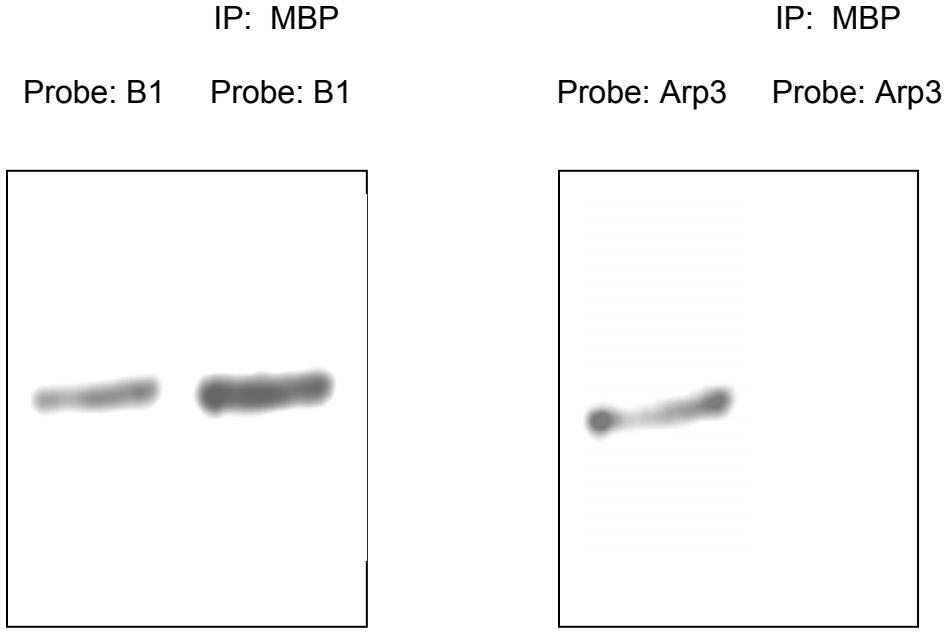

Figure 3.3. The B1 (1-106) fusion protein of V-ATPase and the Arp 2/3 complex do not show a direct interaction by immunoprecipitation of B1 subunit. The B1-MBP fusion protein and the Arp2/3 complex were incubated together. The sample was then incubated with a maltose binding protein antibody. The sample was then immunoprecipitated with protein G beads which bind the antibody. The beads were washed and eluted with sodium dodecyl sulfate. The elution was then probed using the B1 or Arp3 antibodies. B1 was pulled down by the protein G beads but Arp3 was not, indicating a lack of binding between the two proteins.

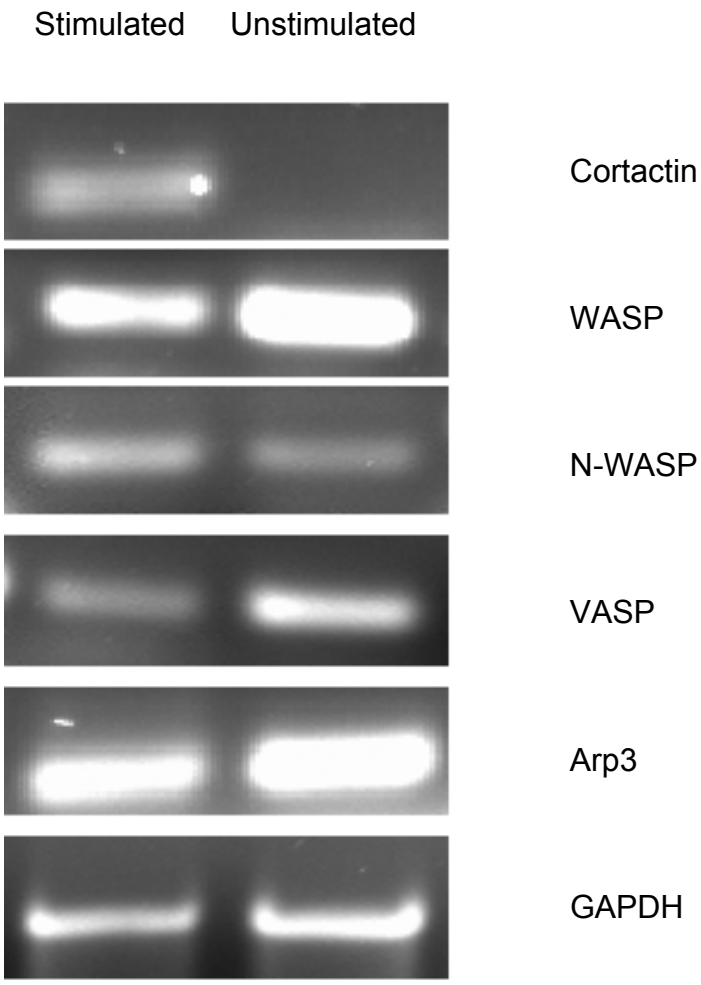

Figure 3.4. Cortactin is preferentially upregulated during osteoclastogenesis as identified by PCR. RAW 264.7 cells were cultured with (stimulated) or without (unstimulated) RANKL. Cells were harvested and RNA was obtained using RNAeasy Mini Kit. RT-PCR was performed using primers specific to cortactin, WASP, N-WASP, VASP and GAPDH (control). Cortactin was the only actin-associated protein preferentially upregulated in response to osteoclastogenesis.

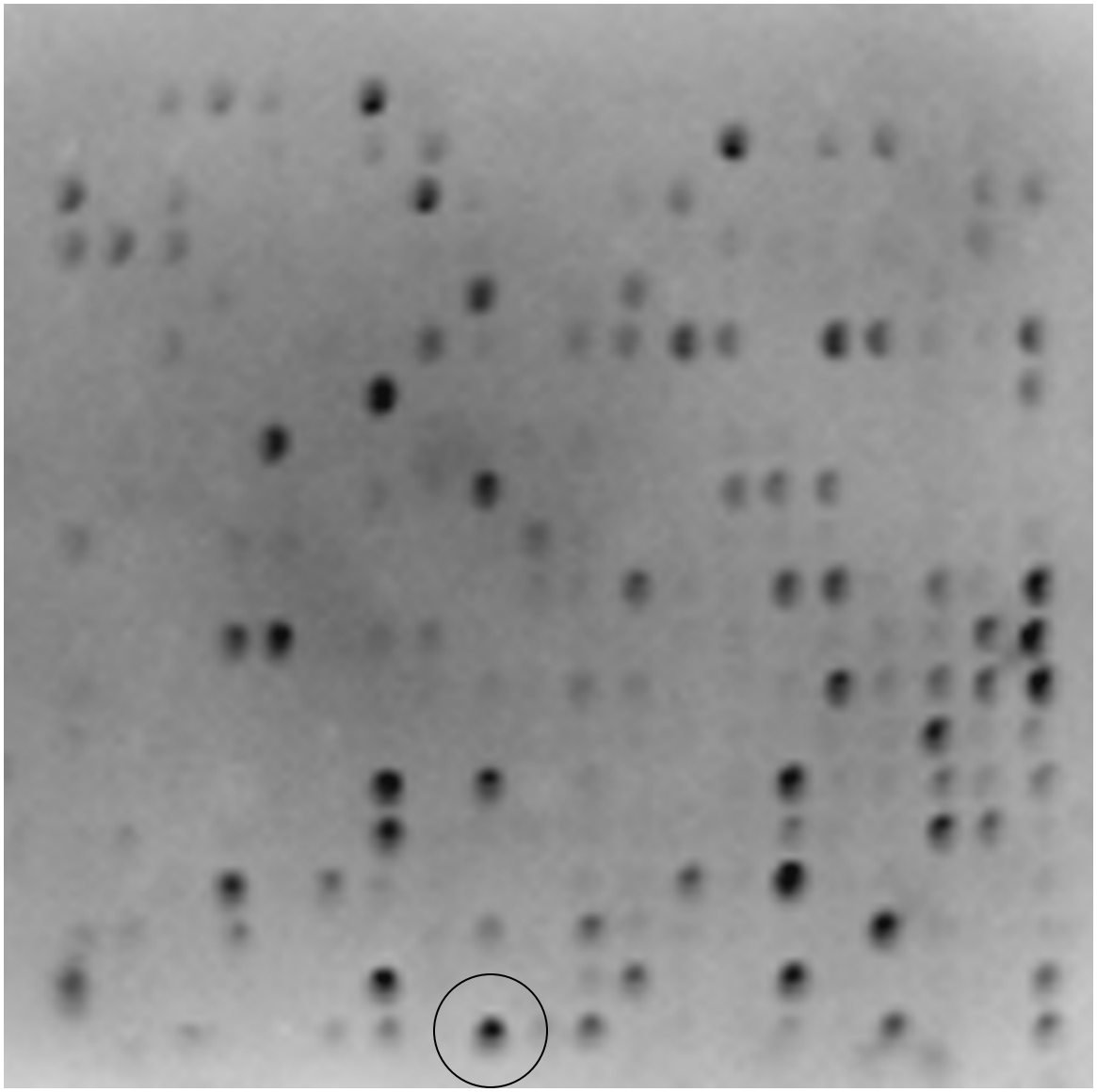

Figure 3.5. Vasodilator stimulated phosphoprotein is identified to have a possible interaction with V-ATPase. Signal Transduction Array by Hypromatrix was probed with biotinylated B2 antibody (work by Sandra Vergara) to identify possible signal transduction molecules which may interact with V-ATPase. Vasodilator stimulated phosphoprotein, an actin associated protein, was identified as having a possible interaction.

Figure 3.6. Immunoprecipitation experiments with the B subunit of V-ATPase Suggests a Possible Direct Linkage between VASP and V-ATPase. RANKL stimulated RAW 264.7 cell lysates were incubated with biotinylated B2 antibody, pulled down on streptavidin agarose, separated by SDS-PAGE and western transfer, and probed with the antibodies of various actin related proteins. Of all the proteins tested, only VASP was pulled down in complex with the B2 subunit of the V-ATPase.

Table 3.1. PCR Primers Used for Identification of Arp2/3 Related Proteins. The sequences of primers used for PCR as well as their positions numbered relative to the AUG start site and the expected product size. All primers were designed against murine sequences.

RT-PCR Target	Position of Primers	Size of Product	Sequence of Primers (5'-3")
VASP	529-548	227 bp	ATTCGGGGTGTCAAGTACAA
	736-755		TTCTGTTGTTCCAGCTCCTC
Cortactin	1442-1461	186 bp	CCTGAGCCTGACTACAGCAT
	1608-1627		GTAGTCATACAGGGCGATGG
n-WASp	425-444	197 bp	GCCAATGAAGAAGAAGCAAA
	602-621		TCTTTGGTGTGGGAGATGTT
WASP	92-111	242 bp	ACATTCCTTCCAACCTCCTC
	314-333		CAGCTCCTGTTCCCAGAGTA
Arp3	750-769	191 bp	AGAGCACCAGAGAGAGCAGA
	921-940		CACACCACACGGCTACTACA
GAPDH (Control)	380-403	711 bp	CCATGTTTGTGATGGGTGTGAACC
	1068-1091		TGTGAGGGAGATGCTCAGTGTTGG

CHAPTER 4
THE ROLE OF CORTACTIN IN OSTEOCLASTOGENESIS

Introduction

Cortactin is a monomeric, long, flexible protein (186) with a multidomain structure consisting of an acidic domain at the amino terminus, followed by 6 and 1/2 tandemly repeated 37 amino acid segments, a helical region, a proline rich region, and a Src homology 3 (SH3) domain at the carboxyl terminus (135, 136, 186). The multidomain structure of cortactin allows a multitude of interactions. Cortactin binds directly to F-actin through sequences in the tandem region while binding to the Arp2/3 complex occurs at the amino terminus (136, 186, 188). Various signaling proteins bind the c-terminal proline rich and SH3 domains (135, 185, 188). Cortactin is a physiologically significant substrate for tyrosine phosphorylation by src kinases (135). This is important because actin ring formation requires the activity of pp60c-src (193, 194). Mutations in c-src in mice results in osteopetrosis and failure of podosome formation (19). Faciogenital dysplasia protein 1 (Fgd1), a CDC42 guanine nucleotide exchange factor, also binds the SH3 domain of cortactin (195). This association allows proper localization of Fgd1 to the actin cytoskeleton (196). Mutations in Fgd1 are implicated in the human disease faciogenital dysplasia (197, 198). The pathology of this disorder includes bone abnormalities.

Cortactin is involved in the activation and stabilization of actin based networks (185, 186). Initially, the role of cortactin was hypothesized as a result of its localization to the same regions as Arp2/3 and n-WASP in vesicles, podosomes, and the actin based rocket tails of *Listeria* (135, 186, 188, 199). The function of cortactin as a regulator of the Arp2/3 complex is two fold. First, cortactin can bind and activate the Arp2/3 complex through binding the Arp3 subunit (186, 188), although its activation potential is four to five fold lower than that of the WASP family proteins (135, 187). Second, cortactin stabilizes Arp2/3 induced branched actin networks, inhibiting their disassembly (135, 187, 200). Recent studies suggest that cortactin, N-WASP, and Arp2/3 form a synergistic, ternary complex to initiate actin polymerization as depicted in Figure 4.1 (186, 188). In this model, N-WASP activates nucleation by interacting with F-actin and the Arp2 and p40 subunits while cortactin stabilizes the branching points by binding to F-actin and the Arp3 subunit (135, 187, 200).

Cortactin's main role may involve the carboxy terminal SH3 domain. This domain allows interactions with various signaling molecules, including src kinases (186, 200). The tyrosine phosphorylation of cortactin occurs in response to integrin ($\alpha v\beta 3$) binding in endothelial cells (200). This is of note as the integrin, $\alpha v\beta 3$, is also the major integrin of mature osteoclasts (55, 56). Cortactin may be responsible for organization of receptor signaling in the region of the sealing zone as it possesses both proper spatial and temporal localization with newly forming actin networks (186, 188, 200).

Cortactin may not be a direct activator of the Arp2/3 complex. However, the multidomain structure of cortactin, in conjunction with its distribution in dynamic cortical actin structures, may allow it to bridge regions of actin reorganization with receptor signaling complexes, protein tyrosine kinases, and/or to recruit proteins that may positively or negatively regulate actin polymerization (186, 188, 200).

Cortactin was previously identified as being preferentially upregulated during osteoclastogenesis. In this study, our objective was to identify the localization of cortactin in the osteoclast and to determine its requirement for actin ring formation.

Materials and Methods

Western blot analysis with quantitation of cortactin

Anti-cortactin antibodies were obtained from Upstate Biotechnology (Charlottesville, VA). RAW 264.7 cells were grown as previously described, plated on 6 well plates, and either left unstimulated or stimulated with RANKL. Cell lysates were collected from both the control and treated cells. Cells were washed twice with ice cold PBS and scraped from the plates. The cells were then detergent solubilized in 0.2% Triton X-100 in PBS. Equal amounts of the lysates were separated by SDS-PAGE, followed by Western Transfer. The nitrocellulose blots were then incubated with anti-cortactin antibodies for one hour, washed three times, incubated with HRP conjugated secondary antibody, washed three times, and incubated with Super Signal Dura West Chemiluminescent Substrate (Pierce, Rockford, IL). The blots were then viewed

on a Fluorochem 8000 (Alpha-Innotech, San Leandro, CA), and quantitation was performed by Spot Densitometry (Fluor-Phor Software, Alpha-Innotech, San Leandro, CA). The integrated density values (IDV) were obtained (white = 65535, black = 0). Background values were subtracted, and the intensities were normalized against the value of actin in the sample. The values were then compared between stimulated and unstimulated cells. The stimulated and unstimulated values were statistically analyzed using the paired t-test, with statistical significance (p) being less than 0.05.

Co-localization of cortactin with actin and Arp3

Cell culture was performed as previously described for RAW 264.7 cells and mouse marrow osteoclasts. To determine the co-localization of cortactin with actin in the actin ring, osteoclasts were fixed in 2% formaldehyde, detergent-permeabilized with 0.2% Triton X-100 in PBS for 10 minutes, washed in PBS and blocked in PBS with 2% BSA (bovine serum albumin) for one hour. Actin filaments were stained with TRITC phalloidin. Cortactin was probed with an anti-cortactin monoclonal antibody (Upstate Biotechnology). Subunit B2 of V-ATPase was detected with an anti-B2 polyclonal antibody (34). Bound antibodies were detected by labeling with CY2 tagged anti-mouse secondary antibody. Osteoclasts were visualized using the MRC-1024 confocal laser scanning microscope and LaserSharp software (Bio-Rad, Hercules, CA). Images were taken in sequential series to eliminate any overlap of emission and analyzed by confocal assistant software.

Immunoprecipitation of actin associated proteins using a GST-cortactin construct

To determine the interaction of cortactin with actin associated proteins in osteoclasts, Glutathione S-transferase (GST)- cortactin prokaryotic expression construct GST-cortactin was obtained from Scott Weed, Ph.D. (West Virginia University, Morgantown, WV). The GST construct was transformed into Escherichia coli strain DH5α. The fusion protein was purified by induction of the bacterium with isopropyl-1-thio-b-D-galactopyranoside. The fusion protein was run on a glutathione-Sepharose 4B column and eluted with 10 mM reduced glutathione in lysis buffer. Cell lysates were obtained from RANKL stimulated RAW 264.7 cells as described previously. Prior to incubation, the cell lysates were centrifuged at high speed to remove any actin to prevent misleading results. The GST-fusion protein conjugated to Sepharose was incubated with cell lysates from RANKL stimulated cells. As a control, Sepharose without the GST-cortactin fusion protein was also incubated with the cell lysates from RANKL stimulated cells. The Sepharose was centrifuged and washed twice with binding buffer lacking ATP. Bound proteins were visualized by Western blotting with anti-Arp3, anti-VASP, anti-E subunit of V-ATPase, anti-WASP (Santa Cruz), and anti-actin (Sigma) antibodies after SDS-PAGE.

Knocking down gene expression of cortactin using siRNA

Five single interfering RNA (siRNA) duplexes to murine cortactin (accession no. NM_007803) were designed and produced by Sequitur (Natick, MA): 120648 (targeting bp 626-644) anti-sense 5'-UCUUGUCUACACGGUC

AGCTT-3', sense 5'-GCUGACCGUGUAGACAA GATT-3'; 120649 (targeting bp 919-937) antisense 5'- GAAACCAGUCUUAUAGUCUTT, sense 5'- AGACUAUA AGACUGGUUUCTT-3'; 120650 (targeting bp 1169-1187) antisense 5'-UAGCACGGAUAUUACUGGUTT-3', sense 5'-ACCAGUAAUAUCCGUGCUATT-3'; 120651 (targeting bp 673-691) antisense 5'-AGACUCAUGCUUCUCCG UCTT-3', sense 5'-GACGGAG AAGCAUGAGU CUTT -3'; 120652 (targeting bp 830-848), antisense 5'-UCUGCACACCAAACUUUCCTT-3', sense 5'-GGAAAG UUUGGUGUGC AGATT-3'; 120653 (control) antisense 5'-UGGUCAUUAUA GGCACGAUTT-3', sense 5'-AUCGUGCCUAUAAUGACCATT-3'. Initial experimentation showed only siRNA 120649 capable of downregulating cortactin; the other siRNAs were used as ineffective controls. In addition, a siRNA known to downregulate cortactin was obtained (Ambion part no. 60931, targeting exon 5) as well as both positive (GAPDH) and negative controls. RANKL stimulated RAW 264.7 cells on glass coverslips in 24 well plates were not transfected or transfected with either 150 nM of the experimental or control siRNA and 2μg/ml Lipofectamine 2000 (Invitrogen) in Opti-MEM media supplemented with RANKL on day 4 of differentiation (at the appearance of multinucleated cells) and monitored for siRNA uptake. A fluorescent oligomer (part no. 2013; Sequitur) was added for uptake assessement. Six hours after transfection, the media was replaced with DMEM with fetal bovine serum and RANKL. The cells were incubated for 48 hours at 37^{o}C in a CO_2 incubator. They were then fixed in 2% paraformaldehyde and viewed for incorporation of the siRNA with the use of the FITC label. Only cells labeled with FITC were identified as having either the

control siRNA or experimental siRNA. The cells were stained with TRITC phalloidin to visualize the actin ring morphology. Osteoclasts were visualized using the MRC-1024 confocal laser scanning microscope and LaserSharp software (Bio-Rad, Hercules, CA). Images were taken in sequential series to eliminate any overlap of emission and analyzed by confocal assistant software.

To determine the downregulation of protein expression, RANKL stimulated RAW 264.7 cells were grown on 6 well plates. On day 6 of differentiation, they were either not transfected or transfected with 150 nM of control or experimental siRNA in 10 µl lipofectamine 2000. The media was replaced with DMEM with FBS and RANKL 6 hours after transfection. The cells were incubated for 48 hours at 37^{o}C in a CO^{2} incubator. The cells were scraped and washed twice with cold PBS. The lysates were centrifuged and the cell pellet was lysed on ice using 150 µl cell extraction buffer (BioSource International, Camarillo, CA, USA) supplemented with protease inhibitor cocktail (Sigma P2714) and phenylmethylsulfonylfluoride (PMSF) for 30 minutes, vortexing every 10 minutes. The cell lysate was then centrifuged at 13,000 rpm for 10 minutes at 4^{o}C. Bradford assay was performed to determine protein concentration. Equal concentrations of proteins were separated by SDS-PAGE, followed by transfer to nitrocellulose. The nitrocellulose blots were incubated overnight in blocking buffer, after which they were incubated with both anti-cortactin and anti-actin antibodies for 2 hours, followed by incubation with secondary horseradish peroxidase labeled antibodies for 1 hour. Chemiluminescent substrate was added and the blots were visualized using an Alpha Innotech Fluorochem 8000.

Results

Cortactin is upregulated at the transcriptional level during osteoclastogenesis

Cortactin protein levels increase during osteoclastogenesis as is verified by Figure 4.2 (184). Increased expression is due to transcriptional rather than translational regulation as was identified by PCR analysis (Figure 3.3). Unlike the other proteins tested, cortactin mRNA was not detected prior to treatment of RAW 264.7 cells with RANKL.

Cortactin in the actin rings of resorbing osteoclasts

Figure 4.3 shows representative micrographs of the staining of activated osteoclasts on dentine bone with anti-cortactin and anti-Arp 3 or phalloidin. As described in previous research, in the activated osteoclast on bone slices, actin is enriched in the ring surrounding the ruffled membrane. Cortactin is shown to be a major element of the actin ring of resorbing osteoclasts.

Cortactin is required for actin ring formation

A new siRNA (120648) was identified that knocked down cortactin expression (Figure 4.4). A commercial siRNA known to downregulate cortactin was also used to confirm our data (Figure 4.6).

Osteoclast-like RANKL stimulated RAW 264.7 cells on 6 well plates were transfected and kept in culture for 48 H. Cortactin was not detected by Western analysis in the cells transfected with effective anti-cortactin siRNAs (Figure 4.4 and 4.6).

RANKL stimulated RAW 264.7 cells on glass coverslips were grown on 24 well plates and transfected with experimental or control siRNAs. The cells were incubated for 48 hours at which time they were fixed. Immunocytochemistry showed normal actin rings in the no treatment and control siRNA groups (Figure 4.5 and 4.7). However, a complete loss of actin ring podosomal organization occurred in the experimental group. Although there was a loss of actin rings, the cells remained viable and well spread.

Cortactin-binding proteins in extracts from osteoclast-like cells

To identify actin-associated proteins that interact with cortactin, pull-down experiments were performed on detergent solubilized extracts of RANKL stimulated R264.7 cells. Recombinant GST-cortactin (Figure 4.8) or vehicle was added to the extracts, and then pulled down with Glutathione Sepharose beads, separated by SDS-PAGE and Western blotted. Consistent with previous reports, cortactin was found to interact with Arp2/3 complex and n-WASp (Figure 4.9). Surprisingly, we detected high levels of Vasodilator-stimulated phosphoprotein (VASP), a regulator of actin polymerization, and V-ATPase subunits (Figure 4.9). Efforts to pulldown cortactin in immunoprecipitations of V-ATPase were not successful. However, we did identify VASP, suggesting a potential complex that includes VASP, cortactin and, V-ATPase (Figure 3.5).

Discussion

As previously shown, cortactin is differentially upregulated during osteoclastogenesis (184). This preferential upregulation in response to RANKL stimulation supports a hypothesis that it is important for osteoclastic bone

resorption and may be a vital component in either V-ATPase translocation to the ruffled membrane or formation of the actin ring.

Cortactin co-localizes with the Arp2/3 complex in the actin ring of osteoclasts. Previous data have shown that cortactin forms a tertiary complex with the Arp2/3 complex and N-WASP to activate actin polymerization and for stabilization of actin based networks (186, 188). Its identification in the actin ring supports its localization to this complex of proteins.

Immunoprecipitation with the GST-cortactin fusion protein identified associations between the Arp2/3 complex and N-WASP, which is consistent with previous studies that demonstrated the complex composed of these proteins plays a role in the regulation of actin polymerization (186, 188). Unexpectedly, cortactin also interacted with V-ATPase and Vasodilator stimulated phosphoprotein. VASP is an actin associated protein that tracks the fast growing end of actin filaments (201, 202). It is still unclear as to the precise mechanism of actin; however, it may be involved in protecting growing actin filaments from capping proteins (201, 202). In addition, the capacity of VASP to concentrate profilactin complex near the fast growing end of actin filaments may be vital (202). This is the first report of VASP and cortactin in the same complex. We currently do not know whether the interaction is direct or indirect. Potential interaction domains are present in the two proteins. VASP contains a src homology region 3 (SH3) binding domain in the proline-rich central region (203), while cortactin has a carboxy-terminal SH3 domain (204). Efforts are underway

to determine whether these domains interact and to explore the functional consequences of the interaction.

The use of siRNA to knock down cortactin results in a loss of actin ring formation which demonstrates that cortactin is crucial for the formation of podosomes and actin rings in osteoclasts. Two separate siRNAs targeting cortactin greatly reduced cortactin levels and disabled the capacity of osteoclasts to form actin rings and podosomes. Together with the fact that cortactin is specifically upregulated during osteoclastogenesis (184), these data suggest that cortactin plays a vital role in osteoclast function.

In summary, we showed that cortactin is required for the formation of the podosomes and actin rings that are vital for osteoclast function. Cortactin interacts with Arp2/3 complex and n-WASp as expected in osteoclasts extracts (186, 188). Novel interactions between cortactin and VASP and cortactin and V-ATPase were identified. Our data are consistent with cortactin playing a role in osteoclasts in the integration of cytoskeletal and membrane dynamics.

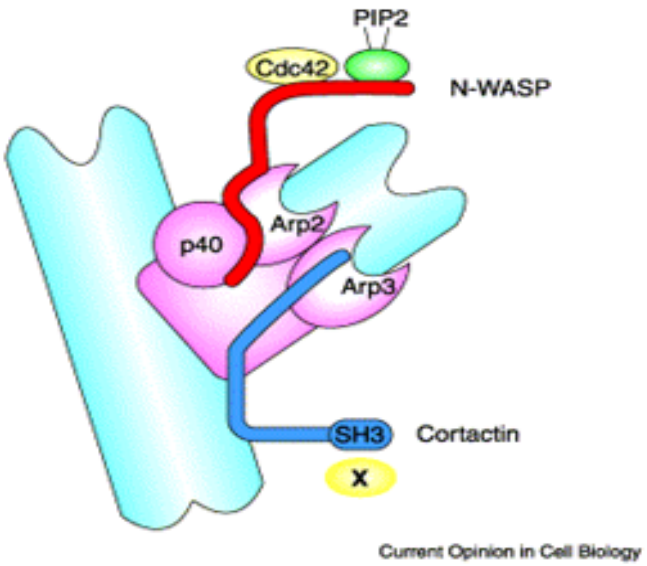

Figure 4.1. Cortactin, N-WASp and Arp2/3 form a synergistic, ternary complex to initiate actin polymerization. The Arp2/3 complex is inactive in its unbound form. Activation of the Arp2/3 complex occurs through the N-WASP family of proteins binding to the Arp2 subunit. Upon activation, a conformation change occurs in between the Arp2 and Arp3 subunits inducing actin polymerization. Cortactin binds to the Arp3 subunit and functions to enhance actin polymerization as well as stabilize the Arp2/3 induced branched actin networks. (Weaver et al. Curr Biol. 2002; 12:1270-1278) (188)

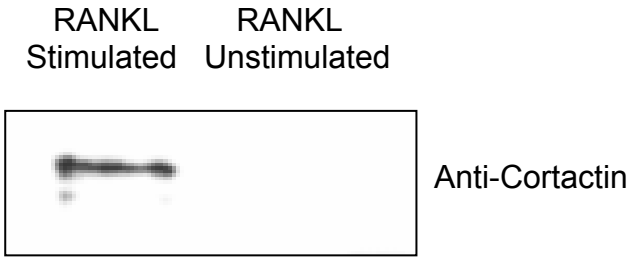

Figure 4.2. Cortactin is upregulated in response to RANKL stimulation. Cell lysates were extracted from unstimulated or RANKL stimulated RAW 264.7 cells. Bradford assay was performed to standardize protein concentrations. Cell lysates were separated by SDS-PAGE and western transfer and probed with anti-cortactin antibody. In unstimulated RAW 264.7 cells, cortactin is undetectable by western analysis; however, upon RANKL stimulation, cortactin expression is induced.

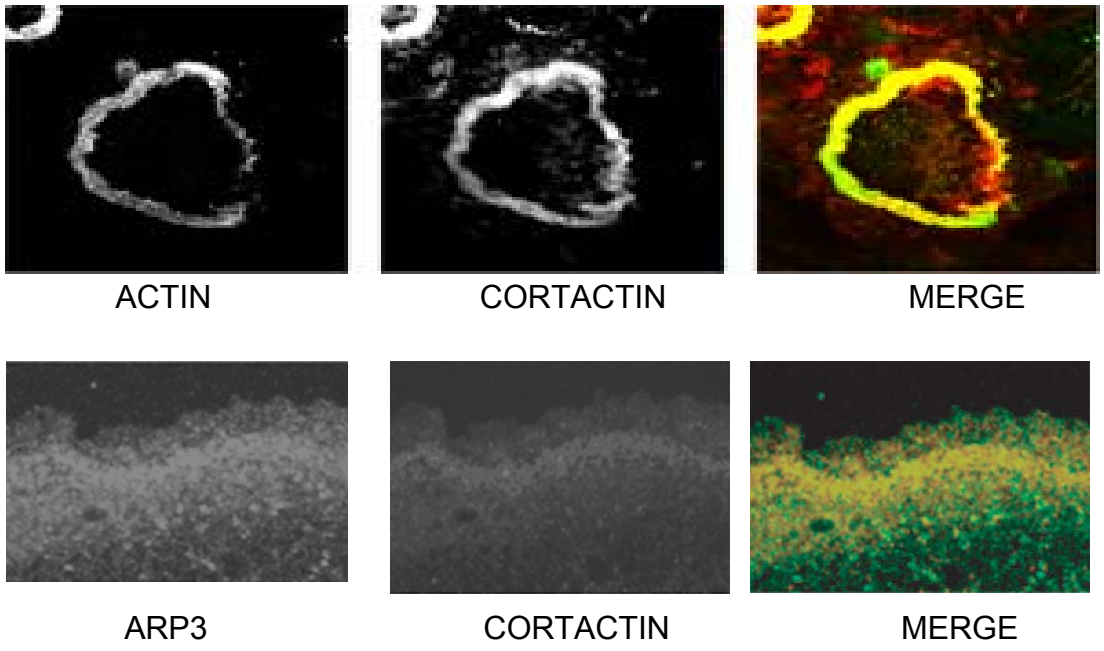

Figure 4.3. Cortactin co-localizes with the podosomal core proteins, actin and the Arp2/3 complex. RAW 264.7 cells were stimulated with RANKL to differentiate into osteoclast-like cells and fixed and stained with anti-cortactin antibody and rhodamine phalloidin or anti-Arp3 antibodies. Note that there is precise co-localization between Arp3 and cortactin and actin and cortactin.

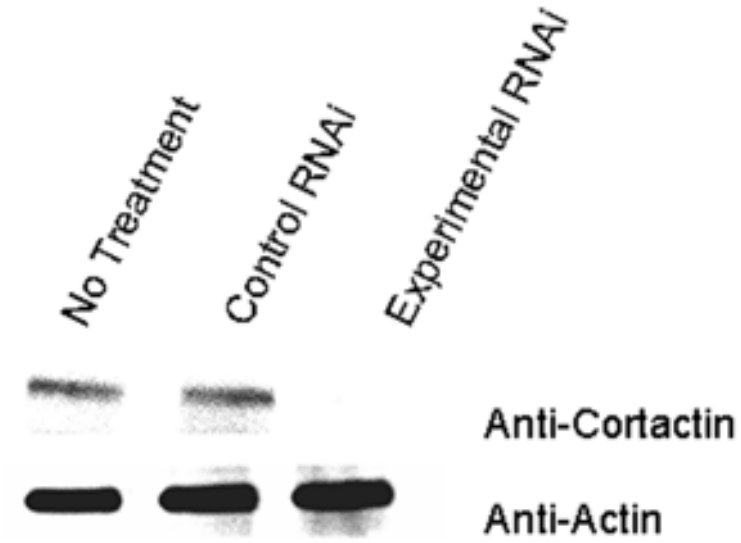

Figure 4.4. siRNA 120649, but not a control siRNA (120653), effectively knocks down the cortactin content to an undetectable level of osteoclast-like cell extract after 30 hours compared with actin. RAW 264.7 cells were stimulated with RANKL. Just as large, multinucleated osteoclasts began to appear, cells were transfected as noted. Cells transfected with siRNA 120649, which had proved effective at knocking down cortactin in preliminary experiments, reduced cortactin levels dramatically compared with either control cells or cells transfected with an ineffective siRNA 120653.

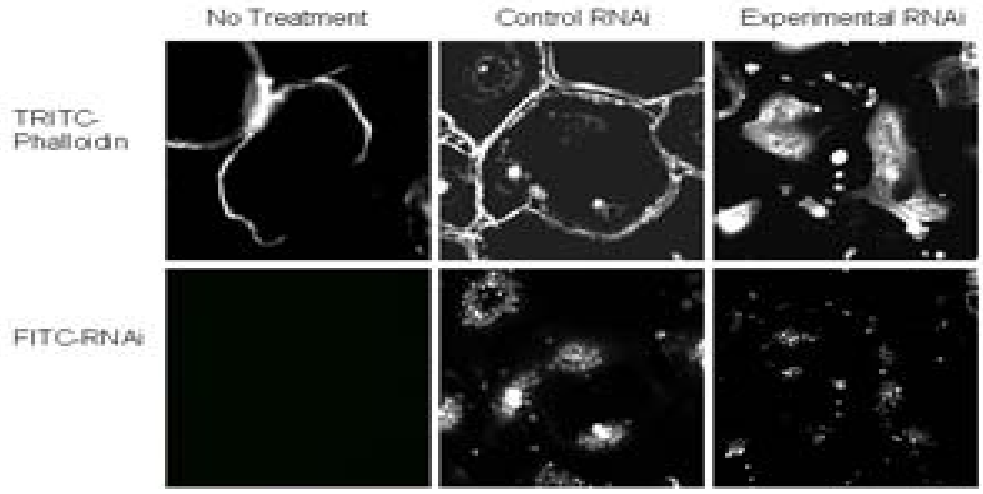

Figure 4.5 Actin rings are disrupted in cortactin knockdown. Untransfected RAW 264.7 osteoclast-like cells or osteoclast-like cells transfected with ineffective siRNA (120653) or effective siRNA (120649) were fixed after 30 hours and examined for the presence of fluorescent oligo marker of transfection (bottom panels) or F-actin by staining with phalloidin (top panels). The photographs are representative cells. The effective siRNA disrupted the ability of the osteoclasts to form actin rings.

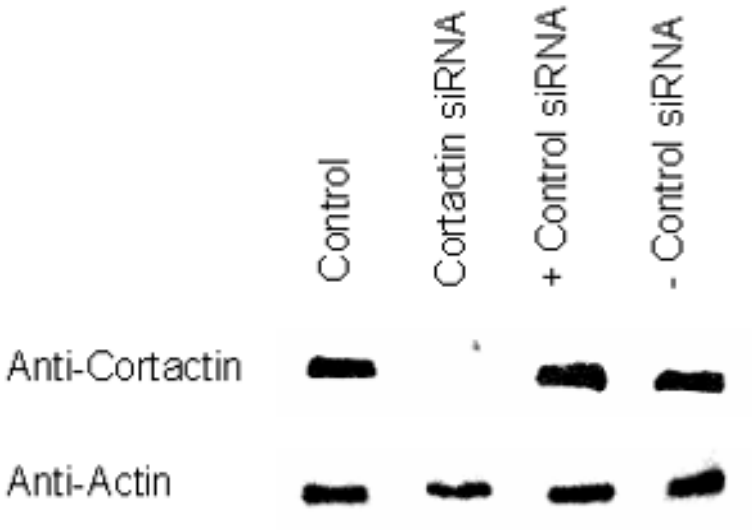

Figure 4.6. An siRNA known to downregulate cortactin (Ambion) effectively knocks down the cortactin content of osteoclast-like cell extract to an undetectable level after 30 hours compared with actin. RAW 264.7 cells were stimulated with RANKL. Just as large, multinucleated osteoclasts began to appear, cells were transfected as noted. Cells transfected with Ambion siRNA, which is known to knock down cortactin levels, reduced cortactin levels dramatically compared with either control cells or cells transfected with either positive or negative controls.

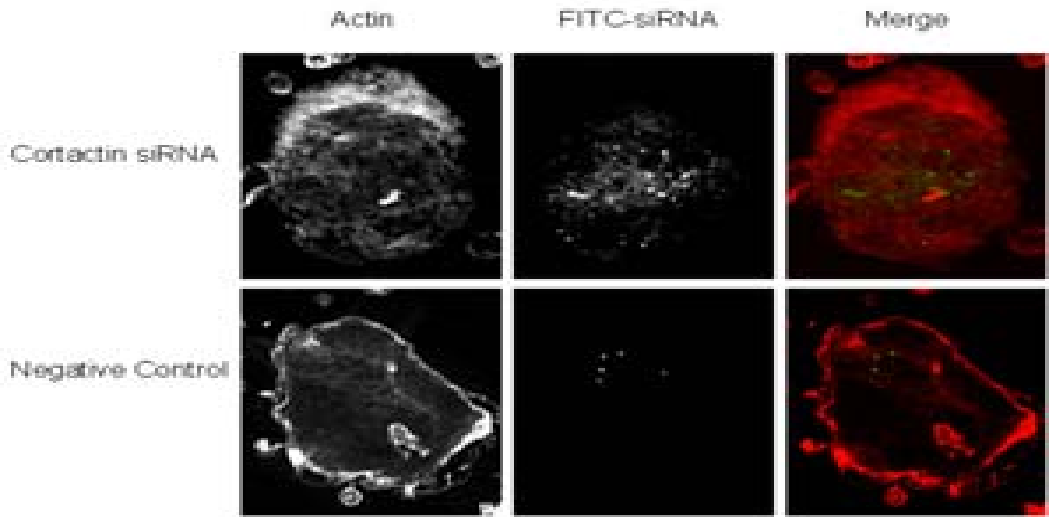

Figure 4.7 Actin rings are disrupted in cortactin knockdown**.** Untransfected RAW 264.7 osteoclast-like cells or osteoclast-like cells transfected with ineffective siRNA (negative control) or effective siRNA (positive control) were fixed after 30 hours and examined for the presence of fluorescent oligo marker of transfection (middle panels) or F-actin by staining with phalloidin (left panels). A merged image is shown in the right panels The photographs are representative cells. The effective siRNA disrupted the ability of the osteoclasts to form actin rings.

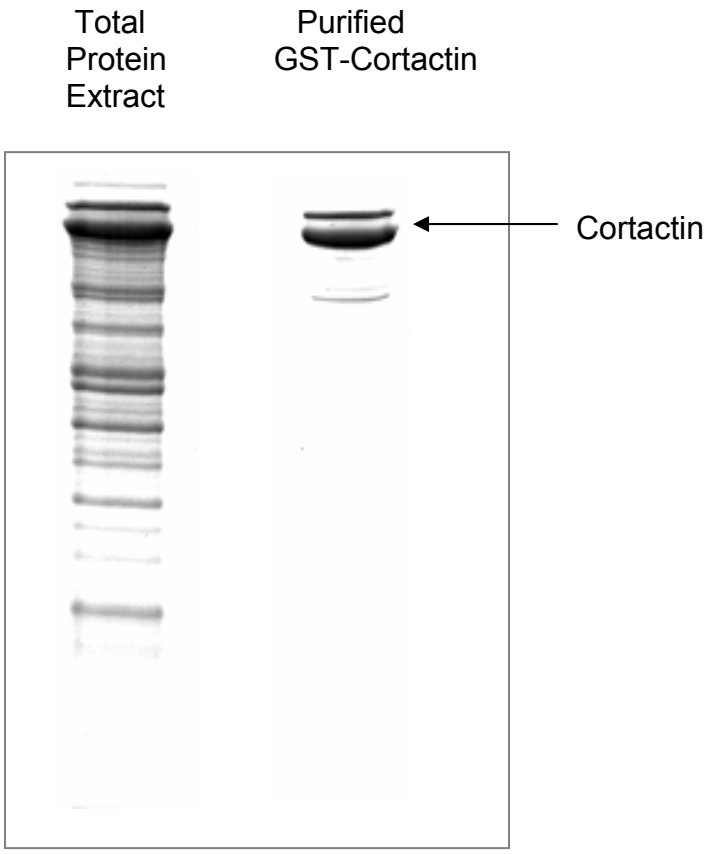

Figure 4.8. Transformation and Purification of GST-cortactin fusion protein. A GST-cortactin fusion protein was obtained from Dr. Scott Weed (West Virginia University, Morgantown, WV). The construct was transformed into E.coli strain DH5a and induced with IPTG. The fusion protein extract was run on a glutathione-sepharose column and eluted with reduced glutathione.

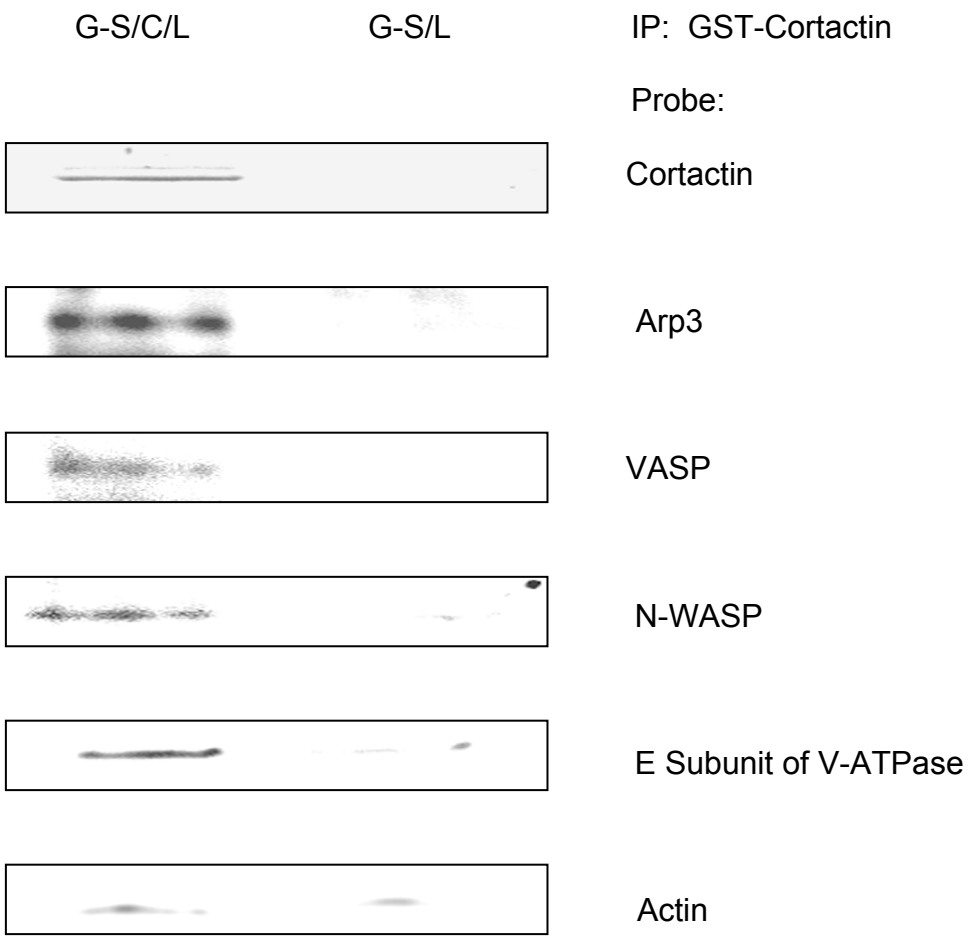

Figure 4.9. Immunoprecipitation Experiments with GST-Cortactin Show a Linkage between Cortactin and Arp3, VASP, N-WASp and the E Subunit of V-ATPase. Cells lysates from RANKL stimulated RAW 264.7 cells were incubated with glutathione sepharose with or without GST-cortactin. The lysates were washed and eluted in loading buffer. They were separated by SDS-PAGE and Western transfer. Bound proteins were then visualized by probing with anti-Arp3, anti-cortactin, anti-VASP, anti-N-WASP, anti-E subunit, and anti-actin.

CHAPTER 5
THE ROLE OF VASP IN OSTEOCLASTOGENESIS

Introduction

Like cortactin, numerous additional proteins have been identified as components of the cytoskeletal machinery. VASP is one such protein. It may act directly as a nucleator of the Arp2/3 complex or indirectly as a structural scaffold for signaling and cytoskeletal proteins such as vinculin, ActA, zyxin, and Fyb/Slap (149, 151).

VASP is a 46 kD protein (203, 205) originally isolated from human platelets and is the founding member of the Ena/VASP family composed of Vasodilator-Stimulated Phosphoprotein (VASP), mammalian Enabled (Mena), and ENA/VASP-like protein (Evl) (Figure 5.1) (203, 205, 206). This family of proteins plays a key role in actin based motility and is localized predominantly at focal adhesions, cell/cell contacts, and regions of highly dynamic actin reorganizations such as lamellipodia (151, 203). The VASP protein contains three primary domains, EVH (Ena/VASP Homology domain) I, proline rich, and EVH2 (189, 203, 206). The EVHI domain is located at the N-terminus and binds actin related proteins such as zyxin, vinculin, and ActA (189, 203, 206). The proline rich region interacts with proteins containing SH3 and WW domains and contains a 4 GP_5 motif which is the binding site of profilin, a G-actin

regulatory protein (189, 203, 206). The EVH2 domain contains the actin binding site and is the location for oligomerization (189, 203, 206).

VASP is phosphorylated by both the Protein Kinase A (PKA) and Protein Kinase G (PKG) pathways (207). The phosphorylated protein has an apparent weight of 50 kD (205, 207). PKA preferentially phosphorylates VASP at Ser157 which is located N-terminal to the $(GP5)_4$ profilin binding site in the proline rich region (189, 203, 206). This phosphorylation site is in close proximity to the ligand binding module which in turn alters the ligand binding properties (189, 203, 206). In addition, it also phosphorylates Thr274 although the consequences of this phosphorylation are not fully understood (189, 203, 206). The PKG pathway preferentially phosphorylates Ser239, but like PKA, will also phosphorylate Thr274 (189, 203, 206). Phosphorylation by the PKA pathway has been shown to diminish F-actin binding, suppressing actin nucleation as well as inhibiting Arp2/3 triggered actin polymerization; thus, it can be a negative regulator of actin polymerization (189, 203, 206).

The PKA pathway is activated in murine osteoclasts in response to calcitonin (207). Calcitonin is a known inhibitor of bone resorption and is used to treat metabolic bone diseases such as osteoporosis and Paget's disease (190, 207). The calcitonin receptor, a 7 transmembrane G-protein coupled receptor, is located on the cell surface of osteoclasts (191, 192). Activation by calcitonin signals the receptor to activate the PKA pathway (190, 191). This could lead to phosphorylation of the VASP protein and in turn to the changes in the organization of F-actin that are known to occur in response to calcitonin.

In this study, our objective was to examine the role of VASP in osteoclastogenesis. We sought to determine the localization of VASP in the osteoclast and well as its requirement for actin ring formation. In addition, we sought to determine what effect phosphorylation of VASP would have on the actin ring of osteoclasts.

Materials and Methods

Distribution of VASP in the actin ring

Cell culture was performed as previously described. For identification of VASP localization, the cells were fixed in 2% formaldehyde, solubilized in 0.2% Triton X-100 in PBS and blocked in PBS with 2% BSA. Cells were stained with rhodamine phalloidin or antibodies recognizing VASP at a dilution of 1:100 in PBS. Secondary antibodies were diluted according to manufacturer's instructions. Osteoclasts were visualized using the MRC-1024 confocal laser scanning microscope and LaserSharp software (Bio-Rad, Hercules, CA). Images were taken in sequential series to eliminate any overlap of emission and analyzed by confocal assistant software.

Effects of calcitonin on actin rings of osteoclasts

Cell culture was performed as previously described. On day 6 of differentiation (many large multinucleated cells present), calcitonin (10nM) was added to the cells and incubated for time points of 1, 2, and 24 hours. For identification of morphological characteristics, the cells were then fixed in 2% formaldehyde, solubilized in 0.2% Triton X-100 in PBS and blocked in PBS with 2% BSA. Cells were stained with rhodamine phalloidin or antibodies recognizing

Arp 3 or phospho-VASP (Ser 157) at a dilution of 1:100 in PBS. Secondary antibodies were diluted according to manufacturer's instructions. Osteoclasts were visualized using the MRC-1024 confocal laser scanning microscope and LaserSharp software (Bio-Rad, Hercules, CA). Images were taken in sequential series to eliminate any overlap of emission and analyzed by confocal assistant software. For assessment of protein expression, RANKL stimulated RAW 264.7 cells on 6 well plates were either untreated or treated with calcitonin (10 nM) for 1, 2 or 24 hours. Cells were then scraped and washed twice with PBS. The pellets were lysed using 250 μl of cell extraction buffer (BioSource International, Camarillo, CA, USA) supplemented with protease inhibitor cocktail (Sigma P2714) and phenylmethylsulfonyl fluoride (PMSF) for 30 minutes on ice with vortexing every 10 minutes. The extract was centrifuged for 10 minutes at 13,000 rpm at 4^{o} C. Bradford assay was performed on the lysates. Equal concentrations of protein were separated by SDS-PAGE, followed by western transfer. The nitrocellulose blots were blocked in blocking buffer overnight and incubated with both anti-VASP and anti-phospho-VASP (Ser 157) antibodies for 2 hours. The bots were washed and incubated with a horseradish peroxidase (HRP)-labeled secondary antibody for 1 hour, followed by incubation with a chemiluminescent substrate. The blots were visualized using an Alpha Innotech Fluorochem 8000. Quantitation was performed using densitometric measurements of integrated density values.

VASP-null colony

To determine the effects of knocking out VASP expression in osteoclasts, three female heterozygous mice and one homozygous VASP knockout male mouse were obtained as a generous gift from Dr. Ulrich Walter (Institute of Clinical Biochemistry and Pathobiochemistry, Wurzberg, Germany). A breeding colony was initiated with approval from the University of Florida Institutional Animal Care and Usage Committee. Based on Mendelian genetics, half of each litter should be homozygous knock out mice and half should be heterozygous. After weaning, a tail sample from each pup was obtained and RNA was extracted with RNAeasy Mini Kit (Qiagen, Valencia, CA) following the manufacturer's instructions and quantified by spectrophotometer. The sequence for VASP was obtained from Gen Bank. Primers were designed as follows: forward 5'-GAGGAGCTGGAACAACA GAA-3'; reverse 5'-CCAGGCAGGAAGTACA GAAA-3'. For standard RT-PCR, 3ug of total RNA were annealed to an oligo-dt primer and first strand cDNA synthesis was performed using Thermoscript RT-PCR System (Invitrogen, Carlsbad, CA) following manufacturer's directions. One-twentieth of the cDNA was subjected to amplification by PCR. PCR was performed under the following conditions: 95^{o}C for 2 minutes, then 35 cycles of 90^{o}C, 30 seconds; 58^{o}C, 30 seconds; 72^{o}C, 30 seconds. One-half of the PCR product was separated on 0.5% agarose gel with ethidium bromide staining for 1 hour. Images were detected using UV transillumination on a Fluorochem 8000 (Alpha-Innotech, San Leandro, CA). Homozygous mice were determined to be those by which PCR with multiple primers was unsuccessful.

Mouse marrow osteoclasts were grown from marrow derived from the long bones of the hind legs of the homozygous VASP knockout and the heterozygous mice. The marrow cells were grown in α-MEM medium with 10% fetal bovine serum (FBS) plus 10^{-8} M 1,25-dihydroxyvitamin D_3 for a period of approximately seven days. The cells were then scraped, plated on 24 well plates, and treated with calcitonin (10nM) for 1 hour. The cells were fixed in 2% paraformaldehyde, detergent-permeabilized with 0.2% Triton X-100 in PBS for 10 minutes, washed in PBS and blocked in PBS with 2% BSA (bovine serum albumin) for one hour. Actin filaments were stained with TRITC phalloidin. VASP was probed with an anti-VASP polyclonal antibody (Santa Cruz Biotechnology, Santa Cruz, CA). Bound antibodies were detected by labeling with CY2 tagged anti-rabbit secondary antibody. Osteoclasts were visualized using the MRC-1024 confocal laser scanning microscope and LaserSharp software (Bio-Rad, Hercules, CA). Images were taken in sequential series to eliminate any overlap of emission and analyzed by confocal assistant software. This protocol was approved by the University of Florida Institutional Animal Care and Usage Committee.

PCR analysis of the ENA/VASP family member, Evl

RNA was extracted from RANKL differentiated RAW 264.7 cells as well as from unstimulated RAW 264.7 cells using RNAeasy Mini Kit (Qiagen, Valencia, CA) and quantified by spectrophotometer. The sequence for evl was obtained from Gen Bank. The following primers were designed: forward 5'-ACCAGCAGGTTGTGATCAAT-3'; reverse 5'-AATAGACCCGGTGTTCT GTG-3'. For standard RT-PCR, 3 μg of total RNA were annealed to an oligo-dt primer and

first strand cDNA synthesis was performed using Thermoscript RT-PCR system following manufacturer's directions. One-twentieth of the cDNA was subjected to amplification by PCR using the above mentioned primers. PCR was performed under the following conditions: 95^{o}C for 2 minutes, then 35 cycles of 90^{o} C, 30 seconds; 58^{o}C, 30 seconds; 72^{o}C, 30 seconds. One half of the PCR product was separated on 0.5% agarose gel with ethidium bromide staining for 1 hour. Images were detected using UV transillumination on a Fluorochem 8000.

Results

VASP is present in the actin rings of osteoclasts.

The actin rings of osteoclasts were stained with anti-VASP or phalloidin. Figure 5.2 is a representative micrograph of the staining. Co-localization was observed between VASP and actin.

VASP is phosphorylated at Serine 157 in response to calcitonin treatment and results in the disruption of the actin ring of osteoclasts.

Osteoclasts were treated with calcitonin at baseline, and cells were fixed and stained with phospho-VASP Serine 157 or Arp3 antibodies at 1, 2 and 24 hour time periods (Figure 5.3). Osteoclasts at baseline showed no phosphorylation of VASP. Treatment with calcitonin caused a phosphorylation of VASP at Serine 153 as observed by the increased signal intensity at 1 and 2 hours. This phosphorylation coincided with a disruption of the microfilament organization in the actin rings from tightly focused rings to broad bands of actin. By 24 hours, the phosphorylation and actin ring morphology were returning to baseline levels.

Western analysis of the calcitonin-treated osteoclasts showed a three fold increase in phosphorylation of VASP at Serine 157 at 1 and 2 hour time points (Figure 5.4). This confirms VASP is phosphorylated in response to calcitonin treatment.

The osteoclasts of mice lacking the VASP gene are able to form actin rings.

Heterozygous female and homozygous male knockout mice were obtained from Ulrich Walter (Institute for Clinical Biochemistry and Pathobiology, Medizinische Universitätsklinik, Würzburg, Germany). The mice were bred and homozygous VASP-null mice were identified by tail DNA isolation (Figure 5.5). Osteoclasts were cultured from the mouse marrow of the hind legs of the VASP deficient mice. The osteoclasts were then fixed and stained with phalloidin or treated with calcitonin and fixed and stained with phalloidin.

Normal actin ring morphology was observed in osteoclasts from VASP-null mice (Figure 5.6). Treatment with calcitonin, which disrupts actin ring morphology by the PKA pathway, disrupted the actin rings of both the control, as expected, and the VASP null osteoclasts. This suggests that calcitonin may exert its functions through another VASP/Ena family member.

Evl is upregulated in response to osteoclast differentiation

To identify other members of the ENA/VASP family that could play a role in osteoclastogenesis, PCR was performed using primers to detect changes in gene expression in evl. Unlike VASP, Evl mRNA was preferentially upregulated during osteoclastogenesis, with a complete lack of detection prior to treatment of RAW 264.7 cells with RANK-L (Figure 5.7).

Discussion

Vasodilator stimulated phosphoprotein is a member of the ENA/VASP family of proteins (190, 192, 203, 206, 207). These proteins localize to areas of dynamic actin polymerization and are known downstream effectors of multiple signaling pathways (189). These studies show that VASP is a component of the actin ring of osteoclasts, which is consistent with its localization to areas of dynamic actin reorganization (205). The function of VASP in the actin ring of osteoclasts is still unknown. However, ENA/VASP proteins bind directly to G-actin and F-actin as well as profilactin and are known to promote the elongation of actin filaments by recruiting profilactin complexes to the sites of dynamic actin reorganization (205, 208-210). VASP also functions to enhance Arp2/3 activity and prevent capping proteins from inhibiting actin polymerization (210). These data strongly suggest that VASP plays a key role in actin dynamics.

VASP has been identified as a substrate for both the PKA and PKG phosphorylation (208, 211, 212). Platelets from VASP null mice have defective PKA signaling and exhibit deficiencies in platelet aggregation (213-215). Calcitonin is a known activator of the PKA pathway and induces changes in the cytoskeleton (191, 192). Treatment of osteoclasts with calcitonin shows a three-fold increase in phosphorylation of VASP at Serine 157 within the first two hours of treatment with a return to baseline by 24 hours. The actin rings of calcitonin-treated osteoclasts were disrupted as the microfilament organization changed from a tightly focused ring to broad bands of actin. By 24 hours, the actin ring morphology had returned to baseline morphology. This is consistent

with data indicating that VASP plays a role in actin filament organization by affecting the branching activity of the Arp2/3 complex. Upon activation of VASP, the density of Arp2/3 induced branching is decreased, resulting in larger and more sparsely branched filaments (216). Upon deactivation, Arp2/3 mediated actin polymerization and branching occurs resulting in a dense, tightly branched network.

Although data confirm that VASP is associated with the reorganization that occurs in the actin ring of osteoclasts, VASP null mice have no real skeletal deficiencies (212-214). Osteoclasts from VASP null mice exhibit normal actin ring morphology. In addition, when treated with calcitonin, the osteoclasts exhibit actin ring disruption similar to that observed in control cells. These findings support the lack of skeletal deficiencies identified in VASP null mice and suggest that VASP may not play a major role in the dynamic actin polymerization found in the podosomes of the actin ring.

The ENA/VASP family consists of three mammalian members, VASP, Mena (mammalian Enabled) and Evl (Ena/VASP-like protein) (211, 217). PKA phosphorylation, as induced by calcitonin, is known to affect two members of the ENA/VASP family, VASP, as our data have shown, and Evl (203, 211). Evl is highly expressed in cells of hematopoietic lineage and has been shown to nucleate actin polymerization (203, 206). In addition, phosphorylation of Evl results in a decrease in nucleation activity (211). These data suggest that Evl may be the Ena/VASP family member that plays a key role in osteoclastogenesis. PCR analysis of unstimulated and RANKL stimulated RAW

264.7 cells indicates that Evl is preferentially upregulated in response to RANKL stimulation, as is seen with cortactin. This preferential upregulation suggests it functions in the dynamic actin reorganizations that occur during osteoclastic differentiation.

In summary, VASP is present in the actin rings of osteoclasts and is phosphorylated at Serine 157 in response to calcitonin treatment, which activates the PI3K pathway. This activation causes a disruption of the actin ring of osteoclasts. Although treatment with calcitonin may indicate a role for VASP in actin ring formation and maintenance, we did not detect any skeletal defects in the VASP knockout mouse. Osteoclasts cultured from VASP knockout mice respond similarly to those from control mice, indicating another ENA/VASP family member may play a more dominant role in osteoclastogenesis. Evl, an ENA/VASP family member, is present in cells of hematopoietic lineage (14) and has been shown to be preferentially upregulated in response to RANKL treatment. Evl may be responsible for the structural changes seen in actin ring morphology when treated with calcitonin.

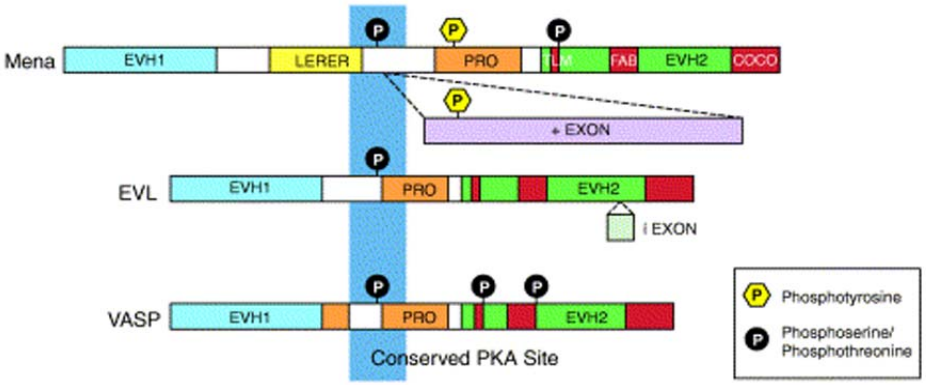

Figure 5.1. The Ena/VASP family. Cartoons of the three mammalian members of the Ena/VASP family are depicted. All three members share a similar domain structure which consists of an amino-terminal EVH1 domain, a central proline-rich region, and a carboxy-terminal EVH2 domain. In addition, all mammalian Ena/VASP proteins share an amino-terminal PKA/PKG phosphorylation site (Ser-157 of VASP). (Kwiatkowski AV et al. Trends Cell Biol. 2003; 13(7):386-92) (206)

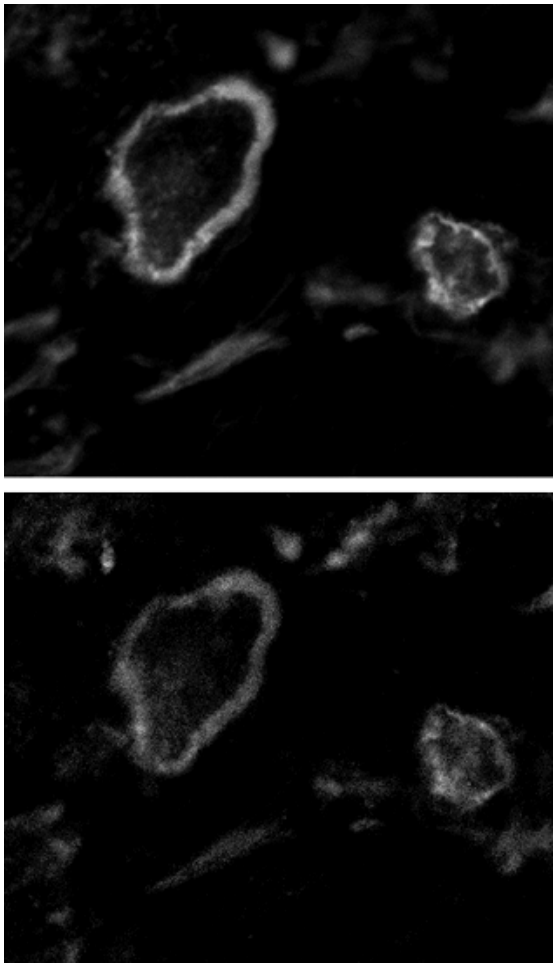

Figure 5.2. VASP is present in the actin ring of osteoclasts. Mouse marrow osteoclasts were cultured on bovine dentin slices for 2 days and then fixed and stained with rhodamine phalloidin and anti-VASP antibody. VASP is observed to co-localize with actin in the podosomes of the actin ring.

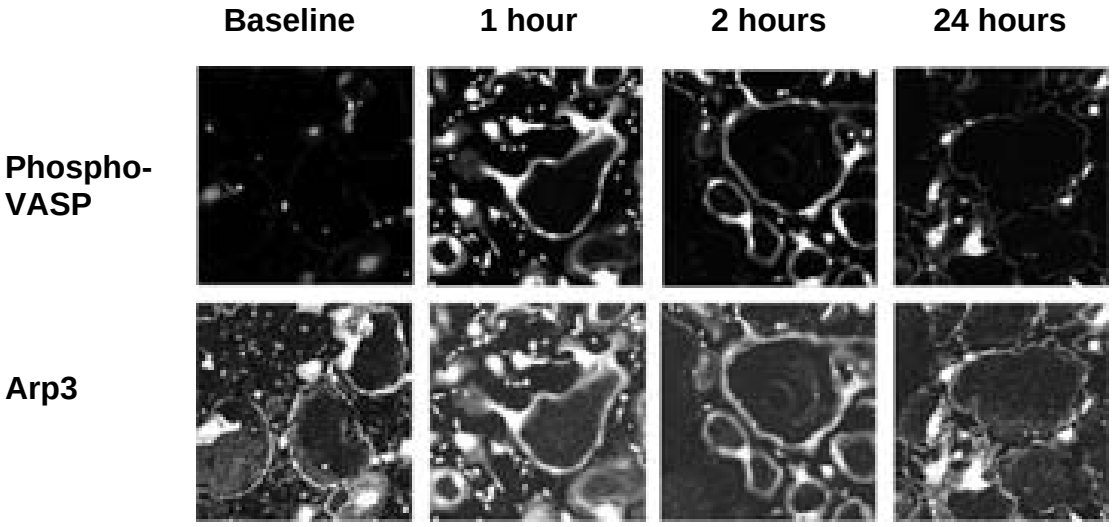

Figure 5.3. VASP is phosphorylated at Serine 157 in response to calcitonin treatment and results in the disruption of the actin ring. RAW 264.7 cells were cultured with RANKL until multinucleated osteoclast-like cells were observed. The cells were then treated with 10 nM calcitonin and fixed at baseline, 1, 2, and 24 hour time points. The cells were stained with antibodies recognizing Arp3 and phospho-VASP Ser 157. Calcitonin treatment caused a phosphorylation of VASP at 1 and 2 hour time points but returned to baseline by 24 hours. A broadening of the actin ring coincided with the observed phosphorylation.

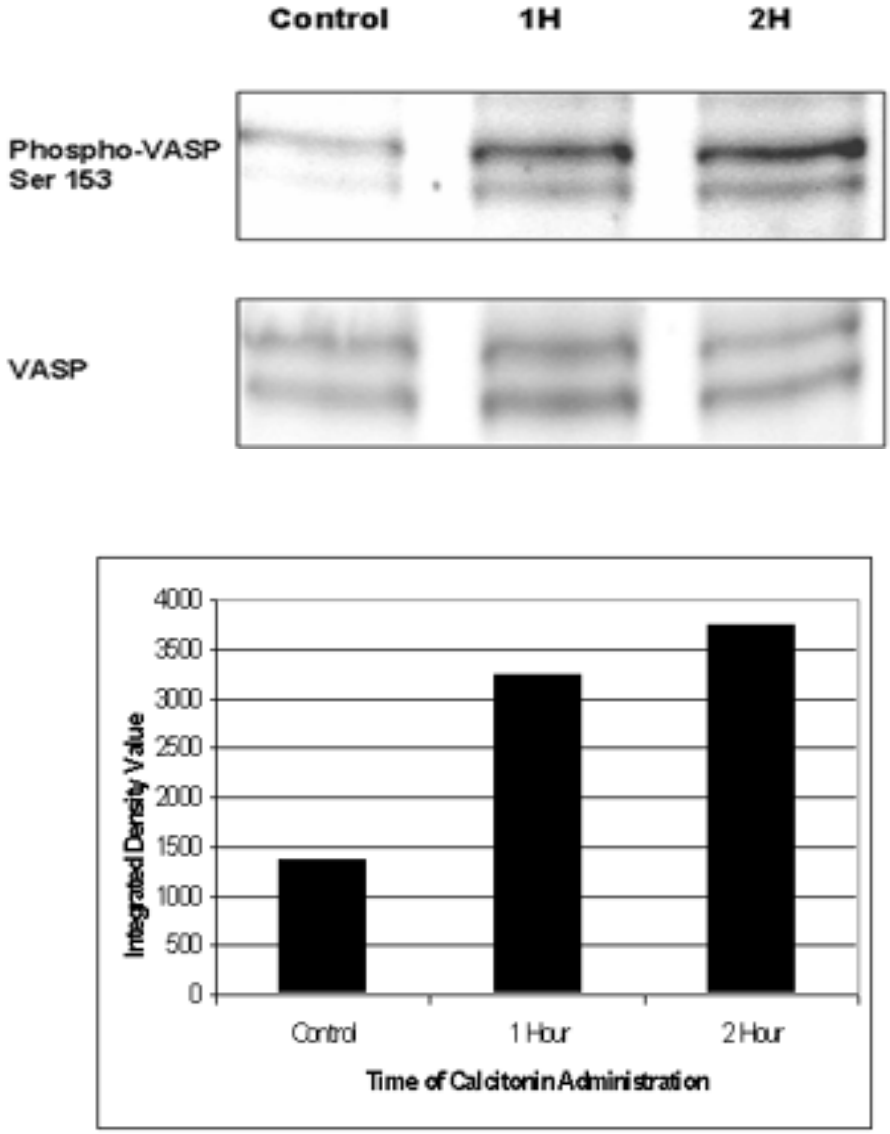

Figure 5.4. Calcitonin induces a three fold increase in phosphorylation levels of VASP at Serine 157. Cell lysates were collected from the RAW 264.7 cells treated with calcitonin at baseline, 1 hour and 2 hours. A Bradford assay was performed to standardize protein concentrations. The lysates were separated by SDS-PAGE and western analysis and probed with either anti- Phospho-VASP (Serine 157) or anti-VASP antibodies. Quantitation was performed on the western blots by densitometry measuring integrated density values.

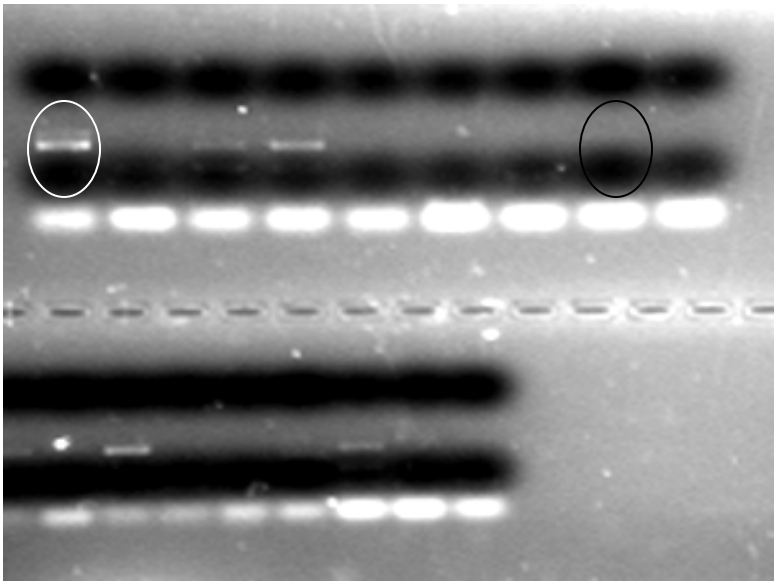

Figure 5.5. Identification of VASP null mice from breeding of heterozygous female with a homozygous male. RNA was extracted from the tail of each pup in the breeding colony. Primers were synthesized against VASP to determine which mice were lacking the VASP gene. The white circle identifies the presence of the VASP gene, while the black circle identifies a VASP null mouse. These identified VASP null mice were then used for immunocytochemical studies.

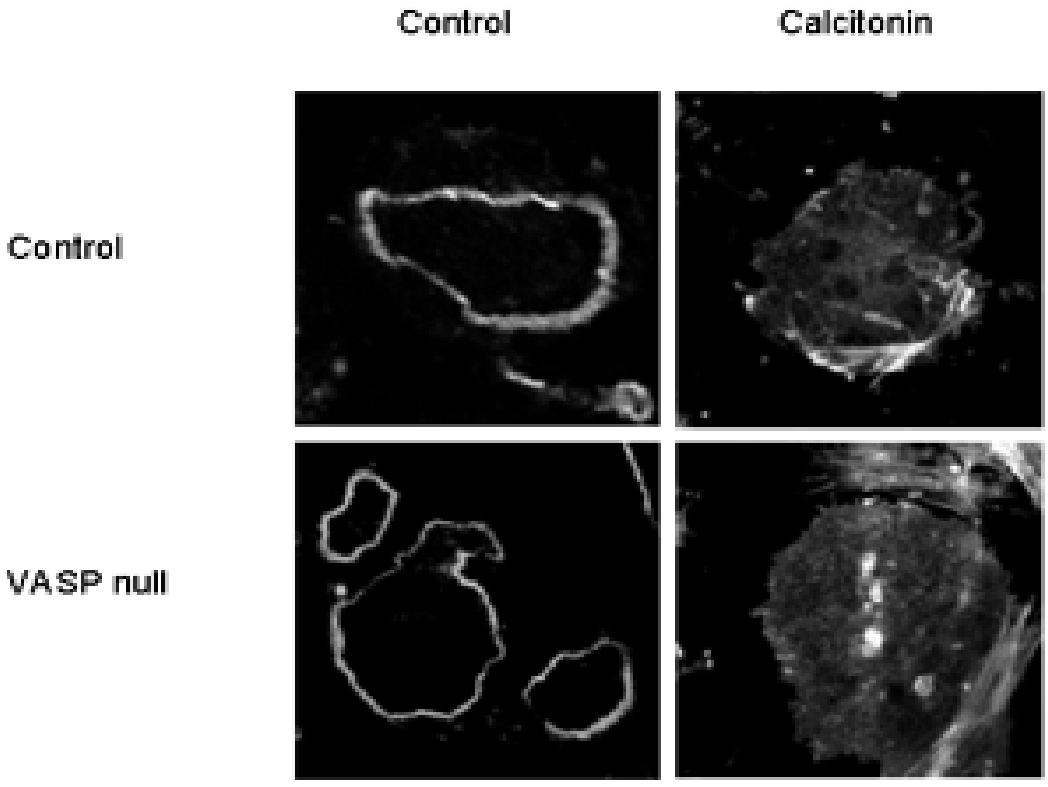

Figure 5.6. Osteoclasts of mice lacking the VASP gene are able to form actin rings and respond to calcitonin in the same fashion as control cells. Osteoclasts were cultured from the mouse marrow of the hind legs of VASP null or control mice. The osteoclasts were either untreated or calcitonin (10 nM) treated for 10 minutes and then fixed and stained with rhodamine phalloidin. The VASP null osteoclasts form actin rings like the controls. In addition, treatment with calcitonin, which disrupts actin ring morphology, similarly disrupts the actin ring in both control and VASP null osteoclasts.

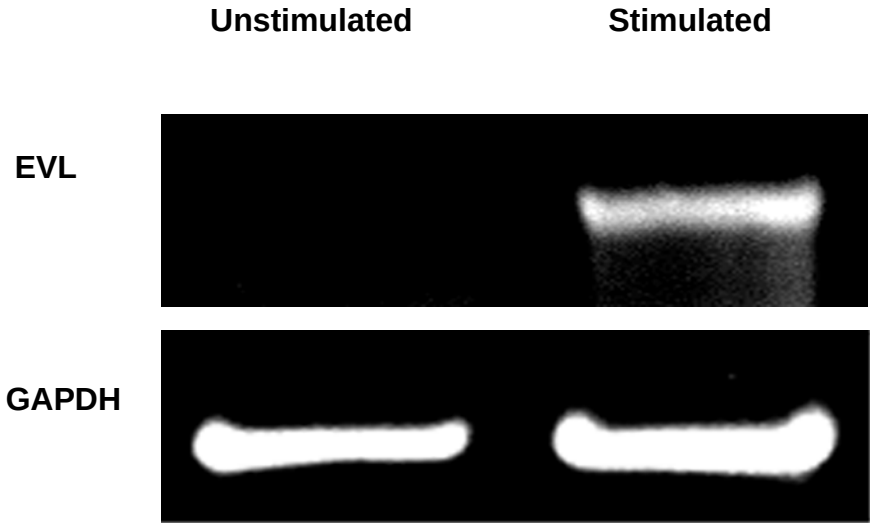

Figure 5.7. Evl, a member of the ENA/VASP family, is upregulated in response to osteoclastogenesis. RNA was extracted from RAW264.7 cells unstimulated or stimulated with RANKL. Primers were designed against Evl, a member of the ENA/VASP family. RT-PCR identifies preferential upregulation of Evl in response to RANKL stimulation.

CHAPTER 6
MODEL AND FUTURE DIRECTIONS

The Model and Hypothesis

This project has tested two novel hypotheses regarding the actin ring of osteoclasts and the association of actin ring proteins with V-ATPase. Our model first proposes that upon activation of the osteoclast, the cell becomes polarized, and the Arp2/3 complex is recruited to the apical membrane. It is hypothesized that the actin polymerization that ensues is Arp2/3 mediated and forms the actin ring. It is possible that this polymerization produces force at the plasma membrane, driving the membrane into the bone and forcing it to conform, creating a tight, yet dynamic seal. To counter the force being applied to the bone at the sealing zone, integrin-mediated focal adhesions elsewhere on the apical surface maintain the osteoclast in position. This hypothesis would account for the dynamic nature of the actin ring and sealing zone as well as the specific exclusion of integrins from the area of the sealing zone.

In addition, it is also hypothesized that the Arp2/3 complex or its associated proteins may bind V-ATPase and that Arp2/3 mediated actin polymerization may be involved in translocation of V-ATPase to and from the ruffled membrane. The association of V-ATPase with actin based networks is first confirmed by the actin binding ability of V-ATPase (9, 11, 218). Several V-

ATPase subunits have been identified to bind actin (9, 11, 218). In addition, in inactivated osteoclasts, F-actin and V-ATPase co-localize in cytosolic vesicles (9). This co-localization is only disrupted upon activation of the cell, where V-ATPase is then inserted into the ruffled membrane and actin is localized to the area of the sealing zone (9). Due to the highly dynamic nature of Arp2/3 mediated actin polymerization and the close proximity of the ruffled membrane and actin ring, this would seem a plausible mechanism.

This study has identified many important characteristics of the actin ring of osteoclasts. We have shown for the first time that the dynamic actin polymerization in the actin ring of osteoclasts is Arp 2/3 mediated. Osteoclast actin rings are now identified as being composed of discrete and dynamic actin based structures, termed podosomes (33, 34, 43). Presented immunocytochemical data confirms the current literature that podosomes are composed of a core of actin and associated proteins, such as the Arp2/3 complex, cortactin and VASP (35, 36). These proteins, when viewed in z-section, are concentrated at the resorptive surface, which is consistent with their role in the force production at the resorptive surface and their incorporation of actin into filaments at the resorptive surface and treadmilling toward the basolateral membrane. In addition, focal adhesion proteins, such as vinculin, do not co-localize with the actin ring but surround the actin ring, as a “cloud” (33, 34). Subsequent to our findings, Jurdic et al. (43) redefined the parameters of the podosomes of the actin ring. The actin ring podosomes differ from individual

podosomes in that the core proteins surround the entire ring instead of each individual podosome, as we observed with vinculin (43).

The dynamic nature of these podosomes was confirmed by various studies. First, rhodamine-actin incorporated into the actin ring of saponin-permeabilized RANKL stimulated RAW 264.7 cells within 10 minutes after treatment. In addition, the inclusion of latrunculin A, which sequesters G-actin, inhibits loss of podosomal structure. This indicates that new polymerization is inhibited while original filaments are treadmilling and disassembling. Second, treatment with various chemical agents known to disrupt actin ring structures, such as wortmannin, calcitonin and cytochalasin D, also show rapid dissolution and relocation of the podosomes in osteoclasts.

Upon stimulation by various factors, proteins are often upregulated in response to specific functions in cells. For the osteoclast, stimulation by RANKL and CSF cause the osteoclast to polarize and specialized structures specific to the resorbing osteoclast to form, specifically the ruffled membrane and the actin ring (8). We identified by PCR and western blot analysis two proteins that were upregulated in response to RANKL stimulation. The upregulation of Arp2 and Arp3 at a translational level and cortactin at a transcriptional level suggest that these proteins play specialized roles in osteoclastogenesis. In addition, their known association with actin related complexes suggests that this role is in the formation of the actin ring.

The function of the Arp2 and cortactin proteins on actin ring formation and osteoclast function were examined via knock down by siRNA. Knock down of

either protein resulted in a decrease in actin rings, confirming actin polymerization is mediated by the Arp2/3 complex. It was interesting to note that the Arp2 knock down cells appeared apoptotic while the cortactin knock down cells appeared viable. These data may support the role of the Arp2/3 complex in cell viability as well as its resorption function although a loss of actin ring formation cannot directly confirm a loss of bone resorption. Chellaiah et al. (165) showed initially that the gelsolin knock out mouse, which appeared to lack a podosomal-based actin ring, was capable of bone resorption albeit much reduced. The hypothesis is that alternative mechanisms of adhesion, such as integrins, are capable of maintaining adequate adhesion for the resorption compartment to remain intact. β3 -/- mice show decreased bone resorption, abnormal ruffled membranes, and increased osteoclast number, most likely caused from stimulation by hyperparathyroidism secondary to the hypocalcemia produced by decreased bone resorption (52). Skeletal remodeling in the β3 -/- mice proceeds even in the absence of $\alpha_v\beta3$; it is hypothesized that an adequate resorption rate is achieved by the increased number of osteoclasts, even in the presence of decreased resorption per osteoclast (52). Further studies with the gelsolin knockout mouse identify a WASP-containing actin ring, capable of maintaining bone resorption, with slightly reduced efficiency (219). These studies suggest that actin ring formation, in addition to integrins, is important for osteoclastic bone resorption as studies have shown that a loss of actin ring formation is concurrent with a reduction in bone resorption (31). The fact that reduced bone resorption has been identified even in the absence of the actin

rings suggests that the osteoclast has alternative adhesive mechanisms to support an extracellular resorption compartment (219). It is reasonable to postulate that for efficient bone resorption, both integrin-based adhesion and actin ring formation are necessary.

Arp2/3 mediated actin polymerization is known to proceed via a complex of proteins, including the Arp2/3 complex, n-WASP, and cortactin (135, 188). The Arp2/3 complex is inactive in its unbound form (136, 137). Activation of the Arp2/3 complex occurs via its interaction with members of the N-WASP family of proteins (136, 137). This interaction causes a conformational change in the structure of the complex, inducing actin polymerization (136, 137). Based on the data generated, as loss of Arp2 and cortactin disrupted actin ring formation, it was logical to propose that actin ring polymerization was a function of this ternary complex. Immunoprecipitation experiments with a GST-cortactin fusion protein pulled down Arp3, N-WASP, VASP, and the E subunit of V-ATPase. Although we cannot confirm if the binding is direct or indirect, the pull down of Arp3 and N-WASP is consistent with the formation of this ternary complex. The binding of V-ATPase and VASP were unexpected. The ability of cortactin to pull down the E subunit of V-ATPase may identify an additional binding partner for V-ATPase that may be involved in its translocation to and from the membrane.

Taken together, these data support the initial hypothesis generated for this project that actin ring formation is a result of Arp2/3 mediated actin polymerization. Based on new methods recently presented, further insights into

the effects of a loss of actin ring formation on bone resorption will be able to be elucidated (Future Directions).

The hypothesis that V-ATPase is translocated throughout the cell via Arp2/3 mediated actin polymerization is attractive as it poses a highly dynamic mechanism of movement and responds appropriately to several chemical mediators. However, current research does not support this hypothesis as we have been unable to show a direct link between V-ATPase and the Arp2/3 complex. A limitation of this study was that only the actin binding sequence of the B1 subunit was used to identify an interaction with the purified Arp2/3 complex. This sequence was used since the Arp2/3 complex and actin share extensive sequence homology; it would seem logical that they may also interact via the same binding site. Unfortunately, interaction was not detected via this sequence.

Although a link was not directly identified between the Arp2/3 complex and V-ATPase, immunoprecipitation experiments with the B-subunit of V-ATPase and signal transduction array did identify VASP as a potential binding partner to V-ATPase. VASP is known to be phosphorylated in response to activation by the PKA and PKG pathways (203, 207). Previous data also show that calcitonin, which activates the PKA pathway, disrupts actin rings (190, 191). When taken together, these data suggest that actin ring disruption may result from the phosphorylation of VASP. VASP is an actin-associated protein that tracks the fast growing end of actin filaments (201). The precise role of VASP remains unclear. However, it may be involved in protecting growing actin filaments ends

from capping proteins (201). Data have also been presented that indicate that VASP has the capacity to concentrate profilactin complex near the fast growing end of actin filaments and this may be vital to ensuring the rapid treadmilling of podosomes (202). One caveat to the role of VASP in osteoclastic bone resorption is that VASP knock out mice have no detected skeletal defects (213, 214). This study identifies that, in fact, VASP is present in the actin rings of osteoclasts and is phosphorylated in response to calcitonin treatment. However, based on immunocytochemical experimentation of osteoclasts of VASP knock out mice, there is no effect on actin ring formation. In addition, the response of the VASP knock out osteoclasts to calcitonin is equal to that of the control. These data suggests that VASP may not play a vital role in osteoclastic bone resorption. However, the Ena/VASP family member, EVL, identified specifically in cells of hematopoietic lineage (211), was found in this study to be preferentially upregulated in response to osteoclastogenesis. This protein warrants further study (Future Directions).

Future Directions

There are several future directions for this research. Previous siRNA knock down studies have lacked the ability to clearly define effects on in vitro bone resorption due to an extremely low efficiency of transfection of mouse marrow cultures. Although RAW 264.7 cells can be efficiently transfected, V-ATPase is not properly located to the ruffled membrane and thus bone resorption does not occur adequately for experimentation. Although the mechanisms of actin ring formation can be studied as there seems to be no effect on the actin

ring, bone resorption assays in RAW cells are suspect. Recent literature has identified a novel method of transfection of siRNAs into mouse marrow cultures (220). Experimental siRNA, along with RNAse inhibitors, are added directly to the mouse marrow osteoclasts prior to scraping and transferring to bovine dentin slices. The siRNA is taken up during transfer onto bone slices. This technique was recently published by Hu et al. (220), who showed successful knock down of the a3 subunit of V-ATPase by this method. Subsequent to that study, we also tested a known siRNA against the a3 subunit of V-ATPase on mouse marrow osteoclasts. Protein expression was reduced approximately 70-80%, which is extremely efficient for mouse marrow osteoclasts. If we are able to get this efficiency when knocking down Arp2 or cortactin with siRNA, we will be able to examine the effects on bone resorption in vitro.

Our hypothesis also focuses on the actin ring being responsible for force production required for the formation of an external resorption compartment. Arp2/3 mediated actin polymerization is known to be capable for force generation as is seen in the actin-based motility of certain pathogens such as *Listeria, Shigella* and *Rickettsia* and the enveloped virus vaccinia (151-153). This actin polymerization that serves as the basis for this movement results in an “actin comet tail”. This movement is involved in the spread of the pathogens from cell to cell (149, 150). Based on the capability of Arp2/3 mediated force generation, the data supporting the requirement of the actin ring for efficient bone resorption and the extremely tight adhesion at the region of the sealing zone, it is plausible that this adhesion is produced by force generation. A long term goal is to study

force generation of the actin ring of osteoclasts using deformable membranes. If force was generated against a deformable membrane, it should be identified as a divot in the membrane.

Another goal is to identify a link between Arp2/3 mediated actin polymerization and V-ATPase translocation. Recent studies have shown that V-ATPase directly binds to aldolase, which functions in glycolysis (26, 27). In addition, aldolase has been shown to interact with actin and actin-associated proteins such as WASP and cortactin (221, 222). These data suggest that aldolase may function as a link between the Arp2/3, cortactin, N-WASP ternary complex and V-ATPase. The dynamic interactions that interplay between these components may prove to be vital for translocation of V-ATPase to and from the plasma membrane. The identification of direct or indirect interactions between these proteins can be identified via immunoprecipitation experiments using GST-cortactin or GST-VCA domain of N-WASP constructs (Dr. Scott Weed, West Virginia University Morgantown, WV) or specific antibodies. Once direct binding partners are identified, specific binding sequences will be determined, and identification of the functional consequences examined by constructing fusion proteins with mutations in the binding region.

The identification of another ENA/VASP family member preferentially upregulated during osteoclastogenesis merits further identification. Based on literature studies, evl, which is highly expressed in hematopoietic cells (211), is the least studied of the three family members. Evl may function as the regulator of profilactin at the active sites of actin polymerization, which, if altered, may

affect actin nucleation rates. Characterization of this protein in the osteoclast model may give many valuable insights into actin ring formation. Initial studies will focus on the localization of evl using immunocytochemical experiments. If co-localized with the actin ring, further studies on the requirement of evl for actin ring formation using knock down studies will be performed. The loss of evl may not completely disrupt actin ring formation but may slow down polymerization; actin polymerization assays might prove useful to identify rate changes based on the presence or absence of evl.

Significance of Study

Bone homeostasis is the maintenance of a delicate balance between two opposite and dynamic processes, bone formation and resorption (2). Bone resorption is a mandatory event in the normal physiological functioning of the human body, required for such processes as human growth, tooth movement, and the maintenance of plasma calcium levels (223). Bone resorption also has extensive implications in disease processes. Enhanced bone resorption is associated with diseases such as malignant hypercalcemia, osteoporosis, osteolytic dysplasia, and metastatic bone tumors (224, 225). Such osteolytic lesions mediate bone resorption by either increasing osteoclastic stimulatory factors to activate differentiation of progenitor cells, activating mature osteoclasts directly, or inducing the immune system to release additional factors to stimulate bone resorption (225, 226). Osteoclastic cells observed in disease states are in general larger in size and number, resulting in an increased resorptive activity and efficiency (227). Morbidity associated with such resorptive diseases includes

pain, pathological fractures, debilitation, and deformity (225, 226). Although these diseases all have different etiologies, in each disease, a resorption lacunae must be segregated by the sealing zone, creating the acidic extracellular compartment, by which the mineralized bone is resorbed (54, 226).

This research has focused on identifying the proteins functioning in the formation of the sealing zone. We have identified for the first time the presence of Arp2/3 in the actin ring and that actin polymerization proceeds via an Arp2/3 mediated process as is shown by knock down of the protein. This process, in contrast to those utilizing formins or SPIRE (228, 229), results in networks of densely branched actin filaments, consistent with podosome structure (33). We have also identified that these branched networks are very dynamic and fairly sensitive to the surrounding environment. At this time, we have not established a mechanism for Arp 2/3 mediated V-ATPase translocation. However, based on these data, it is proposed that the Arp2/3 complex can pose as a target to alter osteoclast function.

We have also identified cortactin as an important protein in the actin ring of osteoclasts. Cortactin stabilizes the Arp2/3 mediated branched filaments (185). The knock down of cortactin in the actin ring of osteoclasts results in a loss of podosomal arrangement of the actin ring but the cells remain viable. This finding is significant as cortactin has also been implicated in cancer metastasis through the formation of podosomal-like invadopodia (230). The modulation of this protein may allow for alterations in bone resorption and cancer metastasis.

Although VASP initially appeared very promising in both its effects on actin ring function and translocation of V-ATPase to and from the ruffled membrane, experimentation proved otherwise. VASP is phosphorylated in response to the protein kinase A pathway (203, 207), which can cause a loosening of the actin ring. However, the osteoclasts from VASP knock out mice had normal actin ring morphology and no skeletal deformities were detected (213, 214). The benefit of studying VASP is the identification of another ENA/VASP family member, evl. Evl may prove to be the family member involved in actin ring dynamics.

The clinical significance of this project is the identification of the podosomal actin ring proteins and the effects of their knock down. It is known that podosomes are not only involved in physiological processes but also in disease states such as cancer (231). We have identified that the knock down of cortactin and Arp2 causes a disruption of podosomal organization. Based on our findings, it is hypothesized that these proteins could be targeted using viral vector therapy and/or osteoclast specific promoters to regulate osteoclastic bone resorption or possibly inhibit cancer metastasis.

REFERENCE LIST

1. Horowitz MC, Xi Y, Wilson K, Kacena MA. Control of osteoclastogenesis and bone resorption by members of the TNF family of receptors and ligands. Cytokine and Growth Factor Reviews. 2001; 12: 9-18.

2. Rousselle AV, Heymann D. Osteoclastic acidification pathways during bone resorption. Bone. 2002; 30(4):533-540.

3. Teitelbaum SL. Osteoclasts, integrins and osteoporosis. J Bone Miner Metab. 2000; 18:344-349.

4. Wada T, Nakashima T, Hiroshi N, Penninger JM. RANKL-RANK signaling in osteoclastogenesis and bone disease. TRENDS in Molecular Medicine. 2005; 20(20):1-9.

5. Stenbeck G, Horton MA. A new specialized cell-matrix interaction in actively resorbing osteoclasts. J Cell Sci. 2000; 113:1577-1587.

6. Redey SA, Razzouk S, Rey C, Bernache-Assollant D, Leroy G, Nardin M, Cournot G. Osteoclast adhesion and activity on synthetic hydroxyapatite, carbonated hydroxyapatite, and natural calcium carbonate: relationship to surface energies. J Biomed Mater Res. 1999; 45(2):140-147.

7. Salo J, Metsikko K, Palokangas H, Lehenkari P, Vaananen HK. Bone-resorbing osteoclasts reveal a dynamic division of basal plasma membrane into two different domains. J Cell Sci. 1996; 109:301-307.

8. Vaananen HK, Zhao H, Mulari M, Halleen JM. The cell biology of osteoclast function. J Cell Sci. 2000; 113:377-381.

9. Lee BS, Gluck SL, Holliday SL. Interaction between vacuolar H^+-ATPase and microfilaments during osteoclast activation. J Biol Chem. 1999; 274(41):29164-29171.

10. Suda T, Nakamura I, Jimi E, Takahashi N. Regulation of osteoclast function. J Bone Miner Res. 1997; 12:869-879.

11. Holliday LS, Lu M, Lee BS, Nelson RD, Solivan S, Zhang L, Gluck SL. The amino-terminal domain of the B subunit of vacuolar H^+-ATPase contains a filamentous actin binding site. J Biol Chem. 2000; 275(41): 32331-32337.

12. Holliday LS, Welgus HG, Fliszar CJ, Veith GM, Jeffrey JJ, Gluck SL. Initiation of osteoclast bone resorption by interstitial collagenase. J Biol Chem. 1997; 272(35):22053-22058.

13. Boyle WJ, Simonet WS, Lacey DL. Osteoclast differentiation and activation. Nature. 2003; 423:337-342.

14. Ash P, Loutit JF, Townsend KMS. Osteoclasts derived from hematopoietic stem cells. Nature. 1980; 283:669-670.

15. Gothlin G, Ericsson J. The osteoclast. Clin Orthoped Rel Res. 1976; 120:201-231.

16. O'Brien EA, Williams JHH, Marshall MJ. Osteoprotegerin ligand regulates osteoclast adherence to the bone surface in mouse calvaria. Biochem Biophys Res Commun. 2000; 274:281-290.

17. Theoleyre S, Wittrant Y, Tat SK, Fortun Y, Redini F, Heymann D. The molecular triad OPG/RANK/RANKL: involvement in the orchestration of pathophysiological bone remodeling. Cytokine and Growth Factor Reviews. 2004; 15:47-475.

18. Ryu J, Kim H, Lee SK, Chang E-J, Kim HJ, Kim H-H. Proteomic identification of the TRAF6 regulation of vacuolar ATPase for osteoclast function. Proteomics. 2005; 5:4152-4160.

19. Nermut MV, Eason P, Hirst EM, Kellie S. Cell/substratum adhesions in RSV-transformed rat fibroblasts. Exp.Cell Res. 1991; 193: 382-397.

20. Tsukii K, Shima N, Mochizuki S, Yamaguchi K, Kinosaki M, Yano K, Shibata O, Udagawa N, Yasuda H, Suda T, Higashio K. Osteoclast differentiation factor mediates an essential signal for bone resorption induced by 1α,25-dihydroxyvitamin D_3, prostaglandin E_2, or parathyroid hormone in the microenvironment of bone. Biochem Biophys Res Commun. 1998; 246:337-341.

21. Yasuda H, Shima N, Nakagawa N, Yamaguchi K, Kinosaki M, Mochizuki S, Tomoyasu A, Yano K, Goto M, Murakami A, Tsuda E, Morinaga T, Higashio K, Udagawa N, Takahashi N, Suda T. Osteoclast differentiation factor is a ligand for osteoprotegerin/ osteoclastogenesis-inhibitory factor and is identical to TRANCE/RANKL. Proc Natl Acad Sci USA. 1998; 95:3597-3602.

22. Suda T. Udagawa N, Nakamura I, Miyaura C, Takahashi N. Modulation of osteocalst differentiation by local factors. Bone. 1995; 17(Suppl.2):87S-91S.

23. Blair HC, Teitelbaum SL, Ghiselli R, Gluck S. Osteoclastic bone resorption by a polarized vacuolar proton pump. Science. 1989; 245:855-857.

24. Ohlsson A, Cumming WA, Paul A, Sly WS. Carbonic anhydrase II deficiency syndrome: recessive osteopetrosis with renal tubular acidosis and cerebral calcification. Pediatrics. 1986; 77(3): 371-381.

25. Whyte MP. Carbonic anhydrase II deficiency. Clin Orthop Relat Res. 1993; 294:52-63.

26. Lu M, Sautin YY, Holliday LS, Gluck SL. The glycolytic enzyme aldolase mediates assembly, expression, and activity of vacuolar H+-ATPase. J Biol Chem. 2004; 279(10):8732-9.

27. Lu M, Holliday LS, Zhang L, Dunn WA, Gluck SL. Interaction between aldolase and vacuolar H+-ATPase: evidence for direct coupling of glycolysis to the ATP-hydrolyzing proton pump. J Biol Chem. 2001; 276(32):30407-13.

28. Schlesinger PH, Blair HC, Teitelbaum SL, Edwards JC. Characterization of the osteoclast ruffled border chloride channel and its role in bone resorption. J Biol Chem. 1997; 272:18636-18643.

29. Holtrop ME, King GJ. The ultrastructure of the osteoclast and its functional implications. Clin Orthop. 1977; 123:177-196.

30. Helfrich MH, Nesbitt SA, Lakkakorpi PT, Barnes MJ, Bodary SC, Shankar G, Mason WT, Mendrick DL, Vaananen HK, Horton MA. β_1 integrins and osteoclast function: involvement in collagen recognition and bone resorption. Bone. 1996; 19(4):317-328.

31. Nakamura I, Takahashi N, Sasaki T, Tanaka S, Udagawa N, Murakami H, Kimura K, Kabuyama Y, Kurokawa T, Suda T, Fukui Y. Wortmannin, a specific inhibitor of phosphatidylinositol-3 kinase, blocks osteoclastic bone resorption. FEBS. 1995; 361:79-84.

32. Lakkakorpi PT, Vaananen HK. Cytoskeletal changes in osteoclasts during the resorptive cycle. Microsc Res Tech. 1996; 33(2):171-81.

33. Destaing O, Saltel F, Geminard J-C, Jurdic P, Bard F. Podosomes display actin turnover and dynamic self-organization in osteoclasts expressing actin-green fluorescent protein. Mol Biol of Cell. 2003; 14:407-416.

34. Luxenburg C, Addadi L, Geiger B. The molecular dynamics of osteoclast adhesions. Eur J Cell Biol. 2006; 85(3-4):203-11.

35. Linder S, Kopp P. Podosomes at a glance. J Cell Sci. 2005. 118(10); 2079-2082.

36. Buccione R, Ortho JD, MA McNiven. Foot and mouth: podosomes, invadopodia and circular dorsal ruffles. Nat Rev Mol Cell Biol. 2004; 5:647-657.

37. Akisaka T, Yoshida H, Inoue S, Shimizu K. Organization of cytoskeletal F-actin, G-actin, and gelsolin in the adhesion structures in cultured osteoclast. J Bone Miner Res. 2001; 16(7):1248-55.

38. Lehto VP, Hovi T, Vartio T, Badley RA and Virtanen I. Reorganization of cytoskeletal and contractile elements during transition of human monocytes into adherent macrophages. 1982. Lab. Invest. 47: 391-199.

39. Pfaff M, Jurdic P. Podosomes in osteoclast-like cells: structural analysis and cooperative roles of paxillin, proline-rich tyrosine kinase 2 (Pyk2) and integrin alphaVbeta3. J Cell Sci. 2001; 114:2775-2786.

40. Moreau V, Tatin F, Varon C, and Genot E. Actin can reorganize into podosomes in aortic endothelail cells, a process controlled by Cdc42 and RhoA. Mol Cell Biol. 2003; 23:6809-6822.

41. Tarone G, Cirillo D, Giancotti FG, Comoglio PM, and Marchisio PC. Rous sarcoma virus-transformed fibroblasts adhere primarily at discrete protrusions of the ventral membrane called podosomes. Exp Cell Res. 1985; 159:141-157.

42. McNiven MA, Baldassarre M, Buccione R. The role of dynamin in the assembly and function of podosomes and invadopodia. Front. Biosci. 2004; 9:1944-1953.

43. Jurdic P, Saltel F, Chabadel A, Destaing O. Podosome and sealing zone: Specificity of the osteoclast model. Eur J Cell Biol. 2006; 85(3-4):195-202.

44. Chellaiah M, Fitzgerald C, Alvarez U, Hruska K. c-Src is required for stimulation of gelsolin-associated phosphatidylinositol 3-kinase. J Biol Chem. 1998; 273:11908-11916.

45. Coue M, Brenner SL, Spector I, Korn ED. Inhibition of actin polymerization by latrunculin A. FEBS letters. 1987; 213:316-318.

46. Yarmola EG, Somasundaram T, Boring TA, Spector I, Bubb MR. Actin-latrunculin A structure and function. J Biol Chem. 2000; 275(36):28120-28127.

47. Burns S, Thrasher AJ, Blundell MP, Machesky L, Jones GE. Configuration of human dendritic cell cytoskeleton by Rho GTPases, the WAS protein, and differentiation. Blood. 2001; 98:1142-1149.

48. Linder S, Aepfelbacher M. Podosomes: adhesion hot-spots of invasive cells. Trends Cell BIol. 2003; 13:376-385.

49. Marchisio PC, D'Urso N, Comoglio PM, Giancotti FG, Tarone G.. Vanadate-treated baby hamster kidney fibroblasts show cytoskeleton and adhesion patterns similar to their Rous sarcoma virus-transformed counterparts. J Cell Biochem. 1988; 37:151-159.

50. Vaananen HK, Karhukorpi EK, Sundquist K, Wallmark B, Roininen I, Hentunen T, Tuukkanen J, Lakkakorpi P. Evidence for the presence of a proton pump of the vacuolar H(+)-ATPase type in the ruffled borders of osteoclasts J Cell Biol. 1990; 111:1305-1311.

51. Zuo J, Jiang J, Chen SH, Vergara S, Gong Y, Xue J, Huang H, Kaku M, Holliday LS. Actin Binding Activity of Subunit B of Vacuolar H(+)-ATPase Is Involved in Its Targeting to Ruffled Membranes of Osteoclasts. J Bone Miner Res. 2006; 21(5): 714-21.

52. McHugh KP, Hodivala-Dilke K, Zheng MH, Namba N, Lam J, Novack D, Feng X, Ross FP, Hynes RO, Teitelbaum SL. Mice lacking β3 integrins are osteosclerotic because of dysfunctional osteoclasts. J Clin Invest. 2000; 105:433-440.

53. Hynes RO. Integrins: versatility, modulation, and signaling in cell adhesion. Cell. 1992; 69:11-25.

54. Duong LT, Lakkakorpi P, Nakamura I, Rodan GA. Integrins and signaling in osteoclast function. Matrix Biol. 2000; 19:97-105.

55. Chambers TJ, Fuller K, Darby JA, Pringle JAS, Horton MA, Monoclonal antibodies against osteoclasts inhibit bone resorption in vitro. J Bone Miner Res. 1986; 1:127-135.

56. Sato M, Garsky MK, Grasser WA, Garsky VM, Murray JM, Gould RJ. Structure-activity studies of the s-echistatin inhibition of bone resorption. J Bone Miner. Res. 1994; 9:1441-1449.

57. Lakkakorpi PT, Horton MA, Helfrich MH, Karhukorpi EK, Vaananen HK. Vitronectin receptor has a role in bone resorption but does not mediate tight sealin zone attachment of osteoclasts to the bone surface. J Cell Biol. 1991; 115:1179-1186.

58. Horton MA, Taylor ML, Arnett TR, Helfrich MH. Arg-Gly-Asp (RGD) peptides and the anti-vitronectin receptor antibody 23C6 inhibit dentine resorption and cell spreading by osteoclasts. Exp Cell Res. 1991; 195:368-375.

59. Masarachia P, Yamamoto M, Leu C-T, Rodan G, Duong LT. Histomorphometric evidence for echistatin inhibition of bone resorption in mice with secondary hyperparathyroidism. Endocrinology. 1998; 139: 1401-1410.

60. Nakamura I, Pilkington MF, Lakkakorpi PT, Lipfert L, Sims SM, Dixon SJ, Rodan GA, Duong LT. Role of $\alpha v\beta 3$ integrin in osteoclast migration and formation of the sealing zone. J Cell Sci. 1999; 112:3985-3993.

61. Masarachia P, Yamamoto M, Rodan GA, Duong LT. Co-localization of the vitronectin receptor $\alpha_v\beta_3$ and echistatin in osteoclasts during bone resorption. J Bone Miner Res. 1995; 10(Suppl 1): S164.

62. Helfrich MH. Osteoclast diseases and dental abnormalities. Archives or Oral Biology. 2005; 50:115-122.

63. Balemans W, Van Wesenbeeck L, Van Hul W. A clinical and molecular overview of human osteopetroses. Calcif Tissue Int. 2005; 77:263-274.

64. Alper SL. Genetic disease of acid-base transporters. Annu Rev Physiol. 2002; 64:899-923.

65. Frattini A, Orchard PJ, Sobacchi C, Giliani S, Abinun M, Mattsson JP, Keeling DJ, Andersson A-K, Wallbrandt P, Zecca L, Notarangelo LD, Vezzoni P, Villa A. Nature Genetics. 2000; 25:343-346.

66. Susani L, Pangrazio A, Sobacchi C, Taranta A, Mortier G, Savarirayan R, Villa A, Orchard P, Vezzoni P, Albertini A, Frattini A, Pagani F. TCIFG1-dependent recessive osteopetrosis: mutation analysis, functional identification of the splicing defects, and in vitro rescue by U1 snRNA. Hum Mutat. 2004; 24(3):225-35.

67. Kornak U, Kasper D, Bosl MR, Kaiser E, Schweizer M, Schulz A, Friedrich W, Delling G, Jentsch TJ. Loss of the ClC-7 chloride channel leads to osteopetrosis in mice and man. Cell. 2001; 104(2):205-15.

68. Waguespack SG, Koller DL, White KE, Fishburn T, Carn G, Buckwalter KA, Johnson M, Kocisko M, Evans WE, Foroud T, Econs MJ. Chloride channel 7 (ClCN7) gene mutations and autosomal dominant osteopetrosis, type II. J Bone Miner Res. 2003; 18(8):1513-1518.

69. Cleiren E, Benichou O, Van Hul E, Gram J, Bollersley J, Singer FR, Beaverson K, Aledo A, Whyte MP, Yoneyama T, deVernejoul MC, Van Hul W. Albers-schonberg disease (autosomal dominant osteopetrosis, type II) results from mutations in the ClCN7 chloride channel gene. Hum Mol Genet. 2001; 10(25):2861-7.

70. Henriksen K, Gram J, Hoegh-Andersen P, Jemtland R, Ueland T, Dziegiel MH, Schaller S, Bollerslev J, Karsdal MA. Osteoclasts from patients with autosomal dominant osteopetrosis type I caused by a T253I mutation in low-density lipoprotein receptor-related protein 5 are normal in vitro, but have decreased resorptive capacity in vivo. Am J Pathol. 2005; 167(5):1341-8.

71. Boyden LM, Mao J, Belsky J, Mitzner L, Farhi A, Mitnick MA, Wu D, Insogna K, Lifton RP. High bone density due to a mutation in LDL-receptor-related protein 5. N Engl J Med 2002; 346:1513–1521.

72. Little RD, Carulli JP, Del Mastro RG, Dupuis J, Osborne M, Folz C, Manning SP, Swain PM, Zhao SC, Eustace B, Lappe MM, Spitzer L, Zweier S, Braunschweiger K, Benchekroun Y, Hu X, Adair R, Chee L, FitzGerald MG, Tulig C, Caruso A, Tzellas N, Bawa A, Franklin B, McGuire S, Nogues X, Gong G, Allen KM, Anisowicz A, Morales AJ, Lomedico PT, Recker SM, Van Eerdewegh P, Recker RR, Johnson ML. A mutation in the LDL receptor-related protein 5 gene results in the autosomal dominant high-bone-mass trait. Am J Hum Genet. 2002; 70:11 19.

73. Kiviranta R, Morko J, Alatalo SL, NicAmhlaoibh R, Risteli J, Laitala-Leinonen T, Vuorio E. Impaired bone resorption in cathepsin K-deficient mice is partially compensated for by enhanced osteoclastogenesis and increased expression of other proteases via an increased RANKL/OPG ratio. Bone. 2005; 36(1):159-172.

74. Li CY, Jepsen KJ, Majeska RJ, Zhang J, Ni R, Gelb BD, Schaffler MB. Mice lacking cathepsin K maintain bone remodeling but develop bone fragility despite high bone mass. J Bone Miner Res. 2006; 21(6):865-875.

75. Ho N, Punturieri A, Wilkin D, Szabo J, Johnson M, Whaley J, Davis J, Clark A, Weiss S, Francomano C. Mutations of CTSK result in pycnodysostosis via a reduction in cathepsin K protein. J Bone Miner res. 1999; 14(10):1649-1653.

76. Sly WS, Hewett-Emmett D, Whyte MP, Yu Y-SL, Tashian RE. Carbonic anhydrase II deficiency identified as the primary defect in the autosomal recessive syndrome of osteopetrosis with renal tubular acidosis and cerebral calcification. Proc Natl Acad Sci USA. 1983; 80:2752-2756.

77. Helfrich MH. Osteoclast diseases. Microsc Res Tech. 2003; 61(6):514-32.

78. Layfield R, Hocking LJ. SQSTM1 and paget's disease of bone. Calcif Tissue Int. 2004; 75(5):347-57.

79. Hocking LJ, Lucas GJ, Daroszweska A, Mangion J, Olavesen M, Cundy T, Nicholson GC, Ward L, Bennett ST, Wuyts W, Van Hul W, Ralston SH. Domain-specific mutations in sequestosome 1 (SQSTM1) cause familial and sporadic paget's disease. Hum Mol Genet. 2002; 11(22):2735-9.

80. Hughes AE, Ralston SH, Marken J, Bell C, MacPherson H, Wallace RG, van Hul W, Whyte MP, Nakatsuka K, Hovy L, Anderson DM. Mutations in TNFRSF11A, affecting the signal peptide of RANK, cause familial expansile osteolysis. Nat Genet. 2000; 24:45-48.

81. Wuyts W, Van Wesenbeeck L, Morales-Piga A, Ralston S, Hocking L, Vanhoenacker F, Westhovens R, Verbruggen L, Anderson D, Hughes A, Van Hul W. Van Wesenbeeck L, Morales-Piga A. Evaluation of the role of RANK and OPG genes in Paget's disease of bone. Bone. 2001; 28:104-107.

82. Hofbauer LC, Huefelder AE. The role of receptor activator of nuclear factor-kB ligand and osteoprotegerin in the pathogenesis and treatment of metabolic bone diseases. J Clin Endocrinol. 2000; 85:2355-2363.

83. Dickson GR, Shirodria PV, Kanis JA, Beneton MN, Carr KE, Mollan RA. Familial expansile osteolysis: a morphological, histomorphometric and serological study. Bone. 1991; 12(5):331-8.

84. Walsh NC, Crotti TN, Goldring SR, Gravallese EM. Rheumatic diseases: the effects of inflammation on bone. Immunol Rev. 2005; 208:228-51.

85. Boyce BF, Li P, Yao Z, Zhang Q, Badell IR, Schwarz EF, O'Keefe RJ, Xing L. TNF-alpha and pathologic bone resorption. Keio J Med. 2005; 54(3): 127-31.

86. Takayanagi H. Inflammatory bone destruction and osteoimmunology. J Periodont Res. 2005; 40:287-293.

87. Harada S-I, Rodan GA. Control of osteoblast function and regulation of bone mass. Nature. 2003; 423:349-355.

88. Cosman F. The prevention and treatment of osteoporosis: a review. Med Gen Med. 2005; 7(2):73.

89. Delaney MF. Strategies for the prevention and treatment of osteoporosis during early menopause. Am. J. Obstet. Gynecol. 2006; 194 (2supplement):S12-22.

90. Rusoff LL. Calcium – osteoporosis and blood pressure. J Dairy Sci. 1987; 20(2):407-13.

91. Hobar C. Osteoporosis and Calcium. eMedicine.com, Inc. http://www.emedicinehealth.com. 2005; accessed 4/2006.

92. Reginster JY, Sarlet N. The treatment of severe menopausal osteoporosis: a review of current and emerging therapeutic options. Treat Endocrinol. 2006; 5(1):15-23.

93. Handy RC, Chesnut CH 3rd, Gass MC, Holick MF, Leib ES, Lewiecki ME, Maricic M, Watts NB. Review of treatment modalities for postmenopausal osteoporosis. South Med J. 2005; 98(10):1000-14.

94. Rosenberg LU, Magnusson C, Lindstrom E, Wedren S, Hall P, Dickman PW. Menopausal hormone therapy and other breast cancer risk factors in relation to the risk of different histological subtypes of breast cancer: a case-control study. Breast Cancer Res. 2006; 8(1):R11.

95. Wu O. Postmenopausal hormone replacement therapy and venous thormboembolism. Gend Med. 2005; 2 Suppl A:S18-27.

96. Rogers MJ. New insights into the molecular mechanism of action of bisphosphonates. Curr Pharm Des. 2003; 9(32):2643-2658.

97. Palomo L. Bissada N, Liu J. Bisphosphanate therapy for bone loss in patients with osteoporosis and periodontal disease: clinical perspectives and review of literature. Quitessence Int. 2006; 37(2):103-107.

98. Luckman SP, Hughes DE, Coxon FP, Graham R, Russell G, Rogers MJ. Nitrogen-containing bisphosphonates inhibit the mevalonate pathway and prevent post-translational prenylation of GTP-binding proteins, including Ras. J Bone Miner Res. 1998; 13(4):581-9.

99. Tanvetayanon T, Stiff PJ. Management of the adverse effects associated with intravenous bisphosphonates. Ann Oncol. 2006; 17(6):897-907.

100. Lanza FL. Gastrointestinal adverse effects of bisphosphonates: etiology, incidence and prevention. Treat Endocrinol. 2002; 1(1):37-43.

101. Badros A, Weikel D, Salama A, Goloubeva O, Schneider A, Rapoport A, Fenton R, Gahres N, Sausville E, Ord R, Meiller T. Osteonecrosis of the jaw in multiple myeloma patients: clinical features and risk factors. J Clin Oncol. 2006; 24(6):945-952.

102. Farrugia MC, Summerlin DJ, Krowiak E, Huntley T, Freeman S, Borrowdale R, Tomich C. Osteonecrosis of the mandible or maxilla associated with the use of new generation bisphosphonates. Laryngoscope. 2006; 116(1):115-120.

103. Melo MD, Obeid G. Osteonecrosis of the jaws in patients with a history of receiving bisphosphonate therapy: strategies for prevention and early recognition. J Am Dent Assoc. 2005; 136(12):1675-81.

104. Greenblatt D. Treatment of postmenopausal osteoporosis. Pharmacotherapy. 2005; 25(4), 574-584.

105. Mahakala A, Thoutreddy S, Kleerekoper M. Prevention and treatment of postmenopausal osteoporosis. Treat Endocrinol. 2003; 2(5): 331-345.

106. Gennari C, Agnusdei D. Calcitonins and osteoporosis. Br J Clin Pract. 1994; 48(4):196-200.

107. Wada S, Yasuda S. Appropriate clinical usage of calcitonin escape phenomenon and intermittent vs daily administration of calcitonin. Clin Calcium. 2001; 11(9):1169-1175.

108. St-Marie CG, Schwartz SL, Hossain A, Desaiah D. Gaich GA. Effect of teriparatide on bone mineral density when given to postmenopausal women receiving HRT. J Bone Miner Res. 2006; 21(2):283-291.

109. Holick MF. PTH(1-34): a novel anabolic drug for treatment of osteoporosis. South Med J. 2005; 98(11):1114-1117.

110. Bilezikian JP. Anabolic therapy for osteoporosis. Int J Fertil Womens Med. 2005; 50(2):53-60.

111. Brixen KT, Christensen PM, Ejersted C, Langdahl BL. Teriparatide (Biosynthetic human parathyroid hormone 1-34): a new paradigm in the treatment of osteoporosis. Basic Clin Pharmacol Toxicol. 2004; 94(6):260-70.

112. Burlet N, Reginster J-Y. Strontium ranelate: the first dual acting treatment for postmenopausal osteoporosis. Clin Orthopaed Rel Res. 2006; 443, 55-60

113. Kocher MS, Kasser JR. Osteopetrosis. Am J Orthop. 2003; 32(5):222-228.

114. Ogbureke KU, Zhao Q, Li YP. Human osteopetroses and the osteoclast V-H^+-ATPase enzyme system. Front Biosci. 2005; 10:2940-2954.

115. Coccia PF, Krivit W, Cervenka J, Clawson C, Kersey JH, Kim TH, Nesbit ME, Ramsay NK, Warkentin PI, Teitelbaum SL, Kahn AJ, Brown DM. Successful bone-marrow transplantation for infantile malignant osteopetrosis. N Engl J Med. 1980; 302(13):701-708.

116. Mogi M, Otogoto J, Ota N, Togari A. Differential expression of RANKL and osteoprotegerin in gingival crevicular fluid of patients with periodontitis. J Dent Res. 2004; 83(2):166-9.

117. Taubman MA, Valverde P, Han X, Kawai T. Immune response: the key to bone resorption in periodontal disease. J Periodontol. 2005; 76(11 Suppl):2033-41.

118. Crotti T, Smith MD, Hirsch R, Soukoulis S, Weedon H, Capone M, Ahern MJ, Haynes D. Receptor activator NF kappaB ligand (RANKL) and osteoprotegerin (OPG) protein expression in periodontitis. J Periodontol Res. 2003; 38(4):380-7.

119. Talic NF, Evans C, Zaki AM. Inhibition of orthodontically induced root resorption with echistatin, an RGD-containing peptide. Am J Orthod Dentofac Orthop. 2006; 129(2):252-60.

120. Al-Qawasami RA, Hartsfield JK Jr, Everett ET, Flury L, Liu L, Foroud TM, Macri JV, Roberts WE. Genetic predisposition to external apical root resorption. Am J Orthod Dentofac Orthop. 2003; 123(3):242-52.

121. Low E, Zoellner H, Kharbanda OP, Darendeliler MA. Expression of mRNA for osteoprotegerin and receptor activator of nuclear factor kappa beta ligand (RANKL) during root resorption induced by the application of heavy orthodontic forces on rat molars. Am J Orthod Dentofac Orthop. 2005; 128(4):497-503.

122. Jager A, Zhang D, Kawarizadeh A, Tolba R, Braumann B, Lossdorfer S, Gotz W. Soluble cytokine receptor treatment in experimental orthodontic tooth movement in the rat. Eur J Orthod. 2005; 27(1):1-11.

123. Dolce C, Vakani A, Archer L, Morris-Wiman JA, Holliday LS. Effects of echistatin and an RGD peptide on orthodontic tooth movement. J Dent Res. 2003; 82(9):682-6.

124. Holliday LS, Vakani A, Archer L, Dolce C. Effects of matrix metalloproteinase inhibitors on bone resorption and orthodontic tooth movement. J Dent Res. 2003; 82(9):687-91.

125. Kanzaki H, Chiba M, Takahashi I, Haruyama N, Nishimura M, Mitani H. Local OPG gene transfer to periodontal tissue inhibits orthodontic tooth movement. J Dent Res. 2004; 83(12):920-5.

126. Yoshimatsu M, Shibata Y, Kitaura H, Chang X, Moriishi T, Hashimoto F, Yoshida N, Yamaguchi A. Experimental model of tooth movement by orthodontic forces in mice and its application to tumor necrosis factor receptor-deficient mice. J Bone Miner Metab. 2006; 24(1):20-7.

127. Sasaki T. Differentiation and functions of osteoclasts and odontoclasts in mineralizerd tissue resorption. Microsc Res Tech. 2003; 61(6):483-95.

128. Machesky LM, Atkinson SJ, Ampe C, Vandekerckhove J, Pollard TD. Purification of a cortical complex containing two unconventional actins from Acanthamoeba by affinity chromatography on profilin-agarose. J Cell Biol. 1994; 127:107-115.

129. Olazabal IM and Machesky LM. Abp1p and cortactin, new “hand-holds” for actin. J Cell Biol. 2001; 154(4):679-682.

130. Welch MD, Iwamatsu A, Mitchison TJ. Actin polymerization is induced by Arp2/3 protein complex at surface of *Listeria monocytogenes.* Nature. 1997; 285:265-269.

131. Machesky LM and Gould KL. The arp2/3 complex: a multifunctional actin organizer. Curr Opin in Cell Biol. 1999; 11:117-121.

132. Winter D, Podtelejnikov AV, Mann M, Li R. The complex containing actin-related proteins Arp2 and Arp3 is required for the motility and integrity of actin patches. Curr Biol. 1997; 7:519-529.

133. Welch MD. The world according to Arp: regulation of actin nucleation by the Arp2/3 complex. Trends in Cell Biology. 1999; 9:423-427.

134. Mullins RD, Heuser JA, Pollard TD. The interaction of Arp2/3 complex with actin-nucleation, high affinity pointed end capping, and formation of branching networks of filaments. Proc Natl Acad Sci USA. 1998; 95:6181-6186.

135. Uruno T, Liu J, Zhang P, Fan Y, Egile C, Li R, Mueller SC, Zhan X. Activation of Arp2/3 complex-mediated actin polymerization by cortactin. Nat Cell Biol. 2001; 3(3):259-266.

136. Schafer DA, Schroer TA. Actin-related proteins. Annu Rev Cell Dev. Biol. 1999; 15:341-363.

137. Mullins RD, Pollard TD. Structure and function of the Arp2/3 complex. Curr Opin in Struct Biol. 1999; 9:244-249.

138. Robinson RC, Turbedsky K, Kaiser DA, Marchand J-B, Higgs HN, Choe S, Pollard TD. Crystal structure of Arp2/3 complex. Science. 2001; 294: 1679-1684.

139. Higgs HN, Pollard TD. Regulation of actin filament network formation through Arp2/3 complex: activation by a diverse array of proteins. Annu Rev Biochem. 2001; 70:649-676.

140. Mullins RD, Stafford WF, Pollard TD. Structure, subunit topology and actin-binding activity of the Arp2/3 complex from Acanthamoeba. J Cell Biol. 1997; 136(2):331-343.

141. Machesky LM, Reeves E, Wientjes F, Mattheyse FJ, Grogan A, Totty NF, Burlingame AL, Hsuan JJ, Segal AW. Mammalian actin-related protein 2/3 complex localizes to regions of lamellipodial protrusion and is composed of evolutionarily conserved proteins. Biochem J. 1997; 328: 105-112.

142. Jay B, Berge-Lefranc JL, Massacrier A, Roessler E, Wallis D, Muenke M, Gastaldi M, Taviaux S, Cau P, Berta P. ARP3beta, the gene encoding a new human actin-related protein, is alternatively spliced and predominantly expressed in brain neuronal cells. Eur J Biochem. 2000; 267(10):2921-2928.

143. Suetsugu S, Miki H, Takenawa T. Spatial and temporal regulation of actin polymerization for cytoskeleton formation through Arp2/3 complex and wasp/wave proteins. Cell Motility and Cytoskeleton. 2002; 51:113-122.

144. Dayel MJ, Holleran EA, Mullins RD. Arp2/3 complex requires hydrolyzable ATP for nucleation of new actin filaments. PNAS. 2001; 98(26):14871-14876.

145. Condeelis J. How is actin polymerization nucleated in vivo? Trends in Cell Biology. 2001; 11(7):288-293.

146. Cooper JA, Schafer DA. Control of actin assembly and disassembly at filament ends. Curr Opin Cell Biol. 2000; 12:97-103.

147. May RC, Caron E, Hall A, Machesky LM. Involvement of the Arp2/3 complex in phagocytosis mediated by FcγR or CR3. Nat Cell Biol. 2000; 2:246-248.

148. Moreau V, Galan J-M, Devilliers G, Haguenauer-Tsapis R, Winsor B. The yeast actin-related protein Arp2p is required for the internalization step of endocytosis. Mol Cell Biol. 1997; 8:1361-1375.

149. Skoble J, Auerbuch V, Goley ED, Welch MD, Portnoy DA. Pivotal role of VASP in Arp2/3 complex-mediated actin nucleation, actin branch-formation, and *Listeria monocytogenes* motility. J Cell Biol. 2001; 155(1): 89-100.

150. Zalevsky J, Grigorova I, Mullins RD. Activation of the Arp2/3 complex by *Listeria* ActA protein. J Biol Chem. 2001; 276(5):3468-3475.

151. Bear JE, Krause M, Gertler FB. Regulating cellular actin assembly. Curr Opin Cell Biol. 2001; 13:158-166.

152. Cudmore S, Cossart P, Griffiths G, Way M. Actin-based motility of vaccinia virus. Nature. 1995; 378:636-638.

153. Taunton J, Rowning BA, Coughlin ML, Wu M, Moon RT, Mitchison TJ, Larabell CA. Actin-dependent propulsion of endosomes and lysosomes by recruitment of N-WASP. J Cell Biol. 2000; 148(3):519-530.

154. Loisel TP, Boujemaa R, Pantaloni D, Carlier MF. Reconstitution of actin based motility of Listeria and Shigella using pure proteins. Nature. 1999; 40:613-616.

155. Welch MD, Mitchison TJ. Purification and assay of the platelet Arp2/3 complex. Methods Enzymol. 1998; 298:52-61.

156. Cooper JA. Effects of cytochalasin and phalloidin on actin. J Cell Biol. 1987; 105:1473-1478.

157. MacLean-Fletcher SD, Pollard TD. Mechanism of action of cytochalasin B on actin. Cell. 1980; 20:329-341.

158. Ziwarl A, Xie MW, Xing Y, Lin L, Zhang PF, Zou W, Saxe JP, Huang J. Novel function of the PI metabolic pathway discovered by a chemical genomics screen by wortmannin. Proc Natl Acad Sci USA. 2003; 100(6):3345-3350.

159. Sato M, Sardana MK, Grasser WA, Garsky VM, Murray JM, Gould RJ. Echistatin is a potent inhibitor of bone resorption in culture. J Cell Biol. 1990; 111(4):1713-23.

160. Pollard TD, Blanchoin L, Mullins RD. Actin dynamics. J Cell Sci. 2001; 114:3-4.

161. Blanchoin L, Amann KJ, Higgs HN, Marchand JB, Kaiser DA, Pollard TD. Direct observation of dendritic actin filament networks nucleated by Arp2/3 complex and WASP/Scar proteins. Nature. 2000; 404(6781):1007-11.

162. Pollard TD, Beltzner CC. Structure and function of the Arp2/3 complex. Curr Opin Struct Biol. 2002;12(6):768-74.

163. Chellaiah MA, Biswas RS, Yuen D. Alvarez UM, Hruska KA. Phosphatidylinositol 3,4,5-triphosphate directs association of Src homology 2-containing signaling proteins with gelsolin. J Biol Chem. 2001; 276:47434-47444.

164. Korn ED. Actin polymerization and its regulation by proteins from nonmuscle cells. Physiol Rev. 1982; 62:672-737.

165. Chellaiah M, Kizer N, Silva M, Alvarez U, Kwiatkowski D. Hruska KA. Gelsolin deficiency blocks podosome assembly and produces increased bone mass and strength. J Cell Biol. 2000; 148:665-678.

166. Li YP, Chen W, Liang Y, Li E, Stashenko P. Atp6i-deficient mice exhibit severe osteopetrosis due to loss of osteoclast-mediated extracellular acidification. Nat Genet. 1999; 23:447-451.

167. Scimeca JC, Franchi A, Trojani C, Parrinello H, Grosgeorge J, Robert C, Jaillon O, Poirier C, Gaudray P, Carle GF. The gene encoding the mouse homologue of the human osteoclast-specific 116 k-Da V-ATPase subunit bears a deletion in osteosclerotic (oc/oc) mutants. Bone. 2000; 26:207-213.

168. Sun-Wada G-H, Wada Y, Futai M. Diverse and essential roles of mammalian vacuolar-type proton pump ATPase: toward the physiological understanding of inside acidic compartments. Biochimica et Biophysica Acta. 2004; 1658:106-114.

169. Gluck SL, Lee BS, Wang SP, Underhill D, Nemoto J, Holliday LS. Plasma membrane V-ATPases in proton-transporting cells of the mammalian kidney and osteoclast. Acta Physiol Scand Suppl. 1998; 643:203-212.

170. Nishi T, Forgac M. The vacuolar (H+)-ATPases--nature's most versatile proton pumps. Nat Rev Mol Cell Biol. 2002; 3:94-103.

171. Lee BS, Holliday LS, Krits I, Gluck SL. Vacuolar H+-ATPase activity and expression in mouse bone marrow cultures. J Bone Miner Res. 1999; 142127-2136.

172. Toyomura T, Oka T, Yamaguchi C, Wada Y, Futai M. Three subunit a isoforms of mouse vacuolar H(+)-ATPase. Preferential expression of the a3 isoform during osteoclast differentiation. J Biol Chem. 2000; 275:8760-8765.

173. Nakamura I, Sasaki T, Tanaka S, Takahashi N, Jimi E, Kurokawa T, Kita Y, Ihara S, Suda T, Fukui Y. Phosphatidylinositol-3 kinase is involved in ruffled border formation in osteoclasts. J Cell Physiol. 1997; 172:230-239.

174. Holliday LS, Bubb MR, Jiang J, Hurst IR, Zuo J. Interactions between vacuolar H^+-ATPases and microfilaments in osteoclasts. J Bioenergentics and Biomembranes. 2005; 37(6):419-423.

175. Vitavska O, Merzendorfer H, Wieczorek H. The V-ATPase subunit C binds to polymeric F-actin as well as to monomeric G-actin and induces cross-linking of actin filaments. J Biol Chem. 2005; 280:1070-1076.

176. Feng X, Novack DV, Faccio R, ORy DS, Aya K, Boyer MI, McHugh KP, Ross FP, Teitelbaum SL. A Glanzmann's mutation in beta 3 integrin specifically impairs osteoclast function. J Clin Invest. 2001; 107:1137-1144.

177. Biswas RS, Baker D, Hruska KA, Chellaiah MA. Polyphosphoinositides-dependent regulation of the osteoclast actin cytoskeleton and bone resorption. BMC Cell Biol. 2004; 5:19.

178. Teti A, Barattolo R, Grano M, Colucci S, Argentino L, Teitelbaum SL, Hruska KA, Santacroce G, Zambonin ZA. Podosome expression in osteoclasts: influence of high extracellular calcium concentration. Boll Soc Ital Biol Sper. 1989; 65:1039-1043.

179. Ramirez A, Faupel J, Goebel I, Stiller A, Beyer S, Stockle C, Hasan C, Bode U, Kornak U, Kubisch C. Identification of a novel mutation in the coding region of the grey-lethal gene OSTM1 in human malignant infantile osteopetrosis. Hum Mutat. 2004;23(5):471-6.

180. Nakamura, I., Takahashi, N., Udagawa, N., Moriyama, Y., Kurokawa, T., Jimi, E., Sasaki, T., and Suda, T. Lack of vacuolar proton ATPase association with the cytoskeleton in osteoclasts of osteosclerotic (oc/oc) mice. FEBS Lett. 1997; 401:207-212.

181. Rajapuprohitam V, Chalhoub N, Benachenhou N, Neff L, Baron R, Vacher J. The mouse osteopetrotic grey-lethal mutation induces a defect in osteoclast maturation/function. Bone. 2001; 28:513-523.

182. Chalhoub N, Benachenhou N, Rajapurohitam V, Pata M, Ferron M, Frattini A, Villa A, Vacher J. Grey-lethal mutation induces severe malignant autosomal recesive osteopetrosis in mouse and human. Nat Med. 2003; 9:399-406.

183. Chen SH, Bubb MR, Yarmola EG, Zuo J, Jiang J, Lee BS, Lu M, Gluck SL, Hurst IR, Holliday LS. Vacuolar H+-ATPase binding to microfilaments: regulation in response to phosphatidylinositol 3-kinase activity and detailed characterization of the actin-binding site in subunit B. J Biol Chem. 2004; 279(9):7988-98.

184. Hiura K, Lim SS, Little SP, Lin A, Sato M. Differentiation dependent expression of tensin and cortactin in chicken osteoclasts. Cell Motil Cytoskeleton. 1995; 30:272-284.

185. Weed SA, Parsons JT. Cortactin: coupling membrane dynamics to cortical actin assembly. Oncogene. 2001; 20:6418-6434.

186. Weaver AM, Karginov AV, Kinley AW, Weed SA, Li Y, Parsons JT, Cooper JA. Cortactin promotes and stabilizes Arp2/3-induced actin filament network formation. Curr.Biol. 2001; 11:370-374.

187. Didry D, Carlier M, Pantaloni D. Synergy between profilin and actin depolymerizing factor (ADF/cofilin) in enhancing actin filament turnover. J Biol Chem. 1999; 273:25602-25611.

188. Weaver AM, Heuser JE, Karginov AV, Lee W, Parsons JT, Cooper JA. Interactions of cortactin and N-WASp with Arp2/3 complex. Curr Biol. 2002; 12:1270-1278.

189. Comerford KM, Lawrence DW, Synnestvedt K, Levi BP, Colgan SP. Role of vasodilator-stimulated phosphoprotein in PKA-induced changes in endothelial junctional permeability. FASEB Journal. 2002; 16:538-585.

190. Harbeck B, Huttelmaier S, Schluter K, Jockusch BM, Illenberger S. Phosphorylation of the vasodilator-stimulated phosphoprotein regulates its interaction with actin. J Biol Chem. 2000; 275(40):30817-30825.

191. Suzuki H, Nakamura I, Takahashi N, Ikuhara T, Matsuzaki K, Isogai Y, Hori M, Suda T. Calcitonin-induced changes in the cytoskeleton are mediated by a signal pathway associated with protein kinase A in osteoclasts. Endocrinol. 1996; 137(11):4685-90.

192. Samura A, Wada SA, Suda S, Iitaka M, Katayama S. Calcitonin receptor regulation and responsiveness to calcitonin in human osteoclast-like cells prepared in vitro using receptor activator of nuclear factor-kB ligand and macrophage colony stimulating factor. Endocrinology. 2000; 141(10): 3774-3782.

193. Weed SA, Karginov AV, Schafer DA, Weaver Am, Kinley AW, Cooper JA, Parsons JT. Cortactin localization to sites of actin assembly in lamellipodia requires interactions with F-actin and the Arp2/3 complex. J Cell Biol. 2000; 151(1):29-40.

194. Soriano P, Montgomery C, Geske R, Bradley A. Targeted disruption of the c-src proto-oncogene leads to osteopetrosis in mice. Cell. 1991; 64:693-702.

195. Hou P, Estrada L, Kinley AW, Parsons JT, Vojtek AB, Gorski JL. Fgd1, the Cdc42 GEF responsible for Faciogenital Dysplasia, directly interacts with cortactin and mAbp1 to modulate cell shape. Hum Mol Genet. 2003; 12:1981-1993.

196. Kim K, Hou P, Gorski JL, Cooper JA. Effect of Fgd1 on cortactin in Arp2/3 complex-mediated actin assembly. Biochemistry. 2004; 43:2422-2427.

197. Orrico A, Galli L, Buoni S, Hayek G, Luchetti A, Lorenzini S, Zappella M, Pomponi MG, Sorrentino V. Attention-deficit/hyperactivity disorder (ADHD) and variable clinical expression of Aarskog-Scott syndrome due to a novel FGD1 gene mutation (R408Q). Am J Med Genet A. 2005; 135:99-102.

198. Pasteris NG, Gorski JL. An intragenic TaqI polymorphism in the faciogenital dysplasia (FGD1) locus, the gene responsible for Aarskog syndrome. Hum Genet. 1995; 96(4):494.

199. Abu-Amer Y, Ross FP, Schlesinger P, Tondravi MM, Teitelbaum SL. Substrate recognition by osteoclast precursors induced s-crc/microtubule association. J Cell Biol. 1997; 137:247-258.

200. Kaksonen M, Peng HB, Rauvala H. Association of cortactin with dynamic actin in lamellipodia and on endosomal vesicles. J cell Sci. 2000; 113:4421-4426.

201. Bear JE, Svitkina TM, Krause M, Schafer DA, Loureiro JJ, Strasser GA, Maly IV, Chaga OY, Cooper JA, Borisy GG, Gertler FB. Antagonism between Ena/VASP proteins and actin filament capping regulates fibroblast motility. Cell. 2002; 109:509-521.

202. Kang F, Laine RO, Bubb MR, Southwick FS, Purich DL. Profilin interacts with the Gly-Pro-Pro-Pro-Pro-Pro sequences of vasodilator-stimulated phosphoprotein (VASP): implications for actin-based Listeria motility. Biochemistry. 1997; 36:8384-8392.

203. Krause M, Dent EW, Bear JE, Loureiro JJ, Gertler FB. Ena/VASP proteins: regulators of the actin cytoskeleton and cell migration. Annu.Rev.Cell Dev.Biol. 2003; 19:541-564.

204. Daly RJ. Cortactin signalling and dynamic actin networks. Biochem.J. 2004; 382:13-25.

205. Reinhard M, Halbrugge M, Scheer U, Wiegand C, Jockusch BM, Walter U. The 46/50 kDa phosphoprotein VASP purified from human platelets is a novel protein associated with actin filaments and focal contacts. EMBO J. 1992; 11:2063-2070.

206. Kwiatkowski AV, Gertler FB, Loureiro JJ. Function and regulation of ENA/VASP proteins. Trends Cell Biol. 2003; 13(7):386-92.

207. Howe AK, Hogan BP, Juliano RI. Regulation of vasodilator-stimulated phosphoprotein phosphorylation and interaction with Able by protein kinase A and cell adhesion. J. Biol Chem. 2002; 277(41):38121-38126.

208. Gertler FB, Niebuhr K, Reinhard M, Wehland J, Soriano P. Mena, a relative of VASP and Drosophila Enabled, is implicated in the control of microfilament dynamics. Cell. 1996; 87:227-239.

209. Bachmann C, Fischer L, Walter U, Reinhard M. The EVH2 domain of the vasodilator-stimulated phosphoprotein mediates tetrameriization, F-actin binding, and actin bundle formation. J Biol Chem. 1999; 274(33):23549-57.

210. Sechi AS, Wehland J. ENA/VASP proteins: multifunctional regulators of actin cytoskeleton dynamics. Front Biosci. 2004; 9:1294-1310.

211. Lambrechts A. Kwiatkowski AV, Lanier LM, Bear JE, Vandekerckhove J, Ampe C, Gertler FB. cAMP-dependent protein kinase phosphorylation of EVL, a Mena/VASP relative, regulates its interaction with actin and SH3 domains. J Biol Chem. 2000; 46(17):36143-36151.

212. Haffner C, Jarchau T, Reinhard M, Hoppe J, Lohmann SM, Walter U. Molecular cloning, structural analysis and functional expression of the proline-rich focal adhesion and microfilament-associated protein VASP. EMBO J. 1995; 14:19-27.

213. Massberg S, Guner S, Konrad I, Arguinzonis MIG, Eigenthaler M, Hemler K, Kersting J, Schulz C, Muller I, Besta F, Nieswandt B, Heinzmann U, Walter U, Gawaz M. Enhanced in vivo platelet adhesion in vasodilator-stimulated phosphoprotein (VASP)-deficient mice. Blood. 2004; 103(1): 136-42.

214. Hauser W, Knobeloch KP, Eigenthaler M, Gambaryan S, Krenn V, Geiger J, Glazova M, Rohde E, Horak I, Walter U, Zimmer M. Megakaryocyte hyperplasia and enhanced agonist-induced platelet activation in vasodilator-stimulated phosphoprotein knockout mice. Proc Natl Acad Sci USA. 1999; 96(14):8120-25.

215. Azodi 99Aszodi A, Pfeifer A, Ahmad M, Glauner M, Zhou XH, Ny L, Andersson KE, Kehrel B, Offermanns S, Fassler R. The vasodilator-stimulated phosphoprotein (VASP) is involved in cGMP- and cAMP-mediated inhibition of agonist-induced platelet aggregation, but is dispensable for smooth muscle function. EMBO J. 1999; 18(1):37-48.

216. Cramer LP. ENA/VASP: Solving a cell motility paradox. Curr Biol. 2002;12(12):417-419.

217. Barzik M, Kotova TI, Higgs HN, Hazelwood L, Hanein D. Gertler FB, Schafer DA. Ena/VASP proteins enhance actin polymerization in the presence of barded end capping proteins. J Biol Chem. 2005; 280(31): 28653-28662.

218. Vitavska O, Wieczorek H, Merzendorfer H. A novel role for subunit C in mediating binding of the H+-V-ATPase to the actin cytoskeleton. J Biol Chem. 2003; 278(20):18499-505.

219. Chellaiah MA. Regulation of actin ring formation by rho GTPases in osteoclasts. J Biol Chem. 2005; 280(38):32930-43.

220. Hu Y, Nyman J, Muhonen P, Vaananen HK, Laitala-Leinonen T. Inhibition of the osteoclast V-ATPase by small interfering RNAs. FEBS Lett. 2005; 579(22):4937-42.

221. Buscaglia CA, Penesetti D, Tao M, Nussenzweig V. Characterization of an aldolase-binding site in the Wiskott-Aldrich syndrome protein. J Biol Chem. 2006; 281(3):1324-31.

222. Waingeh VF, Gustafson CD, Kozliak EI, Lowe SL, Knull HR, Thomasson KA. Glycolytic enzyme interactions with yeast and skeletal muscle F-actin. Biophys J. 2006; 90(4):1371-84.

223. Lazner F, Gowen M, Pavasovic D, Kola I. Osteoporosis and osteopetrosis: two sides of the same coin. Human Molecular Genetics. 1999;8(10):1839-1846.

224. Whyte MP, Reinus WR, Podgornik MN, Mills BG. Familial expansile osteolysis (excessive RANK effect) in a 5-generation American kindred. Medicine. 2002;81(2):101-121.

225. Finley RS. Bisphosphonates in the treatment of bone metastases. Seminars in Oncology. 2002;29(1, Supplement 4):132-138.

226. Good CR, O'Keefe RJ, Puzas E, Schwarz EM, Rosier RN. Immunohistochemical study of receptor activator of nuclear factor kappa-B ligand (RANK-L) in human osteolytic bone tumors. Journal of Surgical Oncology. 2002;79:174-179.

227. Lees RL, Sabharwal VK, Heersche JNM. Resorptive state and cell size influence intracellular pH regulation in rabbit osteoclasts cultured on collagen-hydroxyapatite films. Bone. 2001;28(2):187-194.

228. Higgs HN. Formin proteins: a domain-based approach. Trends Biochem Sci. 2005; 30(6):342-53.

229. Baum B, Kunda P. Actin nucleation: spire - actin nucleator in a class of its own. Curr Biol. 2005; 15(8):R305-8.

230. Bowden ET, Barth M, Thomas D, Glazer RI, Mueller SC.An invasion-related complex of cortactin, paxillin and PKCmu associates with invadopodia at sites of extracellular matrix degradation. Oncogene. 1999; 18(31):4440-9.

231. Mizutani K, Miki H, He H, Maruta H, Takenawa T. Essential role of neural Wiskott-Aldrich syndrome protein in podosome formation and degradation of extracellular matrix in src-transformed fibroblasts. Cancer Res. 2002; 62(3):669-74.

BIOGRAPHICAL SKETCH

Irene Rita Maragos Hurst is the daughter of Drs. Nicolas and Thelma Maragos, and was born and raised in the St. Petersburg area. She was educated at Keswick Christian School and was president and valedictorian of the Class of 1991. Dr. Hurst attended the University of South Florida (1991-1996) where she received degrees in both biology and science education. During her time at USF, Dr. Hurst was actively involved in numerous honor and social organizations, including Kappa Delta Sorority. In 1997, she took a leave from college to teach 7th grade math and science at McLane Middle School in Brandon, FL. The following year, Dr. Hurst enrolled at the University of Louisville College of Dentistry where she received her Doctor of Dental Medicine degree as well as her Master of Science in oral biology. In 2001, Dr. Hurst began a joint Ph.D./residency program at the University of Florida. She completed her orthodontic training in 2006 at the University of Florida College of Dentistry as well as her Ph.D. in biomedical sciences through the College of Medicine.